

Capacity Regions of Two-Receiver Broadcast Erasure Channels with Feedback and Memory

Michael Heindlmaier, *Member, IEEE*, and Shirin Saeedi Bidokhti, *Member, IEEE*,

Abstract

The two-receiver broadcast packet erasure channel with feedback and memory is studied. Memory is modeled using a finite-state Markov chain representing a channel state. Two scenarios are considered: (i) when the transmitter has causal knowledge of the channel state (i.e., the state is visible), and (ii) when the channel state is unknown at the transmitter, but observations of it are available at the transmitter through feedback (i.e., the state is hidden). In both scenarios, matching outer and inner bounds are derived on the rates of communication and the capacity region is determined. It is shown that similar results carry over to channels with memory and delayed feedback, and memoryless compound channels with feedback.

When the state is visible, the capacity region has a single-letter characterization and is in terms of a linear program. Two optimal coding schemes are devised that use feedback to keep track of the sent/received packets via a network of queues: a probabilistic scheme and a deterministic backpressure-like algorithm. The former bases its decisions solely on the past channel state information and the latter follows a max-weight queue-based policy. The performance of the algorithms are analyzed using the frameworks of rate-stability in networks of queues, max-flow min-cut duality in networks, and finite-horizon Lyapunov drift analysis.

When the state is hidden, the capacity region does not have a single-letter characterization and is, in this sense, uncomputable. Approximations of the capacity region are provided and two optimal coding algorithms are outlined. The first algorithm is a probabilistic coding scheme that bases its decisions on the past L feedback sequences and its achievable rate-region approaches the capacity region exponentially fast in L . The second algorithm is a backpressure-like algorithm that performs optimally in the long run.

I. INTRODUCTION

The capacity of broadcast channels (BCs) remains unresolved both without and with feedback (FB). It was shown in [1] that feedback does not increase the capacity of physically degraded BCs. Nevertheless, feedback increases the capacity of general BCs [2], [3] and even partial feedback [4], [5], noisy feedback [6], [7] and rate-limited feedback [8] can help.

The class of memoryless broadcast packet erasure channels (BPECs) is among the few classes of BCs for which the capacity region is known with and without feedback. The capacity region \mathcal{C} for the memoryless BPEC without FB consists of all nonnegative rate pairs (R_1, R_2) satisfying

$$\frac{R_1}{1 - \epsilon_1} + \frac{R_2}{1 - \epsilon_2} \leq 1.$$

The capacity region \mathcal{C}_{fb} of a memoryless BPEC with FB was recently found in [9] for two receivers. The region is characterized by the closure of all non-negative rate pairs (R_1, R_2) such that

$$\begin{aligned} \frac{R_1}{1 - \epsilon_1} + \frac{R_2}{1 - \epsilon_{12}} &\leq 1 \\ \frac{R_1}{1 - \epsilon_{12}} + \frac{R_2}{1 - \epsilon_2} &\leq 1, \end{aligned}$$

where ϵ_1, ϵ_2 are the erasure probabilities at receiver 1 and 2, respectively, and ϵ_{12} is the probability of erasure at both receivers. In particular, feedback increases the capacity and this is of practical interest since the required feedback is only a low-cost ACK/NACK signal that is easy to implement in BPECs. This result has been extended to certain cases of broadcast channels with more number of receivers in [10], [11], [12]. In all these works, the capacity region is achieved using feedback-based coding algorithms that are based on network coding ideas and the converse theorems are proved by proving genie-aided outer bounds on the capacity region. The trick is that the genie helps the receivers such that the broadcast channel becomes a physically degraded one, for which the capacity region with feedback is known based on [1], [13], [14]. In a similar line of work, the capacity region of two-receiver multiple-input BPECs with feedback has been studied in [15] where the capacity region is derived and is shown to be achievable using linear network codes (LNC).

Michael Heindlmaier and S. Saeedi Bidokhti are with the Department for Electrical and Computer Engineering, Technische Universität München, Germany (michael.heindlmaier@tum.de, shirin.saeedi@tum.de).

The authors were supported by the German Federal Ministry of Education and Research in the framework of the Alexander von Humboldt-Professorship. The work of S. Saeedi Bidokhti is also supported by the Swiss National Science Foundation.

The material in this paper was presented in part at the 2014 Allerton Conf. Comm. Control and Computing, USA, and the 2015 IEEE International Symposium on Information Theory, Honolulu, USA.

In this paper, we study BPECs with feedback and channel memory. The problem is motivated by the bursty nature of erasures in practical communication systems, e.g., satellite links [16], [17], [18], [19]. When an erasure channel has memory and there is no feedback, one can use erasure correcting codes for memoryless channels in combination with interleavers that decorrelate the erasures. But it turns out that feedback enables more sophisticated coding methods.

We model channel memory by a finite state machine and a set of state-dependent erasure probabilities. Finite state channel models are a common modeling approach for wireless communication channels, see e.g. [20, Chapter 4.6] or [21] and the references therein. Using a finite state Markov channel model, [22] characterizes the capacity of point-to-point time-varying channels with memory and delayed feedback. The feedback-capacity of point to point channels with general form of memory is characterized using infinite letter characterization in [23], [24], [25]. In particular, it is shown that feedback does not increase the capacity if the channel state information is available at both the transmitter and receiver.

The main result of this paper is the characterization of the feedback capacity of two-receiver-BPECs with hidden and observable memory. More precisely, we study the following two scenarios:

- 1) the transmitter has strictly causal knowledge of the channel state and receives ACK/NACK feedback from both receivers
- 2) the transmitter receives ACK/NACK feedback from the receivers, but does not receive channel state feedback.

In both scenarios, we derive outer bounds on the capacity region, and propose optimal achievable schemes that are of low complexity. Our outer bounds are based on genie-aided arguments. Although the final result has a similar structure as for the memoryless case, these bounds cannot be derived directly using the results of [1], [13], [14]. Our proposed achievable schemes extend the max-weight queue-based algorithms of [9], [11], [26]. The extensions incorporate knowledge about past channel states and change parts of the proof and the corresponding max-weight policy. The techniques generalize to BPECs with delayed feedback.

In a related work that was carried out independently and in parallel by Kuo and Wang [27], it is noted that some of the coding operations proposed in [15] are also useful for BPECs with memory, an achievable rate-region is characterized for channels with memory and causal channel state information, and a scheme is proposed that is optimal in the class of linear codes. Finally, we remark that Dabora and Goldsmith also studied the general broadcast channel with feedback and memory and considered different cooperation scenarios in [28]. Capacity statements were derived only for partial cooperation among receivers.

The rest of the paper is organized as follows: We introduce the notation in Section II and describe the system models for channels with observable memory and channels with hidden memory in Section III. Our main results are summarized in Section IV. In Section V, we derive outer bounds on the capacity. In Section VI we present probabilistic coding schemes and deterministic coding algorithms that achieve the capacity. We introduce some simpler, but suboptimal, coding schemes in Section VII. The numerical performance of the proposed schemes and the role of delayed feedback are discussed in Section VIII. Section IX focusses on the special case of finite-state memoryless channels. We conclude in Section X. Proofs of the theorems can be found in the appendices.

II. NOTATION

Random variables (RVs) are denoted by upper-case letters, e.g. X and their outcomes (values) by lower-case letters, e.g. x . The probability of a RV X taking on the value x given an event \mathcal{E} is written as $\Pr[X = x|\mathcal{E}]$. Often, the conditional event corresponds to another RV Y taking on some value y . This conditional probability is written as $\Pr[X = x|Y = y]$ or equivalently $P_{X|Y}(x|y)$. If the involved RVs are clear from the context, we often write $P(x|y)$ for $P_{X|Y}(x|y)$. The equivalent expressions $\Pr[X|Y]$ and $P_{X|Y}$ are used to address the conditional probability distribution for any outcome of the RVs.

The RVs X, Y, Z form a Markov chain if the joint probability mass function (PMF) P_{XYZ} can be written as $P_{XYZ} = P_X P_{Y|X} P_{Z|Y}$. We write this relationship as $X - Y - Z$. The conditional expectation of a function f of a RV X given another RV Z is itself a RV and is written as $\mathbb{E}[f(X)|Z]$. Using the law of total expectation, we have $\mathbb{E}[f(X)|Z] = \mathbb{E}[\mathbb{E}[f(X)|YZ]|Z]$. If $X - Y - Z$ forms a Markov chain, we can write $\mathbb{E}[f(X)|Z] = \mathbb{E}[\mathbb{E}[f(X)|Y]|Z]$.

A finite sequence (or string) of RVs X_1, X_2, \dots, X_n is denoted by X^n . Often, but not always, this refers to a sequence in time. We write X_t^n if the sequence starts at index t , i.e. $X_t^n = X_t, X_{t+1}, \dots, X_n$. Sequences may have subscripts, e.g. X_j^n denotes $X_{j,1}, X_{j,2}, \dots, X_{j,n}$. This results in one possible ambiguity as X_j^n could also denote X_j, X_{j+1}, \dots, X_n , but in these cases, the meaning will be clear from the context. Vectors are written with underlined letters and can be used as an alternative to the sequence notation, e.g. $\underline{X} = X^n$. These two concepts can be mixed, e.g. \underline{X}^n denotes the sequence of vectors $\underline{X}_1, \dots, \underline{X}_n$. Matrices are written boldface, e.g. \mathbf{A} .

The entropy of a discrete or continuous RV X is written as $H(X)$. Similarly, $H(X|Y)$ denotes the conditional entropy of X given the RV Y . $I(X; Y)$ denotes the mutual information between two RVs X and Y . The mutual information given a RV Z is written as $I(X; Y|Z)$.

General sets are denoted by calligraphic letters, e.g. \mathcal{X} . \mathbb{F}_q denotes the finite field of order q . The cardinality of the finite set \mathcal{X} is written as $|\mathcal{X}|$. If \mathcal{X} is the subset of a larger set \mathcal{Y} , the complement of \mathcal{X} is written as \mathcal{X}^c where $\mathcal{X}^c = \mathcal{Y} \setminus \mathcal{X}$.

The indicator function $\mathbb{1}\{\cdot\}$ takes on the value 1 if the event inside the brackets is true and 0 otherwise. The expression $[a]^+$ is a shorthand notation for $\max(a, 0)$.

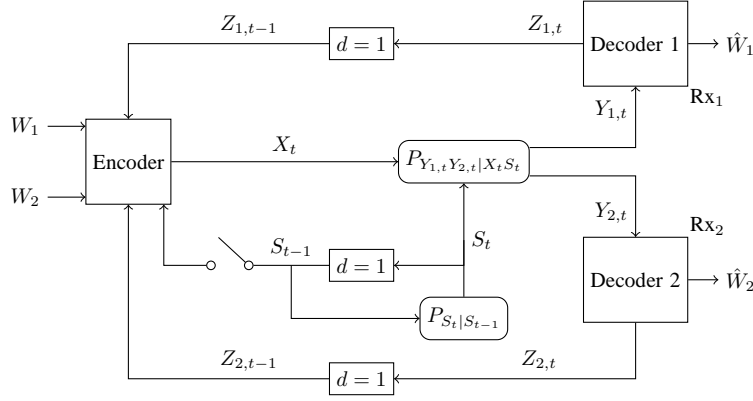


Fig. 1: Block diagram for the BPEC. Depending on whether the switch is closed or not, we call the state visible or hidden. The box marked with $d = 1$ represents a delay of one time unit.

III. SYSTEM MODEL

A transmitter communicates two independent messages W_1 and W_2 (of nR_1 , nR_2 packets, respectively) to two receivers Rx_1 and Rx_2 over n uses of the channel. Communication takes place over a BPEC with memory and feedback as described next.

The input to the broadcast channel at time t , $t = 1, \dots, n$, is denoted by $X_t \in \mathcal{X}$. The channel inputs correspond to packets of ℓ bits; we may represent this by choosing $\mathcal{X} = \mathbb{F}_2^\ell$ with $\ell \gg 1$. Transmission rates are measured in packets per slot, hence all entropies and mutual information terms are considered with logarithms to the base 2^ℓ .

The channel outputs at time t are written as $Y_{1,t} \in \mathcal{Y}$ and $Y_{2,t} \in \mathcal{Y}$, where $\mathcal{Y} = \mathcal{X} \cup \{?\}$. The output $Y_{j,t}$, $j \in \{1, 2\}$, is either X_t (i.e., received perfectly) or ? (i.e., erased).

We define binary random variables $Z_{j,t}$, $j \in \{1, 2\}$, $t = 1, \dots, n$, to indicate if an erasure occurred at receiver j in time t ; i.e. $Z_{j,t} = \mathbb{1}\{Y_{j,t} = ?\}$. Clearly, $Y_{j,t}$ can be expressed as a function of X_t and $Z_{j,t}$, and $Y_{j,t}$ determines $Z_{j,t}$. We denote $(Z_{1,t}, Z_{2,t})$ by \underline{Z}_t and $(Y_{1,t}, Y_{2,t})$ by \underline{Y}_t .

The broadcast channel we study has memory that is modeled via a finite state machine with state S_t at time t . The state evolves according to an irreducible aperiodic time-invariant finite state Markov chain with state space \mathcal{S} and steady-state distribution π_s , $s \in \mathcal{S}$. The initial state S_0 is distributed according to the steady-state distribution. Depending on the current random state of the channel, the erasure probabilities are specified through the conditional distribution $P_{\underline{Z}_t|S_t}$. Note that spatial correlation among the receivers is permitted. The transition probabilities between channel states are known at the transmitter. The sequence \underline{Z}^n is correlated in time in general, hence the channel has memory. Both S^n and \underline{Z}^n are ergodic.

After each transmission, an ACK/NACK feedback is available at the encoder from both receivers. The encoder uses the feedback information to encode its messages W_1 , W_2 . Two setups are considered:

- (i) ACK/NACK feedback and previous state information are available at the encoder:

$$X_t = f_t(W_1, W_2, \underline{Z}^{t-1}, S^{t-1}). \quad (1)$$

- (ii) Only ACK/NACK feedback is available at the encoder:

$$X_t = f_t(W_1, W_2, \underline{Z}^{t-1}). \quad (2)$$

Depending on whether the transmitter knows the previous channel state or not, we call the state *visible* or *hidden* (see also Fig. 1). When the state is visible, the joint probability mass function of the system factorizes as

$$P_{W_1 W_2 X^n S^n Y_1^n Y_2^n Z_1^n Z_2^n} = P_{W_1} P_{W_2} P_{S_0} \left(\prod_{t=1}^n P_{S_t|S_{t-1}} P_{X_t|W_1 W_2 S^{t-1} \underline{Z}^{t-1}} P_{Z_{1,t} Z_{2,t}|S_t} P_{Y_{1,t}|X_t Z_{1,t}} P_{Y_{2,t}|X_t Z_{2,t}} \right).$$

When the state is hidden, the joint probability mass function of the system factorizes as

$$P_{W_1 W_2 X^n S^n Y_1^n Y_2^n Z_1^n Z_2^n} = P_{W_1} P_{W_2} P_{S_0} \left(\prod_{t=1}^n P_{S_t|S_{t-1}} P_{X_t|W_1 W_2 \underline{Z}^{t-1}} P_{Z_{1,t} Z_{2,t}|S_t} P_{Y_{1,t}|X_t Z_{1,t}} P_{Y_{2,t}|X_t Z_{2,t}} \right).$$

The state may be visible either because it is explicitly available at the transmitter or because it can be determined from the available feedback. The latter is illustrated via the following example.

Example 1. Consider a Gilbert-Elliot model [29], [30] with state space $\mathcal{S} = \{\text{GG}, \text{GB}, \text{BG}, \text{BB}\}$ where G and B refer to a good and bad state at each user. Suppose that the channel erases the input in state B and is erasure free in state G; i.e., we have

$$\begin{aligned} P_{\underline{Z}_t|S_t}(0, 0|\text{GG}) &= 1, & P_{\underline{Z}_t|S_t}(0, 1|\text{GB}) &= 1 \\ P_{\underline{Z}_t|S_t}(1, 0|\text{BG}) &= 1, & P_{\underline{Z}_t|S_t}(1, 1|\text{BB}) &= 1. \end{aligned} \quad (3)$$

In such a channel, the feedback \underline{Z}_t determines the channel state S_t , hence $H(S_t|\underline{Z}_t) = 0$, and we thus say that the state is visible. If \underline{Z}_t does not determine S_t , the setup has hidden state, unless S_t is fed back separately. We use a Gilbert-Elliot channel model for our simulations in Section VIII. \square

Given the feedback and the channel state information, the encoder may calculate the statistics of the next channel erasure events. In the visible case, the probabilities of erasure events given the *previous* channel state s are given by

$$\begin{aligned} \epsilon_{12}(s) &\triangleq P_{\underline{Z}_t|S_{t-1}}(1, 1|s), & \epsilon_{1\bar{2}}(s) &\triangleq P_{\underline{Z}_t|S_{t-1}}(1, 0|s), \\ \epsilon_{\bar{1}2}(s) &\triangleq P_{\underline{Z}_t|S_{t-1}}(0, 1|s), & \epsilon_{\bar{1}\bar{2}}(s) &\triangleq P_{\underline{Z}_t|S_{t-1}}(0, 0|s), \\ \epsilon_1(s) &\triangleq \epsilon_{12}(s) + \epsilon_{1\bar{2}}(s), & \epsilon_2(s) &\triangleq \epsilon_{\bar{1}2}(s) + \epsilon_{\bar{1}\bar{2}}(s). \end{aligned} \quad (4)$$

Note that these probabilities do not depend on t in our setup. In the hidden case, the probabilities of erasure events given the past feedback sequence \underline{z}^{t-1} are given by

$$\begin{aligned} \epsilon_{12}(\underline{z}^{t-1}) &\triangleq P_{\underline{Z}_t|\underline{Z}^{t-1}}(1, 1|\underline{z}^{t-1}), & \epsilon_{1\bar{2}}(\underline{z}^{t-1}) &\triangleq P_{\underline{Z}_t|\underline{Z}^{t-1}}(1, 0|\underline{z}^{t-1}), \\ \epsilon_{\bar{1}2}(\underline{z}^{t-1}) &\triangleq P_{\underline{Z}_t|\underline{Z}^{t-1}}(0, 1|\underline{z}^{t-1}), & \epsilon_{\bar{1}\bar{2}}(\underline{z}^{t-1}) &\triangleq P_{\underline{Z}_t|\underline{Z}^{t-1}}(0, 0|\underline{z}^{t-1}), \\ \epsilon_1(\underline{z}^{t-1}) &\triangleq \epsilon_{12}(\underline{z}^{t-1}) + \epsilon_{1\bar{2}}(\underline{z}^{t-1}), & \epsilon_2(\underline{z}^{t-1}) &\triangleq \epsilon_{\bar{1}2}(\underline{z}^{t-1}) + \epsilon_{\bar{1}\bar{2}}(\underline{z}^{t-1}). \end{aligned} \quad (5)$$

In the hidden case, these probabilities depend on t .

The goal is to have each decoder Rx_j reliably estimate $\hat{W}_j = h_j(Y_j^n)$ from its received sequence Y_j^n .

Definition 1. The rate-pair (R_1, R_2) is said to be *achievable* if the error probability $\Pr[\hat{W}_1 \neq W_1, \hat{W}_2 \neq W_2]$ can be made arbitrarily small as n gets large. The *capacity region* is the closure of the set of achievable rate pairs.

For the visible case, we denote the capacity region by $C_{\text{fb}+s}^{\text{mem}}$ and for the hidden case, we denote it by $C_{\text{fb}}^{\text{mem}}$.

In Section VI we also consider a dynamic version of the problem: Instead of having messages W_1, W_2 of rates nR_1, nR_2 we consider packets for Rx_1, Rx_2 arriving in each slot with probability R_1, R_2 , respectively. This dynamic version is modelled and analyzed with a network of queues that captures different coding operations and tracks the number of delivered packets.

For the dynamic version of the problem, we would like to have all the queues in the network *stable* according to the following two stability definitions (e.g. [31], [32, Definition 3.1]):

Definition 2. Let Q_t denote the number of packets in the corresponding queue Q at time t . A queue Q is *rate-stable* if

$$\lim_{n \rightarrow \infty} \frac{Q_n}{n} = 0 \quad \text{with probability 1.} \quad (6)$$

A queue Q is *strongly stable* if

$$\limsup_{n \rightarrow \infty} \frac{1}{n} \sum_{t=1}^n \mathbb{E}[Q_t] < \infty. \quad (7)$$

A network of queues is stable if all queues inside the network are stable [32, Definition 3.2]. The *network stability region* consists of all rate pairs (R_1, R_2) for which all queues in the network are stable.

For the setup in Section VI, we will propose coding algorithms that strongly stabilize the queues. We remark that strong stability implies rate stability [31, Theorem 4] in this setup, but not vice versa.

Remark 1. Capacity Regions vs. Stability Regions: Capacity regions are defined via block-coding and decoding error probability as a criterion, as in Definition 1. Queue stability deals with dynamic packet arrivals (instead of blocks of packets) and measures if the number of packets in the queues grows sublinearly, as in Definition 2. Stability regions can be cast into corresponding block-based rate regions as follows: Suppose that a network of queues is rate-stable for (R_1, R_2) ; i.e., each queue satisfies

$$Q_n = o(n) \quad \text{with probability 1.} \quad (8)$$

In n channel uses, $nR_1 \pm o(n)$ packets arrive for Rx_1 and $nR_2 \pm o(n)$ packets arrive for Rx_2 with high probability for n large enough. Rate stability implies (see (8)) that there are only $o(n)$ packets left in the queues after n channel uses. These remaining packets can be delivered in $o(n)$ slots. Hence, the total number of slots needed to deliver $nR_1 \pm o(n)$ packets for user Rx_1 and $nR_2 \pm o(n)$ packets for Rx_2 is given by $n + o(n)$. The number of slots of the cleanup phase is negligible compared to n , for n getting large, and (R_1, R_2) is achievable in the block-based communication sense.

IV. MAIN RESULTS

Our main results are in the form of matching outer and inner bounds on the capacity region of the two-receiver BPEC with memory and ACK/NACK feedback. We consider both visible and hidden cases.

A. Visible Case

Define $\bar{\mathcal{C}}_{fb+s}^{\text{mem}}$ as the closure of rate pairs (R_1, R_2) for which there exist variables $x_s, y_s, s \in \mathcal{S}$ such that

$$0 \leq x_s \leq 1, \quad 0 \leq y_s \leq 1, \quad \forall s \in \mathcal{S} \quad (9)$$

$$R_1 \leq \sum_{s \in \mathcal{S}} \pi_s (1 - \epsilon_1(s)) x_s \quad (10)$$

$$R_1 \leq \sum_{s \in \mathcal{S}} \pi_s (1 - \epsilon_{12}(s)) (1 - y_s) \quad (11)$$

$$R_2 \leq \sum_{s \in \mathcal{S}} \pi_s (1 - \epsilon_2(s)) y_s \quad (12)$$

$$R_2 \leq \sum_{s \in \mathcal{S}} \pi_s (1 - \epsilon_{12}(s)) (1 - x_s). \quad (13)$$

We show in Section V that $\bar{\mathcal{C}}_{fb+s}^{\text{mem}}$ is an outer bound on the capacity region $\mathcal{C}_{fb+s}^{\text{mem}}$ in the visible case. Moreover, we show in Section VI that the region $\bar{\mathcal{C}}_{fb+s}^{\text{mem}}$ is achievable, leading to the following theorem.

Theorem 1. The capacity region of the BPEC with feedback, memory, and visible state is

$$\mathcal{C}_{fb+s}^{\text{mem}} = \bar{\mathcal{C}}_{fb+s}^{\text{mem}}. \quad (14)$$

Two coding schemes achieving $\bar{\mathcal{C}}_{fb+s}^{\text{mem}}$ are presented in Section VI: In the first scheme the transmitter randomly chooses to send linear combinations of packets according to a probability distribution that depends on the observed state feedback. The optimization of the corresponding probability distribution results in a single-commodity flow problem in a network of virtual queues that reflect the coding operations. The min-cut version of the max-flow problem can be shown to match the outer bounds, proving Theorem 1. The second scheme is a queue-based max-weight backpressure algorithm that operates in on the network of queues. This algorithm strongly stabilizes all queues in the network for all rates inside the capacity region.

The region $\bar{\mathcal{C}}_{fb+s}^{\text{mem}}$ can be achieved by a coding scheme that was first introduced in [27] based on work in [15]. Our contribution is an alternative capacity proof for the visible case that does not require the results of [15] and that is based on standard approaches in network control, whereas [27] requires the more evolved concept of stochastic programming networks [33]. Further, the results carry over to the case of delayed state feedback (Section VIII) and can be easily adapted to the case of hidden states.

Define $\underline{\mathcal{C}}_{fb+s}^{\text{mem}}$ as the closure of rate pairs (R_1, R_2) for which there exist variables $x_s, y_s, s \in \mathcal{S}$, such that

$$0 \leq x_s \leq 1, \quad 0 \leq y_s \leq 1, \quad \forall s \in \mathcal{S} \quad (15)$$

$$x_s + y_s \geq 1, \quad \forall s \in \mathcal{S} \quad (16)$$

$$R_1 \leq \sum_{s \in \mathcal{S}} \pi_s (1 - \epsilon_1(s)) x_s \quad (17)$$

$$R_1 \leq \sum_{s \in \mathcal{S}} \pi_s (1 - \epsilon_{12}(s)) (1 - y_s) \quad (18)$$

$$R_2 \leq \sum_{s \in \mathcal{S}} \pi_s (1 - \epsilon_2(s)) y_s \quad (19)$$

$$R_2 \leq \sum_{s \in \mathcal{S}} \pi_s (1 - \epsilon_{12}(s)) (1 - x_s). \quad (20)$$

We show in Section VII-A that $\underline{\mathcal{C}}_{fb+s}^{\text{mem}}$ is achievable with restricted coding schemes. Note that $\bar{\mathcal{C}}_{fb+s}^{\text{mem}}$ and $\underline{\mathcal{C}}_{fb+s}^{\text{mem}}$ differ only in the constraint (16). In some cases, $\bar{\mathcal{C}}_{fb+s}^{\text{mem}}$ and $\underline{\mathcal{C}}_{fb+s}^{\text{mem}}$ coincide: For example, consider $\bar{\mathcal{C}}_{fb+s}^{\text{mem}}$ when \mathcal{S} has one state only, which models a memoryless BPEC. One may verify that the two regions $\underline{\mathcal{C}}_{fb}^{\text{mem}}$ and $\bar{\mathcal{C}}_{fb}^{\text{mem}}$ match, and that the result of [9] follows by eliminating the variables x_s, y_s . We show in Section IX that this applies more generally to finite state *memoryless* channels, i.e. channels where the sequence \underline{S}^n is i.i.d.

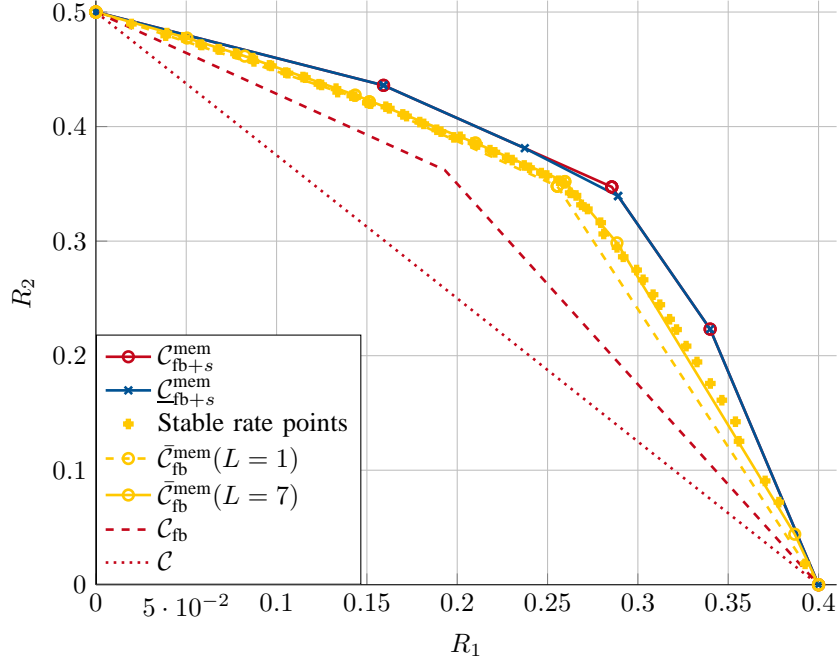


Fig. 2: Capacity region for visible and hidden case. The channel parameters, to be discussed in detail in Section VIII-C, are $\epsilon_1 = 0.6$, $g_1 = 0.1$, $b_1 = 0.15$, $\epsilon_{1G} = 0.2$, $\epsilon_{1B} = 0.866$ and $\epsilon_2 = 0.5$, $g_2 = 0.2$, $b_2 = 0.2$, $\epsilon_{2G} = 0.2$, $\epsilon_{2B} = 0.8$.

B. Hidden Case

Define $\bar{\mathcal{C}}_{n, \text{fb}}^{\text{mem}}$, for every positive integer n , as the closure of rate pairs (R_1, R_2) for which there exist variables $x(\underline{z}^{t-1}), y(\underline{z}^{t-1})$, $t = 1, \dots, n$ such that

$$0 \leq x(\underline{z}^{t-1}) \leq 1, \quad 0 \leq y(\underline{z}^{t-1}) \leq 1 \quad t = 1, \dots, n, \forall \underline{z}^{t-1} \in \{0, 1\}^{2(t-1)} \quad (21)$$

$$R_1 \leq \frac{1}{n} \sum_{t=1}^n \sum_{\underline{z}^{t-1}} P_{\underline{Z}^{t-1}}(\underline{z}^{t-1}) (1 - \epsilon_{11}(\underline{z}^{t-1})) x(\underline{z}^{t-1}) \quad (22)$$

$$R_1 \leq \frac{1}{n} \sum_{t=1}^n \sum_{\underline{z}^{t-1}} P_{\underline{Z}^{t-1}}(\underline{z}^{t-1}) (1 - \epsilon_{12}(\underline{z}^{t-1})) (1 - y(\underline{z}^{t-1})) \quad (23)$$

$$R_2 \leq \frac{1}{n} \sum_{t=1}^n \sum_{\underline{z}^{t-1}} P_{\underline{Z}^{t-1}}(\underline{z}^{t-1}) (1 - \epsilon_{21}(\underline{z}^{t-1})) y(\underline{z}^{t-1}) \quad (24)$$

$$R_2 \leq \frac{1}{n} \sum_{t=1}^n \sum_{\underline{z}^{t-1}} P_{\underline{Z}^{t-1}}(\underline{z}^{t-1}) (1 - \epsilon_{22}(\underline{z}^{t-1})) (1 - x(\underline{z}^{t-1})). \quad (25)$$

Define $\bar{\mathcal{C}}_{\text{fb}}^{\text{mem}} \triangleq \limsup_{n \rightarrow \infty} \bar{\mathcal{C}}_{n, \text{fb}}^{\text{mem}}$. We show in Appendix B that $\bar{\mathcal{C}}_{\text{fb}}^{\text{mem}}$ is an outer bound for the capacity region $\mathcal{C}_{\text{fb}}^{\text{mem}}$ for the hidden case. Unlike for the visible case, $\bar{\mathcal{C}}_{\text{fb}}^{\text{mem}}$ has an infinite-letter characterization. This makes it impossible to compute the outer bound. We derive computable approximations with fast convergence guarantees in Section V. Moreover, we show in Section VI that the region $\bar{\mathcal{C}}_{\text{fb}}^{\text{mem}}$ is achievable using a low-complexity backpressure-like coding algorithm and prove the following theorem.

Theorem 2. The capacity region¹ of the BPEC with feedback, memory and hidden state is

$$\mathcal{C}_{\text{fb}}^{\text{mem}} = \bar{\mathcal{C}}_{\text{fb}}^{\text{mem}}. \quad (26)$$

As an example, Fig. 2 shows the rate regions $\mathcal{C}_{\text{fb}+s}^{\text{mem}}$, $\underline{\mathcal{C}}_{\text{fb}+s}^{\text{mem}}$, \mathcal{C}_{fb} and \mathcal{C} . Stable rate points are points inside $\bar{\mathcal{C}}_{\text{fb}}^{\text{mem}}$, $\bar{\mathcal{C}}_{\text{fb}}^{\text{mem}}(L)$ show computable approximations of $\bar{\mathcal{C}}_{\text{fb}}^{\text{mem}}$, to be introduced in Section V-B.

We present further numerical simulations and the role of delayed feedback in Section VIII.

¹under the assumptions stated in Theorem 5

V. OUTER BOUNDS

A. Visible Case

We prove that $\bar{C}_{\text{fb}+s}^{\text{mem}}$ is an outer bound on the capacity region. The general idea is to show that for any achievable scheme, there are parameters $x_s, y_s, s \in \mathcal{S}$, as in (9) - (13). We find these parameters by relating them to certain mutual information terms.

In order to bound R_1 and R_2 , for any $\delta > 0$, we write the following multi-letter bounds and single-letterize them properly next. For $j \in \{1, 2\}$, we define $\bar{j} \in \{1, 2\}$ such that $\bar{j} \neq j$. Fano's inequality [34, Chapter 2.10] and the independence of the two messages W_1 and W_2 lead to the following bounds:

$$nR_j \leq I(W_j; Y_j^n) + n\delta \quad (27)$$

$$nR_j \leq I(W_j; Y_1^n Y_2^n | W_{\bar{j}}) + n\delta \quad (28)$$

For $j = 1$, the single-letterization is done as follows:

$$\begin{aligned} R_1 - \delta &\leq \frac{1}{n} I(W_1; Y_1^n) \\ &\leq \frac{1}{n} I(W_1; Y_1^n S^{n-1}) \\ &= \frac{1}{n} \sum_{t=1}^n I(W_1; Y_{1,t} S_{t-1} | Y_1^{t-1} S^{t-2}) \\ &= \frac{1}{n} \sum_{t=1}^n [I(W_1; S_{t-1} | Y_1^{t-1} Z_1^{t-1} S^{t-2}) + I(W_1; Y_{1,t} | Y_1^{t-1} S^{t-1})] \\ &\stackrel{(a)}{=} \sum_{t=1}^n \frac{1}{n} I(W_1; Y_{1,t} | Y_1^{t-1} S^{t-1}) \\ &\leq \sum_{t=1}^n \frac{1}{n} I(W_1 Y_1^{t-1} S^{t-1}; Y_{1,t} | S_{t-1}) \\ &\stackrel{(b)}{=} \sum_{t=1}^n \frac{1}{n} I(U_{1,t}; Y_{1,t} | S_{t-1}) \\ &\stackrel{(c)}{=} I(U_{1,T}; Y_{1,T} | S_{T-1} T) \\ &= \sum_{s \in \mathcal{S}} \pi_s I(U_{1,T}; Y_{1,T} | T, S_{T-1} = s). \end{aligned} \quad (29)$$

In the above chain of inequalities, (a) follows because Z_1^{t-1} is a function of Y_1^{t-1} and because of the Markov chain

$$W_1 - Y_1^{t-1} Z_1^{t-1} S^{t-2} - S_{t-1},$$

(b) follows by defining $U_{1,t} = (W_1 Y_1^{t-1} S^{t-1})$, and (c) follows by a standard random time sharing argument with time sharing random variable T . Similarly, one obtains

$$\begin{aligned} R_1 - \delta &\leq \frac{1}{n} I(W_1; Y_1^n Y_2^n | W_2) \\ &\leq \sum_{s \in \mathcal{S}} \pi_s I(U_{1,T}; Y_{1,T} Y_{2,T} | U_{2,T} V_T T, S_{T-1} = s), \end{aligned} \quad (30)$$

where $U_{2,T} = (W_2 Y_2^{T-1} S^{T-1})$ and $V_T = (Y_1^{T-1} Y_2^{T-1} S^{T-1})$. By symmetry, we also have the following bounds:

$$R_2 - \delta \leq \sum_{s \in \mathcal{S}} \pi_s I(U_{2,T}; Y_{2,T} | T, S_{T-1} = s) \quad (31)$$

$$R_2 - \delta \leq \sum_{s \in \mathcal{S}} \pi_s I(U_{2,T}; Y_{1,T} Y_{2,T} | U_{1,T} V_T T, S_{T-1} = s). \quad (32)$$

Remark 2. Note that

- V_T is a function of $(U_{1,T} U_{2,T})$, and
- $\underline{Z}_T - T S_{T-1} - U_{1,T} U_{2,T} V_T X_T$ forms a Markov chain.

The following lemma is based on [35, Lemma 1].

Lemma 3. For every $s \in \mathcal{S}$ and $j \in \{1, 2\}$, we have:

$$I(U_{j,T}; Y_{j,T} | T, S_{T-1} = s) = (1 - \epsilon_j(s)) I(U_{j,T}; X_T | T, S_{T-1} = s) \quad (33)$$

$$I(U_{j,T}; Y_{1,T} Y_{2,T} | U_{\bar{j},T} V_T T, S_{T-1} = s) = (1 - \epsilon_{12}(s)) I(U_{j,T}; X_T | U_{\bar{j},T} V_T T, S_{T-1} = s). \quad (34)$$

Using Lemma 3, we now replace the mutual information terms in (29) - (32) to obtain

$$R_j - \delta \leq \sum_{s \in \mathcal{S}} \pi_s (1 - \epsilon_j(s)) u_s^{(j)} \quad j = 1, 2 \quad (35)$$

$$R_j - \delta \leq \sum_{s \in \mathcal{S}} \pi_s (1 - \epsilon_{12}(s)) z_s^{(j)} \quad j = 1, 2, \quad (36)$$

where $u_s^{(j)}$ and $z_s^{(j)}$ are defined as follows for $j \in \{1, 2\}$, $s \in \mathcal{S}$:

$$u_s^{(j)} = I(U_{j,T}; X_T | T, S_{T-1} = s) \quad (37)$$

$$z_s^{(j)} = I(U_{j,T}; X_T | U_{\bar{j},T} V_T T, S_{T-1} = s). \quad (38)$$

The following Lemma relates these parameters and is proven in Appendix A.

Lemma 4. For every $j \in \{1, 2\}$ and $s \in \mathcal{S}$, we have

$$u_s^{(j)} + z_s^{(\bar{j})} \leq 1.$$

Combining the above results and letting δ go to zero, (R_1, R_2) can be achieved only if there exist variables $u_s^{(1)}$, $u_s^{(2)}$, $z_s^{(1)}$, $z_s^{(2)}$, $s \in \mathcal{S}$, for which the following inequalities hold for all $j \in \{1, 2\}$:

$$0 \leq u_s^{(j)}, z_s^{(j)} \leq 1 \quad (39)$$

$$u_s^{(j)} + z_s^{(\bar{j})} \leq 1 \quad (40)$$

$$R_j \leq \sum_{s \in \mathcal{S}} \pi_s (1 - \epsilon_j(s)) u_s^{(j)} \quad (41)$$

$$R_j \leq \sum_{s \in \mathcal{S}} \pi_s (1 - \epsilon_{12}(s)) z_s^{(j)}. \quad (42)$$

The final step is to show that the above outer bound matches $\bar{C}_{\text{fb}+s}^{\text{mem}}$ defined in (9) - (13). This is done by noting that inequality (40) can be made tight without changing the rate region. The equivalence of the two regions then becomes clear by setting $z_s^{(1)} = 1 - y_s$, $z_s^{(2)} = 1 - x_s$, $u_s^{(1)} = x_s$, and $u_s^{(2)} = y_s$.

B. Hidden Case

Following the same line of arguments as that in Section V-A, we prove in Appendix B that $\bar{C}_{\text{fb}}^{\text{mem}}$ is an outer bound on the capacity region in the hidden case. Unfortunately, unlike the outer bound in the visible case, $\bar{C}_{\text{fb}}^{\text{mem}}$ is not computable. We establish outer and inner approximations to the outer bound $\bar{C}_{\text{fb}}^{\text{mem}}$ which have finite-letter characterizations and are therefore computable.

First note that the predicted erasure probabilities in each time slot t can be computed as

$$P_{\underline{Z}_{t+1} | \underline{Z}^t}(\underline{z}_{t+1} | \underline{z}^t) = \sum_{s \in \mathcal{S}} P_{S_{t+1} | \underline{Z}^t}(s | \underline{z}^t) P_{\underline{Z}_{t+1} | S_{t+1}}(\underline{z}_{t+1} | s). \quad (43)$$

The distribution $P_{\underline{Z}_{t+1} | S_{t+1}}$ does not change with t by assumption of time invariance. The distribution $P_{S_{t+1} | \underline{Z}^t}$ does change, however. A recursive formula to compute $P_{S_{t+1} | \underline{Z}^t}$ on-the-fly using the previously computed distribution $P_{S_t | \underline{Z}^{t-1}}$ and the new feedback sample \underline{z}_t is

$$\begin{aligned} P_{S_{t+1} | \underline{Z}^t}(s | \underline{z}^t) &= \frac{P_{S_{t+1} \underline{Z}_t | \underline{Z}^{t-1}}(s, \underline{z}_t | \underline{z}^{t-1})}{P_{\underline{Z}_t | \underline{Z}^{t-1}}(\underline{z}_t | \underline{z}^{t-1})} \\ &= \frac{\sum_{s' \in \mathcal{S}} P_{S_{t+1} | S_t}(s | s') P_{\underline{Z}_t | S_t}(\underline{z}_t | s') P_{S_t | \underline{Z}^{t-1}}(s' | \underline{z}^{t-1})}{\sum_{s' \in \mathcal{S}} P_{\underline{Z}_t | S_t}(\underline{z}_t | s') P_{S_t | \underline{Z}^{t-1}}(s' | \underline{z}^{t-1})}. \end{aligned} \quad (44)$$

Similarly, the distribution of the channel states based only on the past L feedback samples $P_{S_{t+1} | \underline{Z}_{t-L+1}^t}$ can be written as

$$P_{S_{t+1} | \underline{Z}_{t-L+1}^t}(s | \underline{z}_{t-L+1}^t) = \frac{\sum_{s' \in \mathcal{S}} P_{S_{t+1} | S_t}(s | s') P_{\underline{Z}_t | S_t}(\underline{z}_t | s') P_{S_t | \underline{Z}_{t-L+1}^{t-1}}(s' | \underline{z}_{t-L+1}^{t-1})}{\sum_{s' \in \mathcal{S}} P_{\underline{Z}_t | S_t}(\underline{z}_t | s') P_{S_t | \underline{Z}_{t-L+1}^{t-1}}(s' | \underline{z}_{t-L+1}^{t-1})}. \quad (45)$$

Note that (44) and (45) differ only in whether the distribution of S_t is based on all or only the past L samples. In practice these two distributions do not differ much for a sufficiently large choice of L , where L depends on the mixing time of the Markov chain. This is made precise by the following theorem [36, Theorem 2.1]:

Theorem 5 ([36, Theorem 2.1]). Suppose all entries of the state transition matrix $P_{S_t|S_{t-1}}$ and the distribution matrix $P_{Z_t|S_t}$ are strictly positive. For any observed sequence \underline{z}^t , we have the following bound on the variational distance:

$$\sum_{s \in \mathcal{S}} \left| P_{S_{t+1}|\underline{Z}^t}(s|\underline{z}^t) - P_{S_{t+1}|\underline{Z}_{t-L+1}^t}(s|\underline{z}_{t-L+1}^t) \right| \leq 2(1-\sigma)^L, \quad (46)$$

where $0 < \sigma < 1$ depends on the smallest entry in the matrix $P_{S_t|S_{t-1}}$ and on the ratio of the largest and smallest value in the matrix $P_{Z_t|S_t}$.

Remark 3. The theorem in its original form [36, Theorem 2.1] is more general and only requires the r -th order transition matrix $P_{S_t|S_{t-r}}$ to be strictly positive. We use the weaker form for simplicity.

Corollary 6. For any observed sequence \underline{z}^t , the total variation between $P_{Z_{t+1}|\underline{Z}^t}$ and $P_{Z_{t+1}|\underline{Z}_{t-L+1}^t}$ is bounded by

$$\sum_{\underline{z}_{t+1}} \left| P_{Z_{t+1}|\underline{Z}^t}(\underline{z}_{t+1}|\underline{z}^t) - P_{Z_{t+1}|\underline{Z}_{t-L+1}^t}(\underline{z}_{t+1}|\underline{z}_{t-L+1}^t) \right| \leq 2(1-\sigma)^L. \quad (47)$$

Proof: The proof is deferred to Appendix C. ■

From Corollary 6, we have for any \underline{z}_{t+1} :

$$\left| P_{Z_{t+1}|\underline{Z}^t}(\underline{z}_{t+1}|\underline{z}^t) - P_{Z_{t+1}|\underline{Z}_{t-L+1}^t}(\underline{z}_{t+1}|\underline{z}_{t-L+1}^t) \right| \leq 2(1-\sigma)^L. \quad (48)$$

In Appendix D, we prove an *outer approximation* on $\bar{C}_{\text{fb}}^{\text{mem}}$, for every integer L , as follows:

$$0 \leq x(\underline{z}^L) \leq 1, \quad 0 \leq y(\underline{z}^L) \leq 1 \quad \forall \underline{z}^L \in \{0, 1\}^{2L} \quad (49)$$

$$R_1 \leq \sum_{\underline{z}^L} P_{\underline{Z}^L}(\underline{z}^L)(1 - \epsilon_1(\underline{z}^L))x(\underline{z}^L) + 2(1-\sigma)^L \quad (50)$$

$$R_1 \leq \sum_{\underline{z}^L} P_{\underline{Z}^L}(\underline{z}^L)(1 - \epsilon_{12}(\underline{z}^L))(1 - y(\underline{z}^L)) + 2(1-\sigma)^L \quad (51)$$

$$R_2 \leq \sum_{\underline{z}^L} P_{\underline{Z}^L}(\underline{z}^L)(1 - \epsilon_2(\underline{z}^L))y(\underline{z}^L) + 2(1-\sigma)^L \quad (52)$$

$$R_2 \leq \sum_{\underline{z}^L} P_{\underline{Z}^L}(\underline{z}^L)(1 - \epsilon_{12}(\underline{z}^L))(1 - x(\underline{z}^L)) + 2(1-\sigma)^L. \quad (53)$$

Similarly, an *inner approximation* to the outer bound $\bar{C}_{\text{fb}}^{\text{mem}}$ is given by the following program.

$$0 \leq x(\underline{z}^L) \leq 1, \quad 0 \leq y(\underline{z}^L) \leq 1 \quad \forall \underline{z}^L \in \{0, 1\}^{2L} \quad (54)$$

$$R_1 \leq \sum_{\underline{z}^L} P_{\underline{Z}^L}(\underline{z}^L)(1 - \epsilon_1(\underline{z}^L))x(\underline{z}^L) - 2(1-\sigma)^L \quad (55)$$

$$R_1 \leq \sum_{\underline{z}^L} P_{\underline{Z}^L}(\underline{z}^L)(1 - \epsilon_{12}(\underline{z}^L))(1 - y(\underline{z}^L)) - 2(1-\sigma)^L \quad (56)$$

$$R_2 \leq \sum_{\underline{z}^L} P_{\underline{Z}^L}(\underline{z}^L)(1 - \epsilon_2(\underline{z}^L))y(\underline{z}^L) - 2(1-\sigma)^L \quad (57)$$

$$R_2 \leq \sum_{\underline{z}^L} P_{\underline{Z}^L}(\underline{z}^L)(1 - \epsilon_{12}(\underline{z}^L))(1 - x(\underline{z}^L)) - 2(1-\sigma)^L. \quad (58)$$

Define $\bar{C}_{\text{fb}}^{\text{mem}}(L)$ as the rate region specified by the inequalities

$$0 \leq x(\underline{z}^L) \leq 1, \quad 0 \leq y(\underline{z}^L) \leq 1 \quad \forall \underline{z}^L \in \{0, 1\}^{2L} \quad (59)$$

$$R_1 \leq \sum_{\underline{z}^L} P_{\underline{Z}^L}(\underline{z}^L)(1 - \epsilon_1(\underline{z}^L))x(\underline{z}^L) \quad (60)$$

$$R_1 \leq \sum_{\underline{z}^L} P_{\underline{Z}^L}(\underline{z}^L)(1 - \epsilon_{12}(\underline{z}^L))(1 - y(\underline{z}^L)) \quad (61)$$

$$R_2 \leq \sum_{\underline{z}^L} P_{\underline{Z}^L}(\underline{z}^L)(1 - \epsilon_2(\underline{z}^L))y(\underline{z}^L) \quad (62)$$

$$R_2 \leq \sum_{\underline{z}^L} P_{\underline{Z}^L}(\underline{z}^L)(1 - \epsilon_{12}(\underline{z}^L))(1 - x(\underline{z}^L)). \quad (63)$$

Clearly, $\bar{C}_{\text{fb}}^{\text{mem}}(L)$ is sandwiched between the outer and inner approximations of the outer bound. It thus coincides with the original outer bound $\bar{C}_{\text{fb}}^{\text{mem}}$ exponentially fast with L .

Remark 4. For many examples, the parameter σ in (47) is close to zero. Thus, L must be large (in the order of $L = 10000$) to give meaningful bounds. In numerical examples, we observed that the variational distance decays much faster than predicted by using σ . Often, the variational distance is on the order of 10^{-4} for values like $L = 10$.

VI. OPTIMAL CODING SCHEMES

In this section, we develop codes that achieve the outer bounds stated in Section IV. We show that $C_{\text{fb}+s}^{\text{mem}} = \bar{C}_{\text{fb}+s}^{\text{mem}}$ and $C_{\text{fb}}^{\text{mem}} = \bar{C}_{\text{fb}}^{\text{mem}}$. One of the coding operations that we use to achieve $C_{\text{fb}+s}^{\text{mem}}$ was first proposed in [27] based on a previous result on [15]. We believe that the alternative proof we derive here is conceptually simpler as it does not require knowledge about results and coding schemes in [15]. Our coding schemes build upon well-established results on virtual-queue-based algorithms such as [9], [10], [37]. To analyze the coding scheme, we track packets through a network of queues as explained next.

A. Queue Model

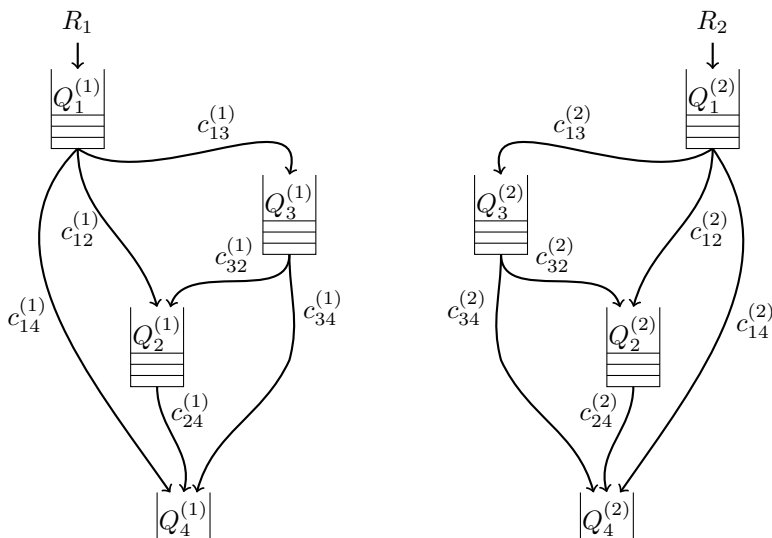


Fig. 3: Networked system of queues.

Consider Fig. 3 that shows a network of queues whose operation we now describe. The transmitter has two buffers $Q_1^{(1)}$, $Q_1^{(2)}$ to store packets destined for Rx_1 , Rx_2 , respectively. We consider dynamic arrivals, where packets for Rx_1 , Rx_2 arrive in each slot according to a Bernoulli process with probability R_1 , R_2 , respectively. These arrived packets are called *original packets*. An analysis for more general arrival processes is possible. The transmitter maintains two additional buffers $Q_2^{(1)}$ (resp. $Q_2^{(2)}$) for packets that have already been sent, but have been received only by Rx_2 (resp. Rx_1). Hence buffer $Q_2^{(1)}$ contains packets that are destined for Rx_1 and have been received at Rx_2 but not at Rx_1 , and vice versa for $Q_2^{(2)}$. These queues are empty before transmission begins. If both $Q_2^{(1)}$ and $Q_2^{(2)}$ are nonempty, the transmitter can send the XOR combination of these original packets. Such a linear combination of original packets from $Q_2^{(1)}$ and $Q_2^{(2)}$ is called a *coded packet*². If both users receive this coded packet, both can decode one desired original packet and two packets per slot are delivered. Since the coding that is used here is a reaction to previous erasure events, we refer to this coding operation as *reactive coding*³.

Another coding operation turns out to be useful: The transmitter can take one packet from $Q_1^{(1)}$ and $Q_1^{(2)}$ each, compute the XOR combination and send it. Note that the packets involved have not been transmitted before (hence have not been received at Rx_1 or Rx_2), so we call this action *proactive coding* or *poisoning*⁴. A poisoned packet is not immediately useful for a receiver upon reception. It may become useful together with a *remedy* packet that enables decoding of original packets that are

²The original packets arriving to $Q_1^{(j)}$ may be coded as well in the sense that error-correcting codes have been employed by lower layers. We use the term *coded packet* to emphasize that information packets for different receivers have been mixed. Alternative terms would be network-coded or inter-session-coded packet.

³The term *reactive coding* is also used in [27], but the meaning is different.

⁴We use this term because of its analogy to the poison-remedy approach in [38].

involved in the linear combination for the poisoned packet: Assume packet $p_l^{(1)}$ was chosen from $Q_1^{(1)}$ and $p_m^{(2)}$ was chosen from $Q_1^{(2)}$, and the poison packet $p_l^{(1)} + p_m^{(2)}$ was transmitted and received by Rx₁ or Rx₂ or both. In that case, $p_l^{(1)}$ is put into an additional queue $Q_3^{(1)}$, likewise $p_m^{(2)}$ is put into $Q_3^{(2)}$. Assume $p_l^{(1)} + p_m^{(2)}$ was received at Rx_j. If, at a later stage, the corresponding *remedy* $p_l^{(1)}$ (or $p_m^{(2)}$) is transmitted and received at Rx_j, both $p_l^{(1)}$ and $p_m^{(2)}$ can be decoded at Rx_j. An example why this can be beneficial is provided in Example 2 ahead.

The system exit for Rx_j is represented by the buffer $Q_4^{(j)}$. Once a packet reaches the intended receiver, it is moved to this queue and leaves the system. These buffers are empty by definition.

With slight abuse of notation, let $Q_{l,t}^{(j)}$ denote the number of packets stored in buffer $Q_l^{(j)}$ at time t . Obviously, $Q_{l,t}^{(j)} \in \mathbb{N}_0$. Define

$$\underline{Q}_t = (Q_{1,t}^{(1)}, Q_{2,t}^{(1)}, Q_{3,t}^{(1)}, Q_{1,t}^{(2)}, Q_{2,t}^{(2)}, Q_{3,t}^{(2)}) \in \mathbb{N}_0^6. \quad (64)$$

Because $Q_{4,t}^{(1)} = Q_{4,t}^{(2)} = 0$ by definition, the vector \underline{Q}_t determines the queue state at time t .

The transmitter selects an action A_t in slot t from the set $\mathcal{A}_5 = \{1, 2, 3, 4, 5\}$, where

- $A_t = 1$ corresponds to sending an uncoded original packet for Rx₁ from $Q_1^{(1)}$
- $A_t = 2$ corresponds to sending an uncoded original packet for Rx₂ from $Q_1^{(2)}$
- $A_t = 3$ corresponds to sending a coded packet from $Q_2^{(1)}$ and $Q_2^{(2)}$
- $A_t = 4$ corresponds to sending a poisoned packet from $Q_1^{(1)}$ and $Q_1^{(2)}$
- $A_t = 5$ corresponds to sending a remedy packet either from $Q_3^{(1)}$ or $Q_3^{(2)}$.

We will explain in detail how action $A_t = 5$ chooses remedy packets in Section VI-C.

Remark 5. An implementation of the described coding scheme could add a header to each packet. The header should include a flag of 3 bits to indicate which of the 5 actions was used. At most two packets will be combined, so one needs two fields of at most $\log_2(nR_1 + nR_2)$ bits each, to indicate which two out of the $nR_1 + nR_2$ packets were involved in the coding operation. The latter two field sizes grow with the block size n , but only logarithmically. For a typical internet protocol (IP) packet of $\ell = 1500 \cdot 8 = 12000$ bits, this overhead would be less than 1% for a block size n larger than 10^9 .

Remark 6. All buffers are physically present at the transmitter. The packets in $Q_2^{(j)}$ however also have to be stored in Rx_j's memory. Packets in $Q_3^{(j)}$ are involved in a poisoned packet. The corresponding poisoned packet is stored in the memory at Rx₁, Rx₂ or at both. In order to let both receivers correctly track the packet movement, each receiver needs feedback about the other receiver's packet erasures. To realize this we require a reliable low-rate forward channel from the transmitter to both receivers. This assumption facilitates the mathematical treatment of the problem.

One can also define a strategy that only uses *reactive* coding, where only the actions 0, 1, 2, 3 are permitted. The corresponding set of admissible actions is called \mathcal{A}_3 . In that case, the queues $Q_3^{(j)}$ are not needed and are always empty. These coding operations suffice to achieve capacity for memoryless channels.

A third possibility is to permit only uncoded packet transmissions, i.e. actions 0, 1, 2. The corresponding set of actions is called \mathcal{A}_2 . In that case, the queues $Q_2^{(j)}$ and $Q_3^{(j)}$ are always empty by definition.

For the visible case, actions at time t are restricted to depend on the *current* queue state \underline{Q}_t and the *previous* channel state S_{t-1} , i.e., the actions are generated by a distribution $P_{A_t|S_{t-1}\underline{Q}_t}$. We choose distributions that do not depend on t . For the hidden case, actions at time t may depend on the *current* queue state \underline{Q}_t and all *previous* ACK/NACK messages up to time t , \underline{Z}^{t-1} , i.e. the actions are generated by a distribution $P_{A_t|\underline{Z}^{t-1}\underline{Q}_t}$.

The following example from [27] demonstrates the necessity of *proactive* coding:

Example 2. Consider the Markov chain in Fig. 4 for $\delta = 0^5$, i.e. the state sequence is $\dots, s_1, s_2, s_1, s_2, \dots$. The stationary distribution is $\pi_{s_1} = \pi_{s_2} = 0.5$.

A packet is never erased when we arrive at state s_1 . In state s_2 , it is received only at Rx₁ or only at Rx₂, both with a chance of 50%. The setup is visible because the feedback determines the state. Consider a strategy with *reactive* coding only, to be introduced in detail in Section VII-A, with actions $A_t \in \mathcal{A}_3$ and corresponding rate region $\underline{\mathcal{C}}_{\text{fb}+s}^{\text{mem}}$. Action $A_t = 3$ is fully beneficial only if both Rx₁ and Rx₂ receive the coded packet, so it should be used only after state s_2 (when the next state is s_1 and no erasure will occur). After state s_1 , one can transmit packets for Rx₁ and packets for Rx₂ 50% of the time each. 50% of these packets are received by the intended receiver and leave the system. The other half is received by the wrong receiver and goes to the buffer for overheard packets, $Q_2^{(j)}$. The reactive coding action $A_t = 3$ can be used after state s_2 only at the pace the overhearing buffers $Q_2^{(1)}$ and $Q_2^{(2)}$ are filled: This will occur at a rate of $\pi_{s_1} P_{A_t|S_{t-1}}(1|s_1)(1 - \epsilon_1(s_1)) = 0.5 \cdot 0.5 \cdot 0.5 = \frac{1}{8}$ for Rx₁ and likewise for Rx₂. Hence $\pi_{s_2} P_{A_t|S_{t-1}}(3|s_2) \leq \frac{1}{8}$, leading to $P_{A_t|S_{t-1}}(3|s_2) = 0.25$. Reactive coding can be used only 25% of the time after s_2 , the remaining time must be distributed among actions 1 and 2, leading to a rate of $(R_1, R_2) = (\frac{7}{16}, \frac{7}{16})$.

⁵A periodic Markov chain is used here for illustration. In general, we consider only aperiodic chains. That would require $\delta > 0$.

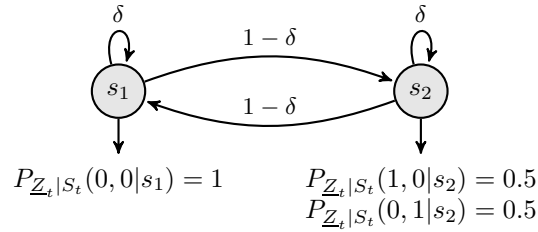


Fig. 4: Example from [27] explaining the usefulness of poisoning.

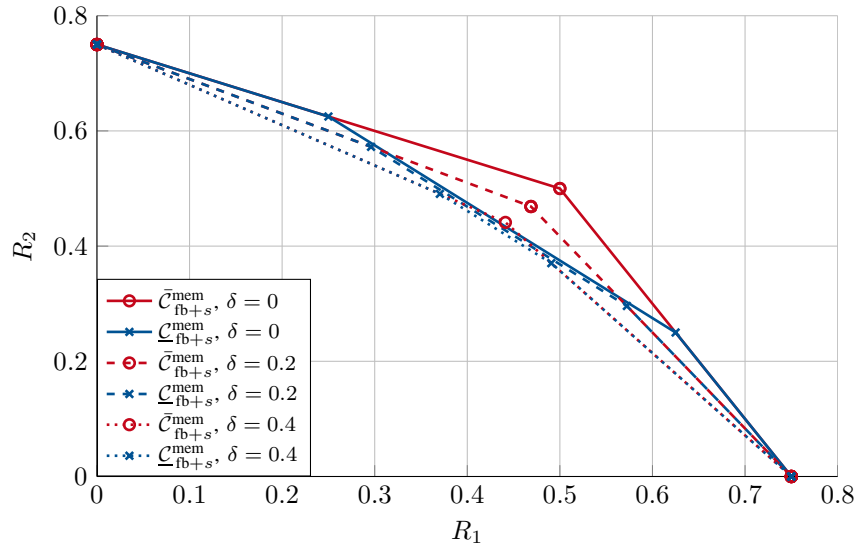


Fig. 5: Rate Regions for the model from Fig. 4, for $\delta = 0$, $\delta = 0.2$ and $\delta = 0.4$. The region $\underline{C}_{fb+s}^{\text{mem}}$ is strictly smaller than $\bar{C}_{fb+s}^{\text{mem}}$.

Now consider the poison-remedy approach, where one always sends a poisoned packet $p_l^{(1)} + p_m^{(2)}$ after state s_1 . This packet is received by either Rx₁ or Rx₂ as state s_2 always follows. Through the ACK/NACK feedback the transmitter is informed about where the poison is received. Assume it has been received at Rx₂: The transmitter now chooses $p_l^{(1)}$ as remedy packet. This packet will be received by both receivers because state s_1 will follow and packets are never erased. Rx₁ gets $p_l^{(1)}$ and Rx₂ can decode $p_m^{(2)}$ from the poison and remedy, hence one packet is transmitted for each user in two time slots, leading to a rate of $(R_1, R_2) = (\frac{1}{2}, \frac{1}{2})$. This rate point is outside of $\underline{C}_{fb}^{\text{mem}}$ and cannot be achieved using reactive coding only. The corresponding regions are plotted in Fig. 5. \square

B. Network Flow

The set of outgoing neighbors of buffer $Q_l^{(j)}$ is written \mathcal{O}_l , hence $m \in \mathcal{O}_l$ if there is a link between $Q_l^{(j)}$ and $Q_m^{(j)}$. Define the following three variables related to the link from buffer $Q_l^{(j)}$ to $Q_m^{(j)}$: Let $C_{lm,t}^{(j)}$ denote the *current link capacity*, i.e. the number of packets that *are allowed* to travel in time slot t . Clearly, $C_{lm,t}^{(j)}$ is in $\{0, 1\}$ and is a deterministic function of the action A_t and on the random erasure events \underline{Z}_t . The values of $C_{lm,t}^{(j)}$ are unknown to the transmitter before the transmission because of the erasures.

The *service rate* on the link in slot t is written as $F_{lm,t}^{(j)}$. $F_{lm,t}^{(j)}$ may be different from $C_{lm,t}^{(j)}$ because the transmitter may decide not to move the packet in the time slot. We write this as

$$F_{lm,t}^{(j)} = E_{lm,t}^{(j)} C_{lm,t}^{(j)}, \quad (65)$$

where $E_{lm,t}^{(j)} \in \{0, 1\}$ is a binary random variable indicating if the link will be activated or not, hence

$$F_{lm,t}^{(j)} \leq C_{lm,t}^{(j)}. \quad (66)$$

The vector \underline{E}_t collects all activator variables in slot t . $F_{lm,t}^{(j)}$ is a deterministic function of A_t , \underline{Z}_t and \underline{E}_t .

Remark 7. The link activation variables can be necessary to control the service rate of a particular link. The 5 actions A_t can control from which set of queues we transmit, but not on which of the outgoing links. The outgoing link is chosen by the erasure pattern and the activation variable lets us decide if we want to go over that link. With this mechanism the transmitter can control the outgoing link flows independently of each other.

The *actual* number of packets travelling on the link in time slot t is denoted $\tilde{F}_{lm,t}^{(j)}$. It can differ from $F_{lm,t}^{(j)}$ because buffer $Q_l^{(j)}$ can be empty:

$$\tilde{F}_{lm,t}^{(j)} = \mathbb{1} \left\{ Q_{l,t}^{(j)} > 0 \right\} E_{lm,t}^{(j)} C_{lm,t}^{(j)} = \mathbb{1} \left\{ Q_{l,t}^{(j)} > 0 \right\} F_{lm,t}^{(j)} \quad (67)$$

The long-term average link flow $f_{lm}^{(j)}$ and link capacity $c_{lm}^{(j)}$ from $Q_l^{(j)}$ to $Q_m^{(j)}$ are defined by

$$f_{lm}^{(j)} = \lim_{n \rightarrow \infty} \frac{1}{n} \sum_{t=1}^n F_{lm,t}^{(j)}, \quad c_{lm}^{(j)} = \lim_{n \rightarrow \infty} \frac{1}{n} \sum_{t=1}^n C_{lm,t}^{(j)} \quad (68)$$

where we assume that the limits exist.

To model external packets arrivals, let $C_{01,t}^{(j)} = F_{01,t}^{(j)}$ denote the indicator random variable if a packet arrived in queue $Q_1^{(j)}$ during time slot t . $C_{01,t}^{(j)}$ is independent of all other random variables in the system, and we have

$$\lim_{n \rightarrow \infty} \frac{1}{n} \sum_{t=1}^n C_{01,t}^{(j)} = \mathbb{E} \left[C_{01,t}^{(j)} \right] = R_j. \quad (69)$$

This definition of dynamic arrivals is slightly different than the block arrival of nR_j packets as in the outer bounds (see Remark 1).

The *flow divergence* [39, Chapter 1.1.2] at buffer $Q_l^{(j)}$ is defined as

$$D_{l,t}^{(j)} = \sum_m F_{lm,t}^{(j)} - \sum_k F_{kl,t}^{(j)}. \quad (70)$$

The flow divergence is thus the difference of the number of packets that can depart from buffer $Q_l^{(j)}$ minus the number of packets that can arrive at $Q_l^{(j)}$ in slot t . For the long-time average flow divergence, we have

$$d_l^{(j)} = \sum_m f_{lm}^{(j)} - \sum_k f_{kl}^{(j)}. \quad (71)$$

The number of packets in queue $Q_l^{(j)}$ evolve according to

$$\begin{aligned} Q_{l,t+1}^{(j)} &= Q_{l,t}^{(j)} - \sum_m \tilde{F}_{lm,t}^{(j)} + \sum_k \tilde{F}_{kl,t}^{(j)} \\ &\leq \left[Q_{l,t}^{(j)} - \sum_m F_{lm,t}^{(j)} \right]^+ + \sum_k F_{kl,t}^{(j)} \end{aligned} \quad (72)$$

where $[x]^+ = \max(x, 0)$. There is an inequality rather than an equality because some queue $Q_k^{(j)}$ might be empty, and $\tilde{F}_{kl,t}^{(j)} \leq F_{kl,t}^{(j)}$.

Each coding scheme leads to a different evolution of the queue state Q_t , as the actions at time t can differ.

The *Rate-Stability* Theorem [31, Theorem 2] states that a queue $Q_{l,t}^{(j)}$ evolving according to (72) is rate-stable if the average arrival rate $\sum_k f_{kl}^{(j)}$ is not larger than the average departure rate $\sum_m f_{lm}^{(j)}$,

$$\sum_k f_{kl}^{(j)} \leq \sum_m f_{lm}^{(j)}, \quad (73)$$

$$\text{hence if } d_l^{(j)} \geq 0. \quad (74)$$

Therefore, satisfying the long-term average capacity constraints is sufficient to ensure rate-stability.

C. Packet Movement

In this section we summarize when packets can leave buffers and move to another one.

First consider cases where uncoded packets are transmitted, i.e. for actions $A_t = 1$ or $A_t = 2$: If an uncoded packet from $Q_1^{(1)}$ is transmitted and received by Rx₁, it is moved to $Q_4^{(1)}$ and leaves the system. If such a packet is only received at Rx₂, it is moved to $Q_2^{(1)}$. If it is erased everywhere, it stays in buffer $Q_1^{(1)}$. Likewise for packets for Rx₂.

poison $p_l^{(1)} + p_m^{(2)}$ received at	remedy	remedy received at Rx ₁	remedy received at Rx ₂	remedy rec. at Rx ₁ and Rx ₂
Rx ₁ only	$p_m^{(2)}$	Rx ₁ decodes both $p_l^{(1)}$ and $p_m^{(2)}$ ⇒ $p_l^{(1)}$ to $Q_4^{(1)}$ (exit) ⇒ $p_m^{(2)}$ to $Q_2^{(2)}$	Rx ₂ gets $p_m^{(2)}$ ⇒ $p_m^{(2)}$ to $Q_4^{(2)}$ (exit) ⇒ Replace $p_l^{(1)}$ with remedy $p_m^{(2)}$ and move to $Q_2^{(1)}$	both Rx ₁ and Rx ₂ decode both $p_l^{(1)}$ and $p_m^{(2)}$ ⇒ $p_l^{(1)}$ to $Q_4^{(1)}$ (exit) ⇒ $p_m^{(2)}$ to $Q_4^{(2)}$ (exit)
Rx ₂ only	$p_l^{(1)}$	Rx ₁ gets $p_l^{(1)}$ ⇒ $p_l^{(1)}$ to $Q_4^{(1)}$ (exit) ⇒ Replace $p_m^{(2)}$ with remedy $p_l^{(1)}$ and move to $Q_2^{(2)}$	Rx ₂ decodes both $p_l^{(1)}$ and $p_m^{(2)}$ ⇒ $p_m^{(2)}$ to $Q_4^{(2)}$ (exit) ⇒ $p_l^{(1)}$ to $Q_2^{(1)}$	both Rx ₁ and Rx ₂ decode both $p_l^{(1)}$ and $p_m^{(2)}$ ⇒ $p_l^{(1)}$ to $Q_4^{(1)}$ (exit) ⇒ $p_m^{(2)}$ to $Q_4^{(2)}$ (exit)
Rx ₁ and Rx ₂	$p_l^{(1)}$	Rx ₁ decodes both $p_l^{(1)}$ and $p_m^{(2)}$ ⇒ $p_l^{(1)}$ to $Q_4^{(1)}$ (exit) ⇒ $p_m^{(2)}$ to $Q_2^{(2)}$	Rx ₂ decodes both $p_l^{(1)}$ and $p_m^{(2)}$ ⇒ $p_m^{(2)}$ to $Q_4^{(2)}$ (exit) ⇒ $p_l^{(1)}$ to $Q_2^{(1)}$	both Rx ₁ and Rx ₂ decode both $p_l^{(1)}$ and $p_m^{(2)}$ ⇒ $p_l^{(1)}$ to $Q_4^{(1)}$ (exit) ⇒ $p_m^{(2)}$ to $Q_4^{(2)}$ (exit)
Resulting capacity:		$C_{34}^{(1)} = 1, C_{32}^{(2)} = 1$	$C_{32}^{(1)} = 1, C_{34}^{(2)} = 1$	$C_{34}^{(1)} = 1, C_{34}^{(2)} = 1$

TABLE I: Packet movement for poisoned packets in $Q_3^{(1)}$ and $Q_3^{(2)}$.

t	A_t	X_t	$Y_{1,t}$	$Y_{2,t}$
1	4	$p_l^{(1)} + p_m^{(2)}$	$p_l^{(1)} + p_m^{(2)}$?
2	5	$p_m^{(2)}$?	$p_m^{(2)}$
3	2	$p_k^{(2)}$	$p_k^{(2)}$?
4	3	$p_m^{(2)} + p_k^{(2)}$	$p_m^{(2)} + p_k^{(2)}$	$p_m^{(2)} + p_k^{(2)}$

TABLE II: Coding example.

For a reactive coding operation, i.e. for $A_t = 3$, suppose $p_l^{(1)} \in Q_2^{(1)}$ and $p_m^{(2)} \in Q_2^{(2)}$. The coded packet $p_l^{(1)} + p_m^{(2)}$ is computed and transmitted. If this packet is received by Rx₁, $p_l^{(1)}$ can be decoded, so it is moved from $Q_2^{(1)}$ to the system exit $Q_4^{(1)}$. If the coded packet is not received by Rx₂, $p_m^{(2)}$ stays in $Q_2^{(2)}$. This also applies vice versa.

In a degenerate case $A_t = 3$ is chosen but either $Q_2^{(1)}$ or $Q_2^{(2)}$ is empty: In this case, only one packet can be delivered per slot, but the queue dynamics as defined in (72) are satisfied for each of the two queue networks individually (see also [40]).

The most complicated packet movement rules apply for the poison/remedy actions and the corresponding buffers: A packet can move from $Q_1^{(j)}$ to $Q_3^{(j)}$ only if it is involved in a poisoned packet. This happens if $A_t = 4$ and the poisoned packet is not erased at both receivers: Suppose $p_l^{(1)} \in Q_1^{(1)}$ and $p_m^{(2)} \in Q_1^{(2)}$ and the poisoned packet $p_l^{(1)} + p_m^{(2)}$ is received at Rx₁, at Rx₂ or at both. Then $p_l^{(1)}$ moves to $Q_3^{(1)}$ and $p_m^{(2)}$ moves to $Q_3^{(2)}$.

A packet can leave $Q_3^{(j)}$ only if a remedy packet was transmitted, i.e. if $A_t = 5$. A remedy packet is always one of the packets that was involved in a proactively coded packet and is stored in either $Q_3^{(1)}$ or $Q_3^{(2)}$. The exact rules describing which packet acts as remedy and how packets leave buffer $Q_3^{(j)}$ are given in Table I. This table appears in similar form in [27].

We explain the following two cases in more detail:

- Assume poison $p_l^{(1)} + p_m^{(2)}$ was received at Rx₁ only and remedy $p_m^{(2)}$ was again received at Rx₁ only: Rx₁ can decode both poisoned packets and hence also knows $p_m^{(2)}$, as if this packet was overheard. So $p_m^{(2)}$ should be moved from $Q_3^{(2)}$ to the buffer for overheard packets, $Q_2^{(2)}$.
- Assume poison $p_l^{(1)} + p_m^{(2)}$ was received at Rx₁ only and remedy $p_m^{(2)}$ was received at Rx₂ only: Obviously, Rx₂ now knows the desired packet $p_m^{(2)}$. The question is if $p_l^{(1)} + p_m^{(2)}$ is of any use for Rx₁: The key observation made in [27] is that $p_m^{(2)}$ is as useful for Rx₁ as the actually desired packet $p_l^{(1)}$: If Rx₁ obtains $p_m^{(2)}$, it can decode $p_l^{(1)}$. So, in order to deliver $p_l^{(1)}$ to Rx₁, we can also deliver $p_m^{(2)}$. The packet $p_m^{(2)}$ however is already known by Rx₂, so it acts like packets that are in buffer $Q_2^{(1)}$. Hence one can replace $p_l^{(1)}$ with the remedy $p_m^{(2)}$ (because $p_m^{(2)}$ is as useful as $p_l^{(1)}$) and put it in buffer $Q_2^{(1)}$.

At a later stage $p_m^{(2)}$ will be XORed with a packet $p_k^{(2)}$ from $Q_2^{(2)}$ (i.e. a packet that has already been received at Rx₁ but not at Rx₂). If Rx₁ receives the linear combination $p_m^{(2)} + p_k^{(2)}$, it can decode $p_m^{(2)}$ because $p_k^{(2)}$ is known. With $p_m^{(2)}$, it can decode the desired packet $p_l^{(1)}$. This is again summarized and visualized in the coding example in Table II.

Taking into account all events described above, we obtain

$$C_{12,t}^{(j)} = \mathbb{1}\{A_t = j\} Z_{j,t} (1 - Z_{\bar{j},t}), \quad F_{12,t}^{(j)} = C_{12,t}^{(j)} E_{12,t}^{(j)}, \quad \tilde{F}_{12,t}^{(j)} = F_{12,t}^{(j)} \mathbb{1}\{Q_{1,t}^{(j)} > 0\} \quad (75)$$

$$C_{13,t}^{(j)} = \mathbb{1}\{A_t = 4\} (1 - Z_{1,t} Z_{2,t}), \quad F_{13,t}^{(j)} = C_{13,t}^{(j)} E_{13,t}^{(j)}, \quad \tilde{F}_{13,t}^{(j)} = F_{13,t}^{(j)} \mathbb{1}\{Q_{1,t}^{(j)} > 0\} \quad (76)$$

$$C_{14,t}^{(j)} = \mathbb{1}\{A_t = j\} (1 - Z_{j,t}), \quad F_{14,t}^{(j)} = C_{14,t}^{(j)} E_{14,t}^{(j)}, \quad \tilde{F}_{14,t}^{(j)} = F_{14,t}^{(j)} \mathbb{1}\{Q_{1,t}^{(j)} > 0\} \quad (77)$$

$$C_{24,t}^{(j)} = \mathbb{1}\{A_t = 3\}(1 - Z_{j,t}), \quad F_{24,t}^{(j)} = C_{24,t}^{(j)} E_{24,t}^{(j)}, \quad \tilde{F}_{24,t}^{(j)} = F_{24,t}^{(j)} \mathbb{1}\{Q_{2,t}^{(j)} > 0\} \quad (78)$$

$$C_{32,t}^{(j)} = \mathbb{1}\{A_t = 5\} Z_{j,t} (1 - Z_{\bar{j},t}), \quad F_{32,t}^{(j)} = C_{32,t}^{(j)} E_{32,t}^{(j)}, \quad \tilde{F}_{32,t}^{(j)} = F_{32,t}^{(j)} \mathbb{1}\{Q_{3,t}^{(j)} > 0\} \quad (79)$$

$$C_{34,t}^{(j)} = \mathbb{1}\{A_t = 5\}(1 - Z_{j,t}), \quad F_{34,t}^{(j)} = C_{34,t}^{(j)} E_{34,t}^{(j)}, \quad \tilde{F}_{34,t}^{(j)} = F_{34,t}^{(j)} \mathbb{1}\{Q_{3,t}^{(j)} > 0\}. \quad (80)$$

Remark 8. The packet movement for reactive coding ($A_t = 4$ and $A_t = 5$) in Table I only considers the non-degenerate case, where $Q_1^{(1)}$ and $Q_1^{(2)}$ are nonempty when $A_t = 4$. The degenerate case when this is not fulfilled is more complicated and studied in detail in Appendix E. However, also the degenerate case can be adapted such that the queue and flow dynamics in (72) and (75) - (80) hold. This allows to use the well-established tools of max-weight backpressure scheduling [41] in Section VI-E, rather than the tools of stochastic programming networks that are used in [27].

The algorithms developed in the following ensure network stability for rate pairs inside $\bar{C}_{\text{fb}}^{\text{mem}}$, which shows that $\bar{C}_{\text{fb}}^{\text{mem}}$ is the capacity region.

D. Probabilistic Scheme

1) *Visible Case:* Consider a strategy that bases decisions for actions only on the previous channel state S_{t-1} , but not on the queue state Q_t . These strategies are called S-only algorithms in [26]. The decisions for A_t are random and independent from previous decisions, according to a stationary probability distribution $P_{A_t|S_{t-1}}$. By the sufficient criterion for rate-stability in (73), rate pairs (R_1, R_2) can be achieved if there is a distribution $P_{A_t|S_{t-1}}$ such that the following flow optimization problem is feasible:

$$R_j \leq f_{12}^{(j)} + f_{13}^{(j)} + f_{14}^{(j)} \quad (81)$$

$$f_{12}^{(j)} + f_{32}^{(j)} \leq f_{24}^{(j)} \quad (82)$$

$$f_{13}^{(j)} \leq f_{32}^{(j)} + f_{34}^{(j)} \quad (83)$$

$$f_{12}^{(j)} \leq c_{12}^{(j)} = \sum_{s \in \mathcal{S}} \pi_s (\epsilon_j(s) - \epsilon_{12}(s)) P_{A_t|S_{t-1}}(j|s) \quad (84)$$

$$f_{13}^{(j)} \leq c_{13}^{(j)} = \sum_{s \in \mathcal{S}} \pi_s (1 - \epsilon_{12}(s)) P_{A_t|S_{t-1}}(4|s) \quad (85)$$

$$f_{14}^{(j)} \leq c_{14}^{(j)} = \sum_{s \in \mathcal{S}} \pi_s (1 - \epsilon_j(s)) P_{A_t|S_{t-1}}(j|s) \quad (86)$$

$$f_{24}^{(j)} \leq c_{24}^{(j)} = \sum_{s \in \mathcal{S}} \pi_s (1 - \epsilon_j(s)) P_{A_t|S_{t-1}}(3|s) \quad (87)$$

$$f_{32}^{(j)} \leq c_{32}^{(j)} = \sum_{s \in \mathcal{S}} \pi_s (\epsilon_j(s) - \epsilon_{12}(s)) P_{A_t|S_{t-1}}(5|s) \quad (88)$$

$$f_{34}^{(j)} \leq c_{34}^{(j)} = \sum_{s \in \mathcal{S}} \pi_s (1 - \epsilon_j(s)) P_{A_t|S_{t-1}}(5|s) \quad \forall j \in \{1, 2\} \quad (89)$$

The link capacities can be written as in (84) - (89) because of the ergodicity of the influencing random processes A^n and \underline{Z}^n in this case. This is a classic flow optimization problem where the individual link capacities on the RHS of (84) - (89) can be adjusted by $P_{A_t|S_{t-1}}$. Note that the disconnected flow networks for R_{x_1} and R_{x_2} are coupled only through the common dependency on $P_{A_t|S_{t-1}}$. For any feasible rate pair, (81) - (83) ensure that $d_i^{(j)} \geq 0$ for every queue $Q_i^{(j)}$. The exact operation of the probabilistic scheme is as follows:

- Solve the above linear program to find suitable values of $P_{A_t|S_{t-1}}$, $c_{lm}^{(j)}$ and $f_{lm}^{(j)}$.
- In each time slot, observe the previous state s , sample the next action randomly from $P_{A_t|S_{t-1}}(\cdot|s)$ and transmit from the corresponding queues.
- Observe the erasure pattern \underline{Z}_t : \underline{Z}_t selects at most one outgoing link from each queue on which a packet can be moved.
- Move packets from queue $Q_l^{(j)}$ to $Q_m^{(j)}$ with probability $\frac{f_{lm}^{(j)}}{c_{lm}^{(j)}}$, i.e. set $E_{lm,t}^{(j)} = 1$ with probability $\frac{f_{lm}^{(j)}}{c_{lm}^{(j)}}$.
- Send the information about moved packets over the low-rate reliable forward link.

The strategy of first observing where a transmitted packet is received and deciding later whether this packet should be logically moved or not appears in similar form in [37]. This mechanism allows to asymptotically achieve a rate of $f_{lm}^{(j)}$ on each link, independent of the other other link flow values $f_{lk}^{(j)}$ departing from the same queue.

By the min-cut max-flow theorem, the flow problem in (81) - (89) is feasible if there is a distribution $P_{A_t|S_{t-1}}$ such that

$$\begin{aligned} R_j &\leq c_{12}^{(j)} + c_{13}^{(j)} + c_{14}^{(j)} \\ &= \sum_{s \in \mathcal{S}} \pi_s (1 - \epsilon_{12}(s)) [P_{A_t|S_{t-1}}(j|s) + P_{A_t|S_{t-1}}(4|s)] \end{aligned} \quad (90)$$

$$\begin{aligned}
R_j &\leq c_{13}^{(j)} + c_{14}^{(j)} + c_{24}^{(j)} \\
&= \sum_{s \in \mathcal{S}} \pi_s \left[(1 - \epsilon_{12}(s)) P_{A_t|S_{t-1}}(4|s) + (1 - \epsilon_j(s)) [P_{A_t|S_{t-1}}(j|s) + P_{A_t|S_{t-1}}(3|s)] \right] \tag{91}
\end{aligned}$$

$$\begin{aligned}
R_j &\leq c_{12}^{(j)} + c_{14}^{(j)} + c_{32}^{(j)} + c_{34}^{(j)} \\
&= \sum_{s \in \mathcal{S}} \pi_s (1 - \epsilon_{12}(s)) [P_{A_t|S_{t-1}}(j|s) + P_{A_t|S_{t-1}}(5|s)] \tag{92}
\end{aligned}$$

$$\begin{aligned}
R_j &\leq c_{14}^{(j)} + c_{24}^{(j)} + c_{34}^{(j)} \\
&= \sum_{s \in \mathcal{S}} \pi_s (1 - \epsilon_j(s)) [P_{A_t|S_{t-1}}(j|s) + P_{A_t|S_{t-1}}(3|s) + P_{A_t|S_{t-1}}(5|s)] \quad \forall j \in \{1, 2\} \tag{93}
\end{aligned}$$

where (90) corresponds to the cut around the buffer $Q_1^{(j)}$, (91) corresponds to the cut around the buffers $Q_1^{(j)}$ and $Q_2^{(j)}$, (92) corresponds to the cut around the buffers $Q_1^{(j)}$ and $Q_3^{(j)}$ and (93) corresponds to the cut around the buffers $Q_1^{(j)}$, $Q_2^{(j)}$ and $Q_3^{(j)}$.

Proposition 7. Suppose $P_{A_t|S_{t-1}}$ is feasible for a rate pair (R_1, R_2) . There exists a distribution $P_{A_t|S_{t-1}}^*$ for which

- (R_1, R_2) is feasible and
- the bounds in (91) and (92) are redundant.

The proof of Proposition 7 is given in Appendix F.

Hence, a rate pair (R_1, R_2) can be achieved if there is a distribution $P_{A_t|S_{t-1}}$ such that

$$R_1 \leq \sum_{s \in \mathcal{S}} \pi_s (1 - \epsilon_1(s)) [P_{A_t|S_{t-1}}(1|s) + P_{A_t|S_{t-1}}(3|s) + P_{A_t|S_{t-1}}(5|s)] \tag{94}$$

$$R_1 \leq \sum_{s \in \mathcal{S}} \pi_s (1 - \epsilon_{12}(s)) [P_{A_t|S_{t-1}}(1|s) + P_{A_t|S_{t-1}}(4|s)] \tag{95}$$

$$R_2 \leq \sum_{s \in \mathcal{S}} \pi_s (1 - \epsilon_2(s)) [P_{A_t|S_{t-1}}(2|s) + P_{A_t|S_{t-1}}(3|s) + P_{A_t|S_{t-1}}(5|s)] \tag{96}$$

$$R_2 \leq \sum_{s \in \mathcal{S}} \pi_s (1 - \epsilon_{12}(s)) [P_{A_t|S_{t-1}}(2|s) + P_{A_t|S_{t-1}}(4|s)]. \tag{97}$$

One can verify that (94) - (97) is equivalent to the outer bound $\bar{C}_{\text{fb}+s}^{\text{mem}}$ in (9) - (13) by setting

$$P_{A_t|S_{t-1}}(1|s) + P_{A_t|S_{t-1}}(3|s) + P_{A_t|S_{t-1}}(5|s) = x_s \tag{98}$$

$$P_{A_t|S_{t-1}}(2|s) + P_{A_t|S_{t-1}}(3|s) + P_{A_t|S_{t-1}}(5|s) = y_s. \tag{99}$$

Note that $x_s + y_s = P_{A_t|S_{t-1}}(1|s) + P_{A_t|S_{t-1}}(2|s) + 2P_{A_t|S_{t-1}}(3|s) + 2P_{A_t|S_{t-1}}(5|s)$ can be less than 1, so constraint (16) is not implicitly required.

Remark 9. The mapping from x_s, y_s $s \in \mathcal{S}$ to $P_{A_t|S_{t-1}}$ defined in (98) - (99) is not unique. In particular, for some valid choices of $P_{A_t|S_{t-1}}$ the constraints in (91) and (92) will *not* be redundant. Proposition 7 however tells us that one can always find a distribution $P_{A_t|S_{t-1}}^*$

- that satisfies (98) - (99) and
- for which (91) and (92) are redundant,

for any values of x_s, y_s $s \in \mathcal{S}$.

This shows that $\bar{C}_{\text{fb}}^{\text{mem}}$ is achievable with the presented coding scheme and hence $\bar{C}_{\text{fb}+s}^{\text{mem}} = C_{\text{fb}+s}^{\text{mem}}$. In Section VI-E, we furthermore show that $C_{\text{fb}+s}^{\text{mem}}$ is achievable using a deterministic algorithm.

2) *Hidden Case:* With the relation between probabilities of actions and parameters x_s and y_s developed for the visible case, we argue that the probabilistic scheme can, in principle, achieve the outer bound for the hidden case as well. For a given rate pair (R_1, R_2) , one must determine a sequence of probability distributions $P_{A_t|\underline{Z}^{t-1}}$, $t = 1, \dots, n$ for the probabilistic scheme with 5 actions. Any value of $x(\underline{z}^{t-1}), y(\underline{z}^{t-1})$ in the outer bound (21) - (25) can be translated into appropriate probability values for $P_{A_t|\underline{Z}^{t-1}}$, as in (98) and (99). Given a certain observed feedback sequence \underline{z}^{t-1} , the transmitter randomly chooses its next action according to the distribution $P_{A_t|\underline{Z}^{t-1}}(\cdot|\underline{z}^{t-1})$.

Similarly, the transmitter can base its actions only on the L past feedback samples $\underline{z}_{t-L}^{t-1}$ according to a stationary distribution $P_{A_t|\underline{Z}_{t-L}^{t-1}}$ and achieve $\bar{C}_{\text{fb}}^{\text{mem}}(L)$ defined in (59) - (63).

According to Corollary 6, the region $\bar{C}_{\text{fb}}^{\text{mem}}(L)$ converges exponentially fast to $\bar{C}_{\text{fb}}^{\text{mem}}$, but also the number of parameters $x(\underline{z}^L), y(\underline{z}^L)$ grows exponentially with L .

We next propose a deterministic scheme that is optimal in the long-run.

A_t	Weight depending on \underline{Q}_t and $S_{t-1} = s$
1	$[1 - \epsilon_1(s)]Q_{1,t}^{(1)} + \epsilon_{12}(s) [Q_{1,t}^{(1)} - Q_{2,t}^{(1)}]^+$
2	$[1 - \epsilon_2(s)]Q_{1,t}^{(2)} + \epsilon_{12}(s) [Q_{1,t}^{(2)} - Q_{2,t}^{(2)}]^+$
3	$[1 - \epsilon_1(s)]Q_{2,t}^{(1)} + [1 - \epsilon_2(s)]Q_{2,t}^{(2)}$
4	$[1 - \epsilon_{12}(s)] \left([Q_{1,t}^{(1)} - Q_{3,t}^{(1)}]^+ + [Q_{1,t}^{(2)} - Q_{3,t}^{(2)}]^+ \right)$
5	$\epsilon_{12}(s) [Q_{3,t}^{(1)} - Q_{2,t}^{(1)}]^+ + [1 - \epsilon_1(s)]Q_{3,t}^{(1)} + \epsilon_{12}(s) [Q_{3,t}^{(2)} - Q_{2,t}^{(2)}]^+ + [1 - \epsilon_2(s)]Q_{3,t}^{(2)}$

TABLE III: Deterministic scheme for the visible case and $A_t \in \mathcal{A}_5$.

A_t	Weight depending on \underline{Q}_t and $\underline{Z}^{t-1} = \underline{z}^{t-1}$
1	$[1 - \epsilon_1(\underline{z}^{t-1})]Q_{1,t}^{(1)} + \epsilon_{12}(\underline{z}^{t-1}) [Q_{1,t}^{(1)} - Q_{2,t}^{(1)}]^+$
2	$[1 - \epsilon_2(\underline{z}^{t-1})]Q_{1,t}^{(2)} + \epsilon_{12}(\underline{z}^{t-1}) [Q_{1,t}^{(2)} - Q_{2,t}^{(2)}]^+$
3	$[1 - \epsilon_1(\underline{z}^{t-1})]Q_{2,t}^{(1)} + [1 - \epsilon_2(\underline{z}^{t-1})]Q_{2,t}^{(2)}$
4	$[1 - \epsilon_{12}(\underline{z}^{t-1})] \left([Q_{1,t}^{(1)} - Q_{3,t}^{(1)}]^+ + [Q_{1,t}^{(2)} - Q_{3,t}^{(2)}]^+ \right)$
5	$\epsilon_{12}(\underline{z}^{t-1}) [Q_{3,t}^{(1)} - Q_{2,t}^{(1)}]^+ + [1 - \epsilon_1(\underline{z}^{t-1})]Q_{3,t}^{(1)} + \epsilon_{12}(\underline{z}^{t-1}) [Q_{3,t}^{(2)} - Q_{2,t}^{(2)}]^+ + [1 - \epsilon_2(\underline{z}^{t-1})]Q_{3,t}^{(2)}$

TABLE IV: Deterministic scheme for the hidden case and $A_t \in \mathcal{A}_5$.

E. Deterministic Scheme

1) *Visible Case:* In the probabilistic scheme, actions are chosen depending on the channel state only. So it might happen that an action is chosen although there is no packet to transmit because the corresponding buffer is empty. To operate the probabilistic scheme one also needs to compute the corresponding distribution $P_{A_t|S_{t-1}}$ that depends on the arrival rates R_1, R_2 . These rates might be unknown to the transmitter ahead of time.

Both drawbacks can be avoided by a max-weight backpressure-like algorithm [41], [42], [43], [32], [26] that bases its actions on both queue and channel states: In each slot t , a weight function is computed for each action. The action with the highest weight is chosen in that slot. In Appendix G-A, we show that the optimal action is

$$A_t = \operatorname{argmax}_{A_t \in \mathcal{A}_5} \sum_{j=1}^2 \sum_{l=1}^3 \sum_{m \in \mathcal{O}_l} [Q_{l,t}^{(j)} - Q_{m,t}^{(j)}]^+ \mathbb{E} \left[C_{lm,t}^{(j)} \middle| \underline{Q}_t = \underline{q}, S_{t-1} = s \right]. \quad (100)$$

Table III lists the weights for each action depending on the current queue state \underline{Q}_t and the previous channel state $S_{t-1} = s$. The dependency of the flow divergence on A_t is based on (70) and (75) - (80).

Theorem 8. The max-weight strategy in Table III strongly stabilizes all queues in the network for every rate pair $(R_1 + \delta, R_2 + \delta) \in \bar{\mathcal{C}}_{\text{fb}+s}^{\text{mem}}$, $\delta > 0$.

The proof is given in Appendix G-A. The proof uses a finite-horizon Lyapunov drift analysis similar to [26], but the analysis must be adapted to account for the previous channel states only instead of the current one. In the model of [44], the authors deal with correlated channels but have the *current* channel state (or an estimate of it) available for the current decision. Similarly, in [43], [45] the current channel state is available at the transmitter. In [46], [47] the authors focus on obtaining channel state information in a scenario that is related to the case of hidden states, however without permitting coding operations. Similarly, [48] investigates the case of delayed channel state information for general networks, without permitting coding operations.

2) *Hidden Case:* Similar to the visible case, the following deterministic max-weight backpressure-like algorithm can be defined. The action is now given by

$$A_t = \operatorname{argmax}_{A_t \in \mathcal{A}_5} \sum_{j=1}^2 \sum_{l=1}^3 \sum_{m \in \mathcal{O}_l} [Q_{l,t}^{(j)} - Q_{m,t}^{(j)}]^+ \mathbb{E} \left[C_{lm,t}^{(j)} \middle| \underline{Q}_t = \underline{q}, \underline{Z}^{t-1} = \underline{z}^{t-1} \right]. \quad (101)$$

Table IV lists the weights for each action depending on the current queue state \underline{Q}_t and the previous feedback state \underline{Z}^{t-1} .

Remark 10. Note that the values of $\epsilon_1(\underline{z}^{t-1})$, $\epsilon_2(\underline{z}^{t-1})$ and $\epsilon_{12}(\underline{z}^{t-1})$ can be recursively computed by (43) and (44) for every t .

Theorem 9. The max-weight strategy in Table IV strongly stabilizes all queues in the network for every rate pair $(R_1 + \delta, R_2 + \delta) \in \bar{\mathcal{C}}_{\text{fb}}^{\text{mem}}$, $\delta > 0$.

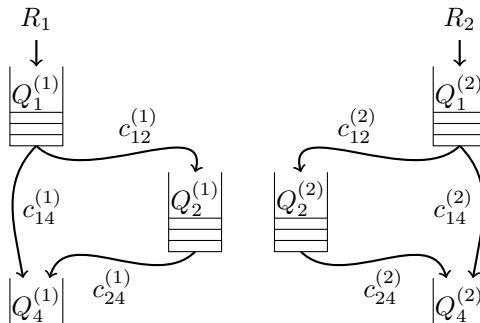
The proof of Theorem 9 is given in Appendix G-B.

A_t	Weight depending on \underline{Q}_t and $S_{t-1} = s$
1	$[1 - \epsilon_1(s)]Q_{1,t}^{(1)} + \epsilon_{12}(s) [Q_{1,t}^{(1)} - Q_{2,t}^{(1)}]^+$
2	$[1 - \epsilon_2(s)]Q_{1,t}^{(2)} + \epsilon_{12}(s) [Q_{1,t}^{(2)} - Q_{2,t}^{(2)}]^+$
3	$[1 - \epsilon_1(s)]Q_{2,t}^{(1)} + [1 - \epsilon_2(s)]Q_{2,t}^{(2)}$

TABLE V: Deterministic scheme with $A_t \in \mathcal{A}_3$.

VII. ACHIEVABLE RATES WITH REACTIVE CODING

In this section, we investigate the performance of schemes that are reactive; i.e., we are restricted to the set of actions \mathcal{A}_3 . The simplified queueing network is shown in Fig. 6. Our focus is on the visible case. All methods can similarly be applied to the hidden case.

Fig. 6: Networked system of queues for reactive coding, $A_t \in \mathcal{A}_3$.

A. Schemes with Infinite-Size Coding Buffers

1) *Probabilistic Scheme*: This scheme adapts the probabilistic scheme in Section VI-D to the action set \mathcal{A}_3 . Using this scheme, the rate tuple (R_1, R_2) can be achieved if there is a distribution $P_{A_t|S_{t-1}}$ on \mathcal{A}_3 such that $\forall j \in \{1, 2\}$:

$$R_j \leq f_{14}^{(j)} + f_{12}^{(j)} \quad (102)$$

$$f_{12}^{(j)} \leq f_{24}^{(j)} \quad (103)$$

$$f_{12}^{(j)} \leq c_{12}^{(j)} = \sum_{s \in \mathcal{S}} \pi_s P_{A_t|S_{t-1}}(j|s) (\epsilon_j(s) - \epsilon_{12}(s)) \quad (104)$$

$$f_{14}^{(j)} \leq c_{14}^{(j)} = \sum_{s \in \mathcal{S}} \pi_s P_{A_t|S_{t-1}}(j|s) (1 - \epsilon_j(s)) \quad (105)$$

$$f_{24}^{(j)} \leq c_{24}^{(j)} = \sum_{s \in \mathcal{S}} \pi_s P_{A_t|S_{t-1}}(3|s) (1 - \epsilon_j(s)). \quad (106)$$

Note that the region described by (102) - (106) is equivalent to the rate region $\underline{\mathcal{C}}_{\text{fb}}^{\text{mem}}$ described in (17) - (20).

This may be seen by turning the flow problem in (102) - (106) to the min-cut formulation and setting

$$P_{A_t|S_{t-1}}(1|s) = 1 - y_s, \quad P_{A_t|S_{t-1}}(2|s) = 1 - x_s, \quad P_{A_t|S_{t-1}}(3|s) = x_s + y_s - 1. \quad (107)$$

The mapping from $x_s, y_s, s \in \mathcal{S}$ is unique in this case. Inequality (16) ensures that $P_{A_t|S_{t-1}}(3|s) \geq 0$. This inequality is implicitly required but does not appear in the outer bound $\bar{\mathcal{C}}_{\text{fb}}^{\text{mem}}$ and makes this approach suboptimal in general.

2) *Deterministic Scheme*: To avoid the drawbacks of the probabilistic scheme, a max-weight algorithm with action set \mathcal{A}_3 can be defined. In each slot t , the transmitter chooses the action with maximal weight as follows: For an observed current queue state $\underline{Q}_t = \underline{q}_t$ and previous channel state $S_{t-1} = s$, the action is given by

$$A_t = \operatorname{argmax}_{A_t \in \mathcal{A}_3} \sum_{j=1}^2 \sum_{l=1}^2 \sum_{m \in \mathcal{O}_l} [Q_{l,t}^{(j)} - Q_{m,t}^{(j)}]^+ \mathbb{E} \left[C_{lm,t}^{(j)} \middle| \underline{Q}_t = \underline{q}_t, S_{t-1} = s \right]. \quad (108)$$

Table V explicitly lists the weights for each action depending on \underline{Q}_t and $S_{t-1} = s$.

The strategy in Table V strongly stabilizes all queues in the network for every rate pair $(R_1 + \bar{\delta}, R_2 + \bar{\delta}) \in \underline{\mathcal{C}}_{\text{fb}}^{\text{mem}}$. The proof is similar to the proof of Theorem 8 and is omitted.

3) *Combination of Memoryless Strategies*: Looking at the characterization of $\underline{\mathcal{C}}_{\text{fb}+s}^{\text{mem}}$ in (15) - (20), one may wonder if this rate region can be attained by simply *combining* memoryless capacity achieving schemes. Let $\mathcal{C}_{\text{fb}+s}(s)$, $s \in \mathcal{S}$, denote the capacity region of a memoryless BPEC with feedback and erasure probabilities $P_{\mathcal{Z}_t|S_{t-1}}(\cdot|s)$. Capacity achieving algorithms for memoryless BPECs with feedback are derived in [9].

A combination of memoryless capacity achieving schemes may be described as follows:

- Choose fractions $\alpha_s \geq 0$ and $\beta_s \geq 0$ such that $\sum_{s \in \mathcal{S}} \alpha_s = \sum_{s \in \mathcal{S}} \beta_s = 1$ and $(\alpha_s R_1, \beta_s R_2) \in \pi_s \mathcal{C}_{\text{fb}+s}(s)$, for all $s \in \mathcal{S}$.
- Take $n\alpha_s R_1$ packets for Rx_1 and $n\beta_s R_2$ packets for Rx_2 to be transmitted only when the previous channel state is equal to $S_{t-1} = s$, $s \in \mathcal{S}$. For each previous state $s \in \mathcal{S}$, the transmitter chooses an optimal memoryless strategy corresponding to a memoryless BPEC with feedback and erasure probabilities $P_{\mathcal{Z}_t|S_{t-1}}(\cdot|s)$.

The transmitter needs to maintain a set of queues for each state. If Algorithm III of [9] is chosen as the capacity-achieving algorithm, the coding buffers contain at most one packet per session. Hence, at most $|\mathcal{S}|$ packets must be stored at each receiver.

Using the above scheme, for large n , one can asymptotically achieve the performance of the memoryless strategy for each state s with the corresponding capacity region $\mathcal{C}_{\text{fb}+s}(s)$. The overall rate region achievable by this strategy, called \mathcal{R}_{\oplus} , is thus a weighted combination of the individual memoryless rate regions (for each state s):

$$\mathcal{R}_{\oplus} = \bigoplus_{s \in \mathcal{S}} \pi_s \mathcal{C}_{\text{fb}+s}(s) \quad (109)$$

where \oplus denotes the set addition operator⁶ (Minkowski sum).

We show in Fig. 8 that \mathcal{R}_{\oplus} can be strictly smaller than $\underline{\mathcal{C}}_{\text{fb}+s}^{\text{mem}}$.

Remark 11. Note that each memoryless rate region $\mathcal{C}_{\text{fb}+s}(s)$, $s \in \mathcal{S}$, is a polytope defined by linear inequalities. However, the polytope generated by the Minkowski sum is *not* equal to the one defined by the sum of the individual polytope constraints, as in $\underline{\mathcal{C}}_{\text{fb}+s}$. That would be the case, for example, if the memoryless rate regions were polymatroids, as pointed out in [34, Chapter 15.3.3],[49]. In that case, \mathcal{R}_{\oplus} would be equal to $\underline{\mathcal{C}}_{\text{fb}+s}^{\text{mem}}$. However, this is not the case in general.

B. Uncoded Transmission

An alternative strategy is one without coding between sessions. Hence the action space is reduced to \mathcal{A}_2 , the coding buffers $Q_2^{(j)}$ are always empty by definition, but channel memory can still be exploited: The strategy will be useful to distinguish the gains due to channel memory and the gains due to coding.

Such a strategy has been proposed in several references, e.g. [26, Chapter 3], under the assumption that the *current* channel state is known. Using manipulations similar to the proof of Theorem 8, one can show that the optimal backpressure policy for this scheme is

$$A_t = \underset{A_t \in \mathcal{A}_2}{\operatorname{argmax}} \sum_{j=1}^2 \mathbb{E} \left[Q_{1,t}^{(j)} C_{14,t}^{(j)} | Q_t = \underline{q}, S_{t-1} = s \right]. \quad (110)$$

A packet for Rx_1 is transmitted if $Q_{1,t}^{(1)}(1 - \epsilon_1(s)) > Q_{1,t}^{(2)}(1 - \epsilon_2(s))$, otherwise a packet for Rx_2 .

One can show that this scheme can achieve rate pairs (R_1, R_2) if there exist variables x_s , $s \in \mathcal{S}$, such that

$$0 \leq x_s \leq 1 \quad (111)$$

$$R_1 \leq \sum_{s \in \mathcal{S}} \pi_s (1 - \epsilon_1(s)) x_s \quad (112)$$

$$R_2 \leq \sum_{s \in \mathcal{S}} \pi_s (1 - \epsilon_2(s)) (1 - x_s). \quad (113)$$

We call this region \mathcal{R}_{unc} .

VIII. NUMERICAL RESULTS

This section compares the rate regions achieved by the proposed schemes.

⁶For example, $\pi_1 \mathcal{R}_1 \oplus \pi_2 \mathcal{R}_2 = \{\pi_1 \underline{r}_1 + \pi_2 \underline{r}_2 | \underline{r}_1 \in \mathcal{R}_1, \underline{r}_2 \in \mathcal{R}_2\}$.

A. Visible Case

Our main focus will be on the visible Gilbert-Elliot model outlined in Example 1: We assume that the individual channels to Rx_1 and Rx_2 are both Gilbert-Elliot channels with states G and B. The broadcast channel state space is therefore given by $\mathcal{S} = \{GG, GB, BG, BB\}$ where G and B respectively refer to a good and bad state at each receiver. Transitions from state B to state G occur with probability g_j for Rx_j , $j = 1, 2$. Similarly, a transition from state G to state B occurs with probability b_j for Rx_j . For simplicity, these transitions are independent across the two users. The corresponding finite state Markov chain is summarized in Fig. 7.

In the visible case, where an erasure occurs always in state B and never in state G, the long-term average erasure probability at Rx_j is

$$\epsilon_j = \frac{b_j}{g_j + b_j}. \quad (114)$$

Given an average erasure probability ϵ_j , g_j determines b_j and specifies the channel to Rx_j .

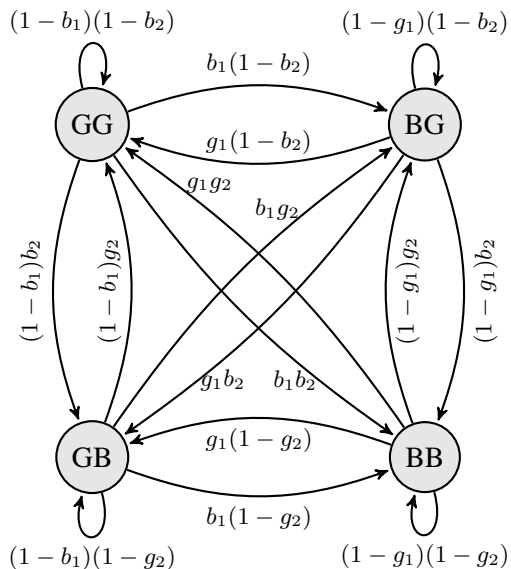


Fig. 7: Markov Chain of channel state space \mathcal{S} with transition probabilities.

We first compare the regions $\mathcal{C}_{fb+s}^{\text{mem}}$, $\underline{\mathcal{C}}_{fb+s}^{\text{mem}}$ and \mathcal{R}_{\oplus} for the strategy combining the memoryless schemes in Section VII-A3: Fig. 8 shows that \mathcal{R}_{\oplus} is smaller than $\underline{\mathcal{C}}_{fb+s}^{\text{mem}}$, despite their similar structure. $\underline{\mathcal{C}}_{fb+s}^{\text{mem}}$ almost matches the capacity region $\mathcal{C}_{fb+s}^{\text{mem}}$ for this example, so $\mathcal{C}_{fb+s}^{\text{mem}}$ is omitted for clarity. For comparison, we also plot the memoryless capacity regions for the same average erasure probabilities with (\mathcal{C}_{fb}) and without feedback (\mathcal{C}). The scaled individual rate regions $\pi_s \mathcal{C}_{fb+s}(s)$ for the $|\mathcal{S}| = 4$ memoryless states are shown as well. Their Minkowski sum results in \mathcal{R}_{\oplus} .

As a second example, Fig. 9 shows the capacity region for a channel with parameters $\epsilon_1 = 0.5$, $\epsilon_2 = 0.5$, $g_1 = 0.2$, $g_2 = 0.3$. Again, the difference between $\underline{\mathcal{C}}_{fb+s}^{\text{mem}}$ and the capacity region $\mathcal{C}_{fb+s}^{\text{mem}}$ is small. The strategy for \mathcal{R}_{\oplus} does not achieve capacity, but has a good performance.

We also compare queue backlog of the deterministic schemes corresponding to $\mathcal{C}_{fb+s}^{\text{mem}}$, $\underline{\mathcal{C}}_{fb+s}^{\text{mem}}$ and \mathcal{R}_{\oplus} ⁷, for the parameter set $\epsilon_1 = 0.6$, $g_1 = 0.1$, $\epsilon_2 = 0.5$, $g_2 = 0.2$: The corresponding rate regions are shown in Fig. 10a. We pick four rate points close to the boundary of all regions: One point lies inside all three regions, one lies inside $\underline{\mathcal{C}}_{fb+s}^{\text{mem}}$ and $\mathcal{C}_{fb+s}^{\text{mem}}$ but outside of \mathcal{R}_{\oplus} , etc. Finally, one rate point lies outside of all regions. This is illustrated in Fig. 10b.

For all four points we apply the corresponding algorithms and keep track of the aggregate queue backlog, i.e. the total number of packets stored in all queues in the system. Results are shown in Fig. 11: For the point inside all three regions (Fig. 11a), all queues are stable, but the capacity-achieving algorithm in Table III has the lowest aggregate backlog on average. If a point lies outside a rate region (e.g. outside of \mathcal{R}_{\oplus} in Fig. 11b), the corresponding queueing system becomes unstable. For the point outside of all regions, all systems are unstable and the average backlog grows slowest for the capacity-achieving scheme.

The same behavior can be seen if we apply the algorithms to the 2-state example in Example 2, for $\delta = 0$ and $R_1 = R_2 = 0.499$. As expected, Fig. 12 shows that the capacity-achieving strategy stabilizes the queueing network for the example in Fig. 4, whereas the other strategies do not.

⁷For \mathcal{R}_{\oplus} , we apply the scheme in Table V for each state s individually. For single-state channels, the scheme in Table V is capacity achieving. This explains that the aggregate backlog can be larger than $|\mathcal{S}|$, in contrast to the argumentation in Section VII-A3.

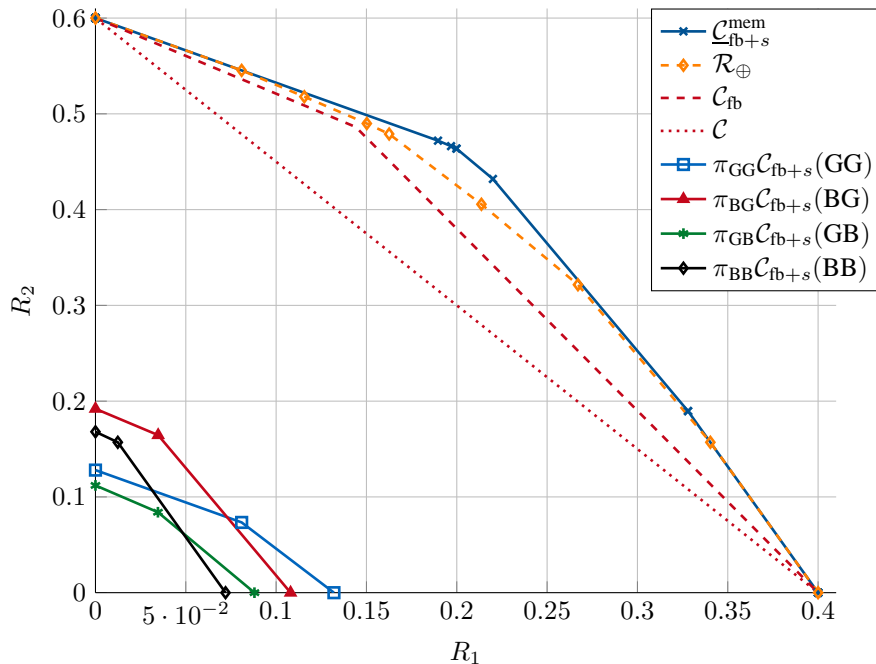


Fig. 8: Individual rate regions and Minkowski sum \mathcal{R}_{\oplus} for $\epsilon_1 = 0.6$, $\epsilon_2 = 0.4$, $g_1 = 0.3$, $g_2 = 0.7$. The region $\underline{\mathcal{C}}_{\text{fb}+s}^{\text{mem}}$ is strictly larger. For comparison, the corresponding capacity regions for memoryless channels with the same average erasure probability are shown for the cases with and without feedback. The difference between $\underline{\mathcal{C}}_{\text{fb}+s}^{\text{mem}}$ and $\bar{\mathcal{C}}_{\text{fb}+s}^{\text{mem}}$ is negligible in this case, so $\bar{\mathcal{C}}_{\text{fb}+s}^{\text{mem}}$ is omitted.

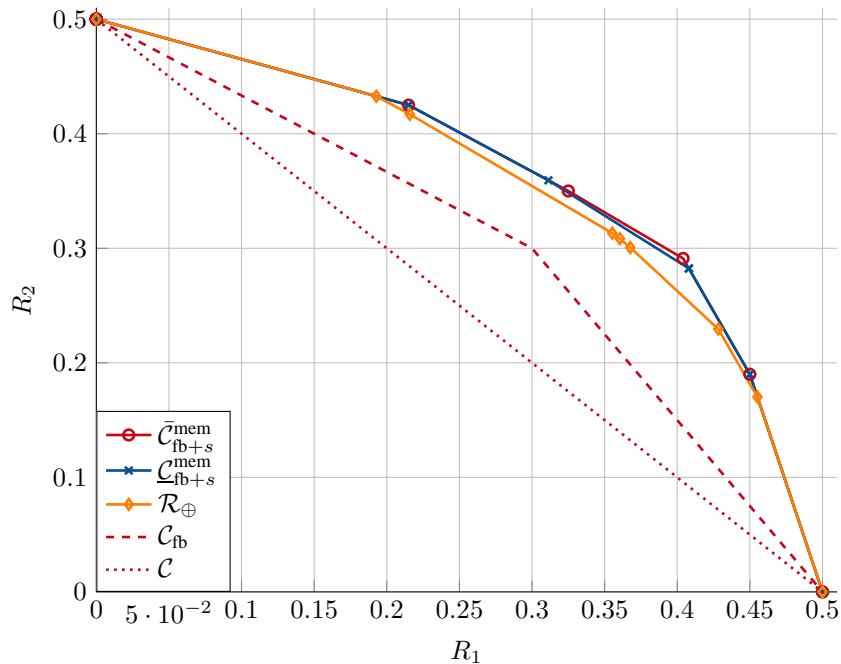


Fig. 9: Rate regions for $\epsilon_1 = 0.5$, $\epsilon_2 = 0.5$, $g_1 = 0.2$, $g_2 = 0.3$.

Fig. 13 shows an example with oscillatory channel memory. The uncoded strategy performs well, the combination of memoryless strategies achieves an even larger region. Again, $\underline{\mathcal{C}}_{\text{fb}+s}^{\text{mem}}$ is only slightly smaller than $\mathcal{C}_{\text{fb}+s}^{\text{mem}}$.

B. Delayed Feedback

The result in Theorem 1 extends to scenarios where feedback and channel state become available at the encoder with more than a single symbol-time delay. Consider a delay of $d \geq 1$ time units. In the converse, one can obtain the corresponding

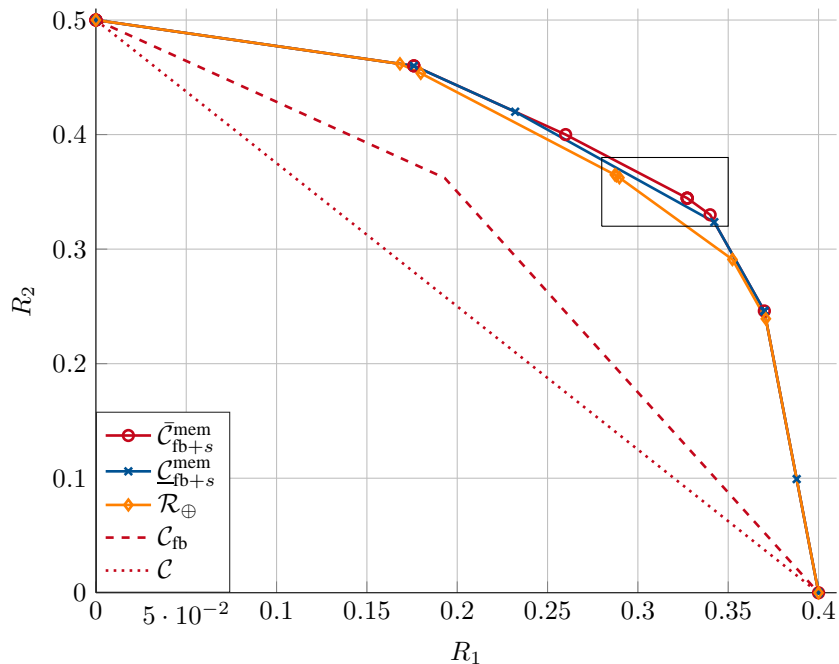
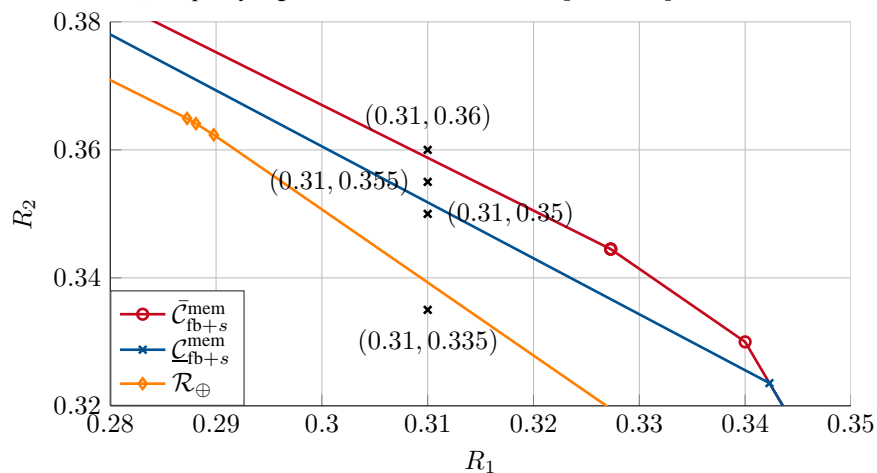
(a) Capacity region for $\epsilon_1 = 0.6$, $\epsilon_2 = 0.5$, $g_1 = 0.1$, $g_2 = 0.2$.(b) Zoom in capacity region for $\epsilon_1 = 0.6$, $\epsilon_2 = 0.5$, $g_1 = 0.1$, $g_2 = 0.2$.

Fig. 10: Capacity region for $\epsilon_1 = 0.6$, $\epsilon_2 = 0.5$, $g_1 = 0.1$, $g_2 = 0.2$ and zoomed selection. The marked rate points are simulated in Fig. 11.

bounds by replacing the sequences S^{T-1} , Y_1^{T-1} , Z_1^{T-1} , Y_2^{T-1} and Z_2^{T-1} with S^{T-d} , Y_1^{T-d} , Z_1^{T-d} , Y_2^{T-d} and Z_2^{T-d} .

The capacity region $\mathcal{C}_{\text{fb}+s}^{\text{mem}}(d)$ and achievable region $\mathcal{C}_{\text{fb}+s}^{\text{mem}}(d)$ thus have a characterization as in (9) - (13), (15) - (20), by redefining the erasure probabilities in (4) as

$$\begin{aligned} \epsilon_{12}(s) &= P_{Z_t|S_{t-d}}(1, 1|s), & \epsilon_{1\bar{2}}(s) &= P_{Z_t|S_{t-d}}(1, 0|s), \\ \epsilon_{\bar{1}2}(s) &= P_{Z_t|S_{t-d}}(0, 1|s), & \epsilon_{\bar{1}\bar{2}}(s) &= P_{Z_t|S_{t-d}}(0, 0|s), \\ \epsilon_1(s) &= \epsilon_{12}(s) + \epsilon_{1\bar{2}}(s), & \epsilon_2(s) &= \epsilon_{12}(s) + \epsilon_{\bar{1}2}(s). \end{aligned}$$

The corresponding deterministic achievable scheme as in Section VI-E uses these redefined conditional erasure probabilities to obtain the same description as in Table III.

Fig. 14 shows the effect of feedback delay for a Gilbert-Elliot channel with parameters $\epsilon_1 = 0.6$, $g_1 = 0.1$, $\epsilon_2 = 0.5$, $g_2 = 0.1$. Observe that delayed feedback shrinks both $\mathcal{C}_{\text{fb}+s}^{\text{mem}}(d)$ and $\mathcal{C}_{\text{fb}+s}^{\text{mem}}(d)$, as the state information becomes less useful. After a feedback delay of $d = 10$ time units, the region $\mathcal{C}_{\text{fb}+s}^{\text{mem}}(d = 10)$ is almost the same as for the memoryless case. In general this depends on the convergence speed of the state Markov chain towards its stationary distribution. It is interesting to

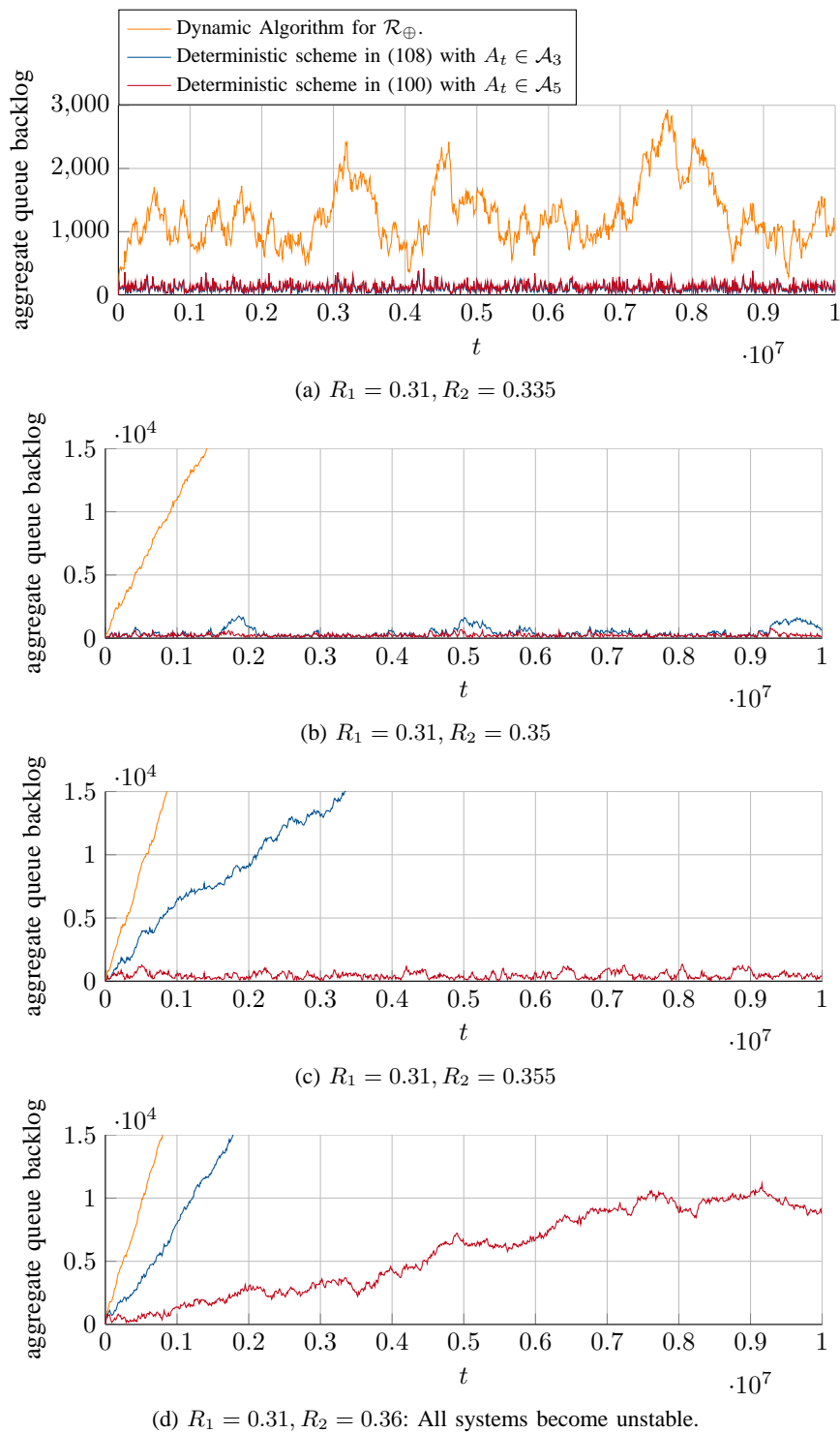


Fig. 11: Aggregate queue backlog for different algorithms and rate points.

see that, as d increases, the difference between $\underline{C}_{fb+s}^{\text{mem}}$ and C_{fb+s}^{mem} becomes smaller. $\underline{C}_{fb+s}^{\text{mem}}$ and C_{fb+s}^{mem} match for the memoryless single-state BPEC, a result further generalized in Section IX.

C. Hidden Case

For the hidden case, we consider a variation on the Gilbert-Elliot model used before. Suppose there is a nonzero erasure probability in both states G and B, where ϵ_{jG} is the erasure probability at Rx $_j$ when in state G and ϵ_{jB} when in state B. Typically one chooses $\epsilon_{jG} < \epsilon_{jB}$.

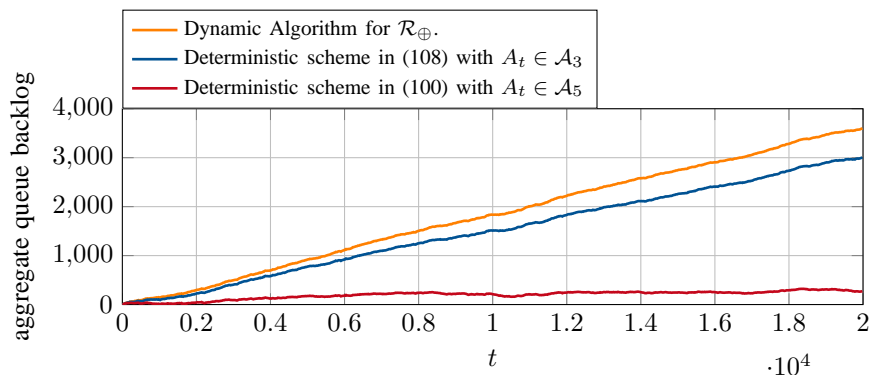


Fig. 12: Aggregate queue backlog for the three different strategies, for the state model as in Fig. 4, $\delta = 0$ and $R_1 = R_2 = 0.499$.

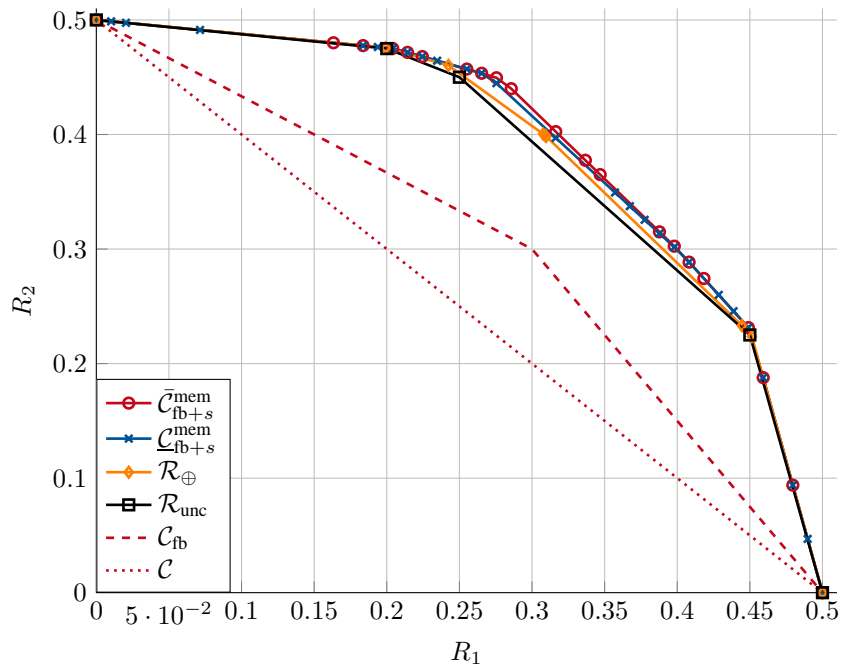


Fig. 13: Rate regions for $\epsilon_1 = \epsilon_2 = 0.5$, $g_1 = 0.8$, $g_2 = 0.9$.

The long-term average erasure probability at Rx_j is

$$\epsilon_j = \pi_G \epsilon_{jG} + \pi_B \epsilon_{jB} = \frac{g_j \epsilon_{jG} + b_j \epsilon_{jB}}{g_j + b_j}. \quad (115)$$

Because all erasure events can happen in every state, the corresponding setup is hidden if only ACK/NACK feedback is available. In Fig. 2 in Section IV we plot the L -th order approximations $\bar{C}_{fb}^{\text{mem}}(L)$ of the outer bounds, as defined in Section V, for $L = 1$ and $L = 7$. We observe that $\bar{C}_{fb}^{\text{mem}}(L_1) \subset \bar{C}_{fb}^{\text{mem}}(L_2)$ for $L_1 < L_2$. We also plot rate pairs that lead to a stable queuing network when the deterministic scheme in Table IV is used⁸. Both curves provide an almost equivalent characterization of the capacity region C_{fb}^{mem} .

As a second example, define the following 3-state channel model with transition matrix \mathbf{P} , $\mathbf{P}_{ij} = P_{S_t|S_{t-1}}(j|i)$ and erasure distribution matrix \mathbf{E} . Each row of \mathbf{E} corresponds to a distribution $[P_{Z_t|S_t}(0, 0|s), P_{Z_t|S_t}(0, 1|s), P_{Z_t|S_t}(1, 0|s), P_{Z_t|S_t}(1, 1|s)]$:

$$\mathbf{P} = \begin{bmatrix} 0.7 & 0.2 & 0.1 \\ 0.2 & 0.4 & 0.4 \\ 0.3 & 0.01 & 0.69 \end{bmatrix} \quad (116)$$

$$\mathbf{E} = \begin{bmatrix} 0.75 & 0.1 & 0.1 & 0.05 \\ 0.2 & 0.2 & 0.3 & 0.3 \\ 0 & 0.1 & 0.2 & 0.7 \end{bmatrix} \quad (117)$$

⁸The decision if the queuing system is stable or not was made by inspection after a simulation of $n = 10^7$ time slots.

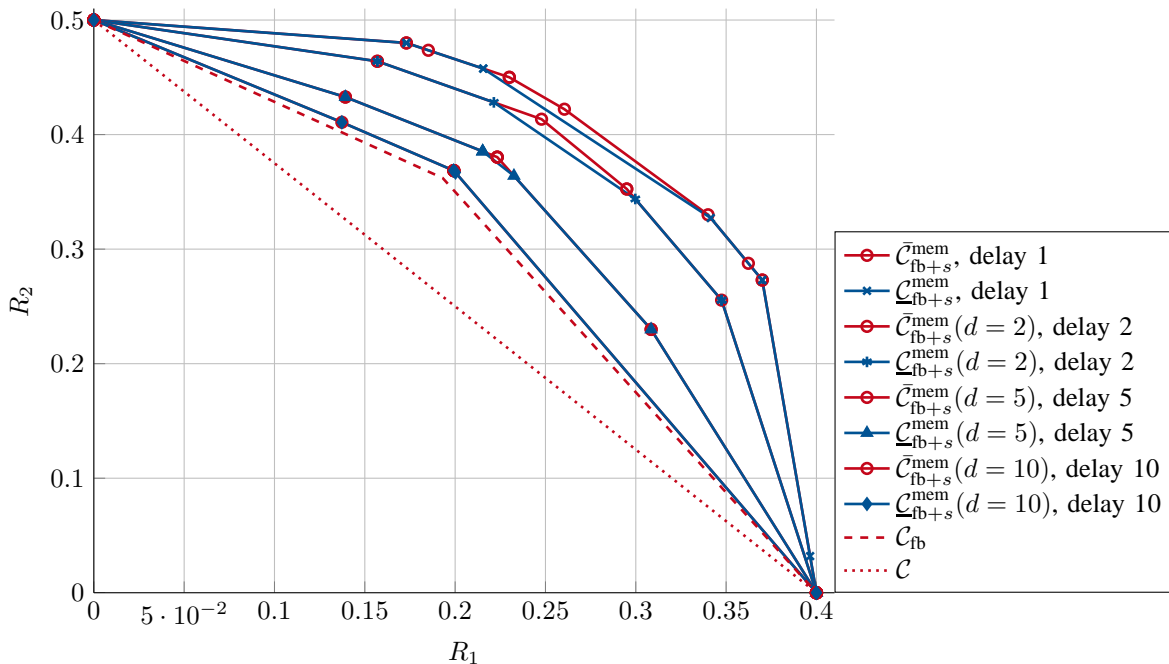


Fig. 14: Capacity regions with delayed feedback, for $\epsilon_1 = 0.6$, $g_1 = 0.1$, $\epsilon_2 = 0.5$, $g_2 = 0.1$.

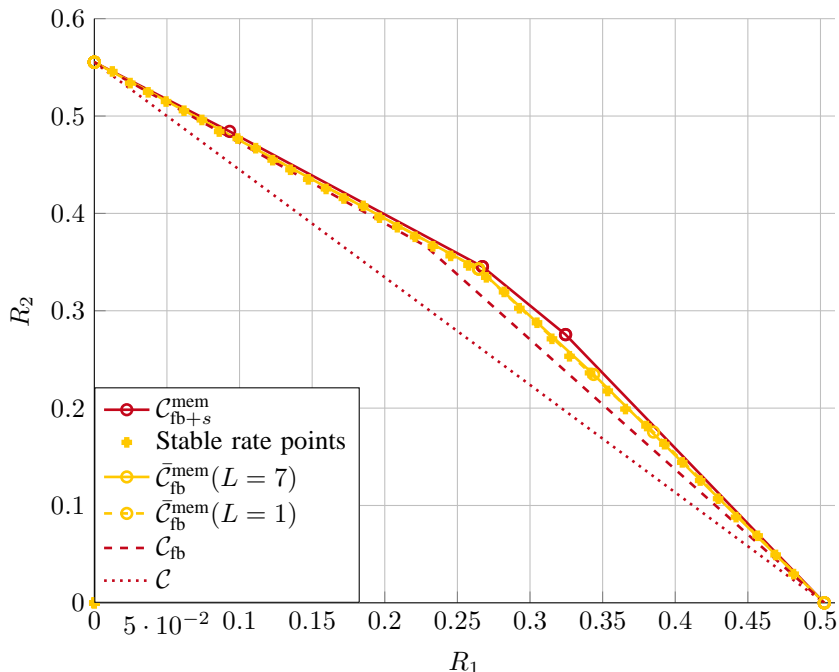


Fig. 15: Capacity region for hidden case, 3-state model as described in (116) and (117).

Note that the channels between Rx_1 and Rx_2 are correlated in this case. The long-term average erasure probabilities are given by $\epsilon_1 = 0.497$, $\epsilon_2 = 0.445$, $\epsilon_{12} = 0.329$. Results including stable rate pairs are shown in Fig. 15.

IX. MEMORYLESS CASE

This section deals with the case of finite-state *memoryless* broadcast packet erasure channels. The erasure probabilities still depend on the current channel state according to $P_{Z_t|S_t}$, but the state sequence S^n is i.i.d. The results in Theorem 1 include this setup as a special case.

Because strictly causal state feedback does not give information about future transmissions, there is no difference between the visible and hidden case here. We show that reactive coding achieves capacity in this case. This is remarkable because this

means that proactive coding is required only when the state sequence is correlated. Our argumentation will build on geometric properties of the memoryless rate regions that we derive next.

A. Memoryless BPEC without Feedback

Recall that the capacity region \mathcal{C} for the memoryless BPEC without FB consists of all rate pairs

$$(R_1, R_2) \geq 0 : \frac{R_1}{1 - \epsilon_1} + \frac{R_2}{1 - \epsilon_2} \leq 1. \quad (118)$$

\mathcal{C} thus has the triangular shape shown in Fig. 16, for $\epsilon_1 = 0.6$, $\epsilon_2 = 0.4$.

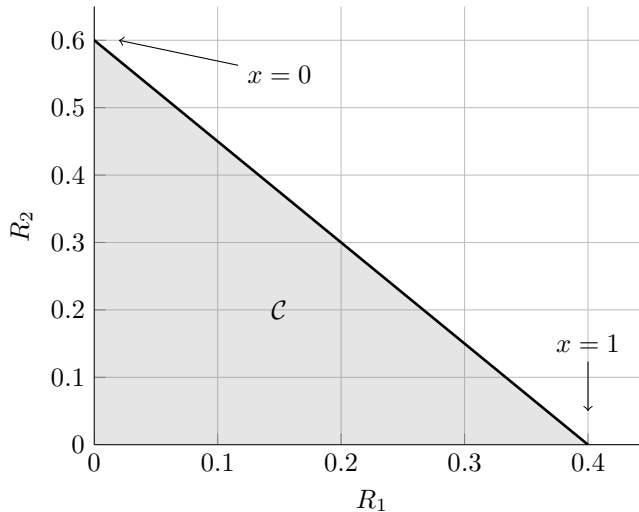


Fig. 16: Capacity region for $\epsilon_1 = 0.6$, $\epsilon_2 = 0.4$.

An alternative representation is in terms of the following feasibility problem: A rate pair (R_1, R_2) is in the capacity region \mathcal{C} if there is a variable x such that

$$\begin{aligned} 0 &\leq x \leq 1 \\ 0 &\leq R_1 \leq (1 - \epsilon_1)x \\ 0 &\leq R_2 \leq (1 - \epsilon_2)(1 - x). \end{aligned} \quad (119)$$

The variable x defines the point at the boundary of the capacity region: $x = 0$ describes the corner point $(R_1, R_2) = (0, 1 - \epsilon_2)$ and $x = 1$ describes the corner point $(R_1, R_2) = (1 - \epsilon_1, 0)$, as illustrated in Fig. 16. All other choices of x lead to a point on the boundary between these corner points. Every particular choice of x gives a subset of the region \mathcal{C} .

The variable x has a natural interpretation as the time sharing fraction of a probabilistic strategy with action set \mathcal{A}_2 and $x = P_{A_t}(1)$.

B. Memoryless BPEC with Feedback

For this case, the capacity region consists of all rate pairs $(R_1, R_2) \in \mathcal{C}_{\text{fb}} = \mathcal{C}_1 \cap \mathcal{C}_2$, where

$$\begin{aligned} \mathcal{C}_1 &= \left\{ (R_1, R_2) \geq 0 : \frac{R_1}{1 - \epsilon_1} + \frac{R_2}{1 - \epsilon_{12}} \leq 1 \right\} \\ \mathcal{C}_2 &= \left\{ (R_1, R_2) \geq 0 : \frac{R_1}{1 - \epsilon_{12}} + \frac{R_2}{1 - \epsilon_2} \leq 1 \right\}. \end{aligned}$$

An alternative representation is in terms of the following feasibility problem: A rate pair (R_1, R_2) is in the capacity region \mathcal{C}_{fb} if there are variables x, y , such that

$$0 \leq x \leq 1 \quad (120)$$

$$0 \leq R_1 \leq (1 - \epsilon_1)x \quad (121)$$

$$0 \leq R_2 \leq (1 - \epsilon_{12})(1 - x) \quad (122)$$

$$0 \leq y \leq 1 \quad (123)$$

$$0 \leq R_1 \leq (1 - \epsilon_{12})(1 - y) \quad (124)$$

$$0 \leq R_2 \leq (1 - \epsilon_2)y \quad (125)$$

where (120) - (122) account for \mathcal{C}_1 and (123) - (125) account for \mathcal{C}_2 .

The variable x defines a point on the boundary of \mathcal{C}_1 and y defines a point on the boundary of \mathcal{C}_2 , as illustrated in Fig. 17a. Consider points on the boundary of \mathcal{C}_{fb} , marked with red dashes in Fig. 17a: For $x \geq x^*$, the boundary points are specified by \mathcal{C}_1 only, i.e. by (120) - (122), for $y \geq y^*$, the boundary points are specified by \mathcal{C}_2 only, i.e. by (123) - (125). Here, x^* and y^* specify the values of x and y that determine the point where the lines defining \mathcal{C}_1 and \mathcal{C}_2 intersect, as shown in Fig. 17a.

For a particular choice of x and y , one obtains a subset of \mathcal{C}_{fb} , as shown in Fig. 17b. If x and y are chosen arbitrarily, the corresponding subset of the capacity region can lie strictly inside \mathcal{C}_{fb} , i.e. it does not contain points on the boundary of \mathcal{C}_{fb} . This is the case in the example in Fig. 17b, where one inequality from (120) - (122) is binding for R_1 and one inequality from (123) - (125) is binding for R_2 .

To obtain *boundary points* of \mathcal{C}_{fb} (drawn in red in Fig. 17a), the binding inequalities should be either both from (121), (122) or both from (124), (125), see Fig. 17c. Hence, for $x \geq x^*$, the value of y should be chosen such that (120) - (122) are more restrictive than (123) - (125) for both R_1 and R_2 , i.e. the following two inequalities hold:

$$(1 - \epsilon_1)x \leq (1 - \epsilon_{12})(1 - y) \quad (126)$$

$$(1 - \epsilon_{12})(1 - x) \leq (1 - \epsilon_2)y \quad (127)$$

An immediate consequence of (127) is the condition

$$\frac{1 - \epsilon_{12}}{1 - \epsilon_2}(1 - x) \leq y, \quad (128)$$

and as $\frac{1 - \epsilon_{12}}{1 - \epsilon_2} \geq 1$, this leads to the following constraint for the feasibility problem above:

$$x + y \geq 1 \quad (129)$$

Similarly, for $y \geq y^*$, the value of x should be chosen such that (123) - (125) are more restrictive than (120) - (122) for both R_1 and R_2 :

$$(1 - \epsilon_{12})(1 - y) \leq (1 - \epsilon_1)x \quad (130)$$

$$(1 - \epsilon_2)y \leq (1 - \epsilon_{12})(1 - x) \quad (131)$$

As before, a consequence of (130) is that $x + y \geq 1$. Hence, this constraint implicitly holds for all pairs of x and y describing a point on the boundary of \mathcal{C}_{fb} .

The constraint (129) is redundant and does not restrict the set defined by \mathcal{C}_{fb} .

Again, the numbers x and y have a natural interpretation in conjunction with a probabilistic scheme on action set \mathcal{A}_3 : By letting $y = 1 - P_{A_t}(1)$, $x = 1 - P_{A_t}(2)$, $x + y = 1 + P_{A_t}(3)$, the rate region can be characterized by parameters of a probabilistic strategy with reactive coding only. This was to be expected, as it was shown in [9] that reactive coding achieves the capacity region for the memoryless case. The constraint $x + y \geq 1$ ensures that $P_{A_t}(3) \geq 0$.

C. Memoryless Compound BPEC with Feedback

Recall that the capacity region $\mathcal{C}_{fb+s}^{\text{mem}}$ differs from the rate region achieved with reactive coding $\underline{\mathcal{C}}_{fb+s}^{\text{mem}}$ only through the constraint

$$x_s + y_s \geq 1 \quad \forall s \in \mathcal{S}. \quad (132)$$

We saw in Section VIII that this makes $\underline{\mathcal{C}}_{fb+s}^{\text{mem}}$ strictly smaller than $\mathcal{C}_{fb+s}^{\text{mem}}$ in general.

For the finite-state memoryless case, note that

$$P_{S_t|S_{t-1}}(s|s') = P_{S_t}(s) = \pi_s. \quad (133)$$

It follows that $\epsilon_j(s)$ is independent of s and equal to the *average* erasure probability

$$\epsilon_j(s) = \bar{\epsilon}_j = \sum_{s' \in \mathcal{S}} \pi_{s'} P_{Z_j|S_t}(1|s') \quad \forall s \in \mathcal{S}. \quad (134)$$

One can define $\epsilon_{12}(s) = \bar{\epsilon}_{12}$ correspondingly. The capacity region $\mathcal{C}_{fb+s}^{\text{mem}}$ simplifies to

$$0 \leq x_s \leq 1, \quad 0 \leq y_s \leq 1 \quad (135)$$

$$R_1 \leq (1 - \bar{\epsilon}_1) \sum_{s \in \mathcal{S}} \pi_s x_s \quad (136)$$

$$R_1 \leq (1 - \bar{\epsilon}_{12}) \left(1 - \sum_{s \in \mathcal{S}} \pi_s y_s \right) \quad (137)$$

$$R_2 \leq (1 - \bar{\epsilon}_{12}) \sum_{s \in \mathcal{S}} \pi_s y_s \quad (138)$$

$$R_2 \leq (1 - \bar{\epsilon}_2) \left(1 - \sum_{s \in \mathcal{S}} \pi_s x_s \right). \quad (139)$$

We can define new variables

$$x' = \sum_{s \in \mathcal{S}} \pi_s x_s \quad (140)$$

$$y' = \sum_{s \in \mathcal{S}} \pi_s y_s. \quad (141)$$

One obtains a characterization that is similar to the single-state memoryless case:

$$0 \leq x' \leq 1, \quad 0 \leq y' \leq 1$$

$$R_1 \leq (1 - \bar{\epsilon}_1) x'$$

$$R_1 \leq (1 - \bar{\epsilon}_{12}) (1 - y')$$

$$R_2 \leq (1 - \bar{\epsilon}_{12}) y'$$

$$R_2 \leq (1 - \bar{\epsilon}_2) (1 - x')$$

Any feasible choice of $x_s, y_s, s \in \mathcal{S}$ leads to a particular value of x' and y' . From the previous section we know that we can restrict us to those pairs $x_s, y_s, s \in \mathcal{S}$ leading to values of x' and y' satisfying the constraint

$$x' + y' \geq 1 \quad (142)$$

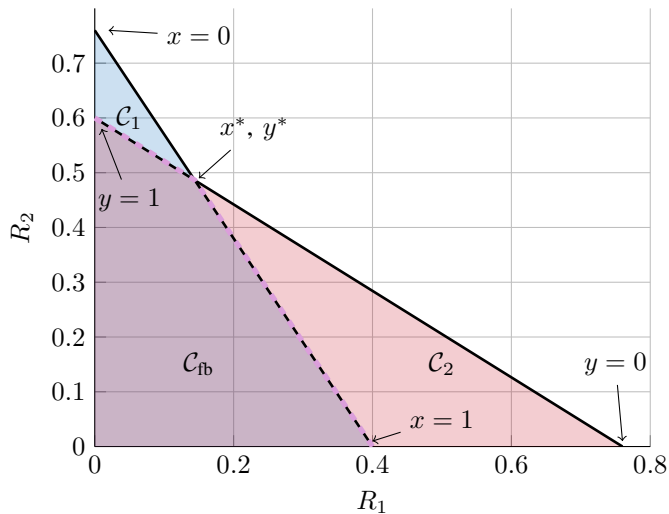
without shrinking the rate region. For every pair of x', y' satisfying (142) that resulted from a particular choice of x_s, y_s , we can find $|\mathcal{S}|$ pairs \hat{x}_s, \hat{y}_s that

- yield the same values x', y' as the original choice x_s, y_s , hence
- lead to the same bounds in (135) - (139) and
- satisfy (132), as we can set

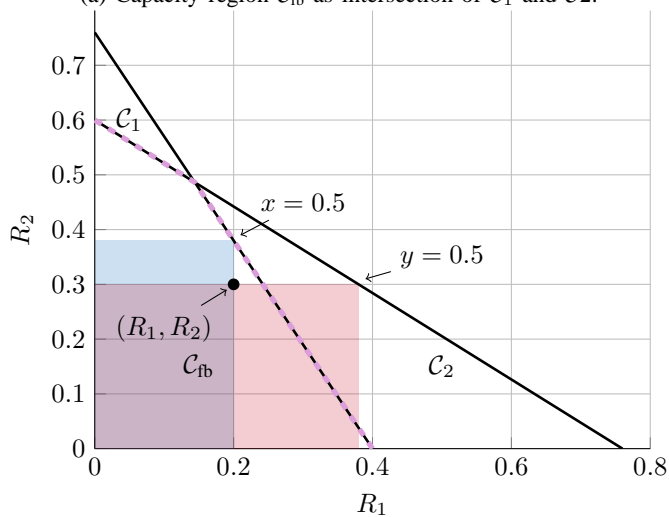
$$\begin{aligned} \hat{x}_s &= x' \\ \hat{y}_s &= y' \quad \forall s \in \mathcal{S}. \end{aligned} \quad (143)$$

This shows that $\underline{C}_{\text{fb}+s}^{\text{mem}} = C_{\text{fb}+s}^{\text{mem}}$ and hence reactive coding achieves capacity.

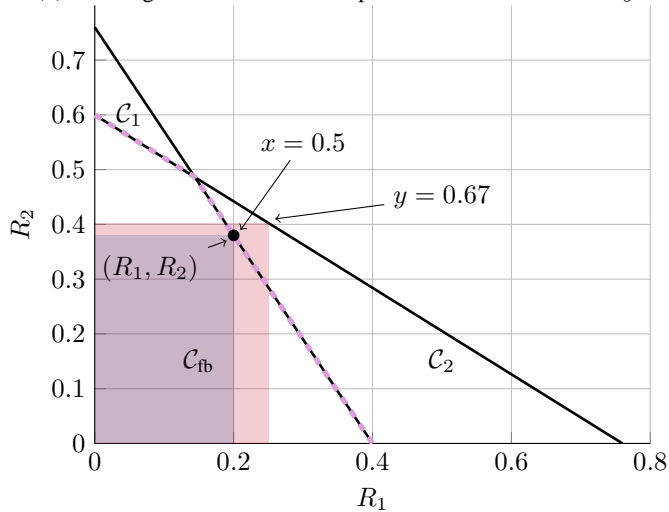
The choice in (143) means that the probability distributions $P_{A_t|S_{t-1}}$ are independent of S_{t-1} , hence the strategy does not need to adapt to the previous state.



(a) Capacity region C_{fb} as intersection of C_1 and C_2 .



(b) Rate region achievable for a particular choice of x and y .



(c) Rate region achievable for a suitable choice of x and y such that only one constraint set is binding.

Fig. 17: Capacity region for $\epsilon_1 = 0.6$, $\epsilon_2 = 0.4$, $\epsilon_{12} = \epsilon_1 \epsilon_2$.

X. CONCLUSION

This paper studied two-receiver finite-state broadcast packet erasure channels (BPECs) with feedback and memory, represented by a finite-state model. Two different cases were investigated: In the case of a visible channel state, the transmitter knows the channel state strictly causally, in addition to the channel output feedback. In the case of a hidden channel state, the transmitter only has channel output feedback. For both situation, we derived novel outer bounds on the capacity region. Similar to the work in [27], we formulate coding schemes as a queueing problem that can be analyzed with standard approaches from network control. The coding schemes can be formulated as linear network flow problems, where we showed that the dual min-cut representation matches the outer bounds. Hence the coding schemes are optimal and achieve any point inside the capacity region. We complemented these results with suboptimal algorithms, delayed feedback and derivations about finite-state memoryless BPECs.

There are multiple directions to extend the work in this paper: The K -receiver setup is well studied for the memoryless case, some results could carry over to the case with channel memory. Thinking towards practical application, schemes dealing with lossy feedback, unknown channel models and time-varying channels are highly desirable.

APPENDIX A PROOF OF LEMMA 4

Using (37) and (38) for $j = 1, 2$, we have

$$u_s^{(1)} + v_s^{(2)} \leq u_s^{(j)} + I(U_{j,T} V_T; X_T | U_{j,T} T, S_{T-1} = s) \quad (144)$$

$$= I(U_{j,T} U_{j,T} V_T; X_T | T, S_{T-1} = s), \quad (145)$$

$$\leq 1 \quad (146)$$

where the last inequality holds because $\log |\mathcal{X}| = 1$.

APPENDIX B $\bar{C}_{\text{FB}}^{\text{MEM}}$ IS AN OUTER BOUND ON THE CAPACITY REGION IN THE HIDDEN CASE

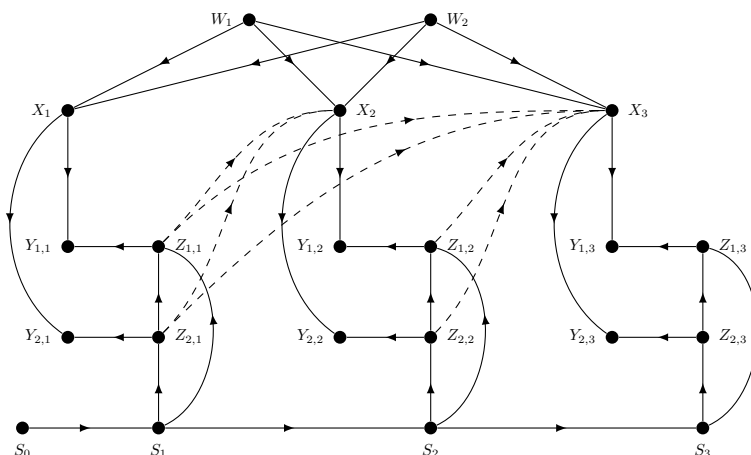


Fig. 18: Bayesian network for the two-receiver BPEC with memory and ACK/NACK feedback (hidden state), for $n = 3$ and $d = 1$. Dependencies due to feedback are drawn with dashed lines.

Similar to the visible case and using Fano's inequality, we write:

$$\begin{aligned} R_1 - \delta &\leq \frac{1}{n} I(W_1; Y_1^n) \\ &\leq \frac{1}{n} I(W_1; Y_1^n Z_2^{n-1}) \\ &= \frac{1}{n} \sum_{t=1}^n I(W_1; Y_{1,t} Z_{2,t-1} | Y_1^{t-1} Z_2^{t-2}) \\ &= \frac{1}{n} \sum_{t=1}^n [I(W_1; Z_{2,t-1} | Y_1^{t-1} Z_1^{t-1} Z_2^{t-2}) + I(W_1; Y_{1,t} | Y_1^{t-1} Z_2^{t-1})] \\ &\stackrel{(a)}{=} \sum_{t=1}^n \frac{1}{n} I(W_1; Y_{1,t} | Y_1^{t-1} Z_1^{t-1} Z_2^{t-1}) \end{aligned}$$

$$= \frac{1}{n} \sum_{t=1}^n \sum_{\underline{z}^{t-1}} P_{\underline{Z}^{t-1}}(\underline{z}^{t-1}) I(W_1; Y_{1,t} | Y_1^{t-1}, \underline{Z}^{t-1} = \underline{z}^{t-1}). \quad (147)$$

In the above chain of inequalities, (a) follows because \underline{Z}_1^{t-1} is a function of Y_1^{t-1} and $W_1 - Y_1^{t-1} \underline{Z}_1^{t-1} \underline{Z}_2^{t-2} - \underline{Z}_{2,t-1}$ forms a Markov chain for every t . Markov chains can be checked in the Bayesian network in Fig. 18.

In a similar manner, we write

$$\begin{aligned} R_1 - \delta &\leq \frac{1}{n} I(W_1; Y_1^n Y_2^n | W_2) \\ &= \frac{1}{n} \sum_{t=1}^n I(W_1; Y_{1,t} Y_{2,t} | W_2 Y_1^{t-1} Y_2^{t-1}) \\ &\stackrel{(a)}{=} \frac{1}{n} \sum_{t=1}^n \sum_{\underline{z}^{t-1}} P_{\underline{Z}^{t-1}}(\underline{z}^{t-1}) I(W_1; Y_{1,t} Y_{2,t} | W_2 Y_1^{t-1} Y_2^{t-1}, \underline{Z}^{t-1} = \underline{z}^{t-1}) \end{aligned} \quad (148)$$

where (a) follows because \underline{Z}^{t-1} is a function of Y_1^{t-1}, Y_2^{t-1} .

Adapting Lemma 3 for every t , \underline{z}^{t-1} and $j \in \{1, 2\}$, we obtain

$$\begin{aligned} I(W_j; Y_{j,t} | Y_j^{t-1}, \underline{Z}^{t-1} = \underline{z}^{t-1}) \\ = (1 - \epsilon_j(\underline{z}^{t-1})) I(W_j; X_t | Y_j^{t-1}, \underline{Z}^{t-1} = \underline{z}^{t-1}), \end{aligned} \quad (149)$$

$$\begin{aligned} I(W_j; Y_{1,t} Y_{2,t} | W_2 Y_1^{t-1} Y_2^{t-1}, \underline{Z}^{t-1} = \underline{z}^{t-1}) \\ = (1 - \epsilon_{12}(\underline{z}^{t-1})) I(W_j; X_t | W_2 Y_1^{t-1} Y_2^{t-1}, \underline{Z}^{t-1} = \underline{z}^{t-1}). \end{aligned} \quad (150)$$

As for the visible case, define variables for $j \in \{1, 2\}$ and any \underline{z}^{t-1} :

$$u^{(j)}(\underline{z}^{t-1}) = I(W_j; X_t | Y_j^{t-1}, \underline{Z}^{t-1} = \underline{z}^{t-1}) \quad (151)$$

$$v^{(j)}(\underline{z}^{t-1}) = I(W_j; X_t | W_j Y_1^{t-1} Y_2^{t-1}, \underline{Z}^{t-1} = \underline{z}^{t-1}) \quad (152)$$

Adapt Lemma 4 to obtain the relation

$$u^{(j)}(\underline{z}^{t-1}) + v^{(\bar{j})}(\underline{z}^{t-1}) \leq 1, \quad j \in \{1, 2\}, \forall t, \underline{z}^{t-1}. \quad (153)$$

We obtain the following outer bound:

$$0 \leq u^{(j)}(\underline{z}^{t-1}) \leq 1, \quad 0 \leq v^{(j)}(\underline{z}^{t-1}) \leq 1 \quad \forall t, \underline{z}^{t-1} \quad (154)$$

$$u^{(j)}(\underline{z}^{t-1}) + v^{(\bar{j})}(\underline{z}^{t-1}) \leq 1 \quad \forall t, \underline{z}^{t-1} \quad (155)$$

$$R_j \leq \frac{1}{n} \sum_{t=1}^n \sum_{\underline{z}^{t-1}} P_{\underline{Z}^{t-1}}(\underline{z}^{t-1}) (1 - \epsilon_j(\underline{z}^{t-1})) u^{(j)}(\underline{z}^{t-1}) \quad (156)$$

$$R_j \leq \frac{1}{n} \sum_{t=1}^n \sum_{\underline{z}^{t-1}} P_{\underline{Z}^{t-1}}(\underline{z}^{t-1}) (1 - \epsilon_{12}(\underline{z}^{t-1})) v^{(j)}(\underline{z}^{t-1}). \quad (157)$$

Similar to the visible case, one obtains the outer bound $\bar{C}_{\text{fb}}^{\text{mem}}$ in (21) - (25), by setting $v^{(1)}(\underline{z}^{t-1}) = 1 - y(\underline{z}^{t-1})$, $v^{(2)}(\underline{z}^{t-1}) = 1 - x(\underline{z}^{t-1})$, $u^{(1)}(\underline{z}^{t-1}) = x(\underline{z}^{t-1})$, and $u^{(2)}(\underline{z}^{t-1}) = y(\underline{z}^{t-1})$.

APPENDIX C PROOF OF COROLLARY 6

$$\begin{aligned} &\sum_{\underline{z}_{t+1}} \left| P_{\underline{Z}_{t+1} | \underline{Z}^t}(\underline{z}_{t+1} | \underline{z}^t) - P_{\underline{Z}_{t+1} | \underline{Z}_{t-L+1}^t}(\underline{z}_{t+1} | \underline{z}_{t-L+1}^t) \right| \\ &= \sum_{\underline{z}_{t+1}} \left| \sum_{s \in \mathcal{S}} \left(P_{\underline{Z}_{t+1} S_{t+1} | \underline{Z}^t}(\underline{z}_{t+1}, s | \underline{z}^t) - P_{\underline{Z}_{t+1} S_{t+1} | \underline{Z}_{t-L+1}^t}(\underline{z}_{t+1}, s | \underline{z}_{t-L+1}^t) \right) \right| \\ &= \sum_{\underline{z}_{t+1}} \left| \sum_{s \in \mathcal{S}} \left(P_{S_{t+1} | \underline{Z}^t}(s | \underline{z}^t) - P_{S_{t+1} | \underline{Z}_{t-L+1}^t}(s | \underline{z}_{t-L+1}^t) \right) P_{\underline{Z}_{t+1} | S_{t+1}}(\underline{z}_{t+1} | s) \right| \\ &\leq \sum_{s \in \mathcal{S}} \left| P_{S_{t+1} | \underline{Z}^t}(s | \underline{z}^t) - P_{S_{t+1} | \underline{Z}_{t-L+1}^t}(s | \underline{z}_{t-L+1}^t) \right| \sum_{\underline{z}_{t+1}} P_{\underline{Z}_{t+1} | S_{t+1}}(\underline{z}_{t+1} | s) \end{aligned}$$

$$= \sum_{s_t} \left| P_{S_{t+1}|\underline{Z}^t}(s|\underline{z}^t) - P_{S_{t+1}|\underline{Z}_{t-L+1}^t}(s|\underline{z}_{t-L+1}^t) \right|, \quad (158)$$

where the inequality is due to the triangle inequality.

APPENDIX D APPROXIMATION OF OUTER BOUNDS FOR THE HIDDEN CASE

We prove inequality (50). The other inequalities follow similarly.

$$\begin{aligned} R_1 &\leq \frac{1}{n} \sum_{t=1}^n \sum_{\underline{z}^{t-1}} P_{\underline{Z}^{t-1}}(\underline{z}^{t-1})(1 - \epsilon_1(\underline{z}^{t-1}))x(\underline{z}^{t-1}) \\ &\stackrel{(a)}{\leq} \frac{1}{n} \sum_{t=1}^n \sum_{\underline{z}^{t-1}} P_{\underline{Z}^{t-1}}(\underline{z}^{t-1}) \left((1 - \epsilon_1(\underline{z}_{t-L}^{t-1}) + 2(1 - \sigma)^L) x(\underline{z}^{t-1}) \right) \\ &= \frac{1}{n} \sum_{t=1}^n \left[\left(\sum_{\underline{z}^{t-1}} P_{\underline{Z}^{t-1}}(\underline{z}^{t-1})(1 - \epsilon_1(\underline{z}_{t-L}^{t-1}))x(\underline{z}^{t-1}) \right) \right. \\ &\quad \left. + 2(1 - \sigma)^L \left(\sum_{\underline{z}^{t-1}} P_{\underline{Z}^{t-1}}(\underline{z}^{t-1})x(\underline{z}^{t-1}) \right) \right] \\ &\stackrel{(b)}{\leq} \frac{1}{n} \sum_{t=1}^n \sum_{\underline{z}_{t-L}^{t-1}} \left(P_{\underline{Z}_{t-L}^{t-1}}(\underline{z}_{t-L}^{t-1}) (1 - \epsilon_1(\underline{z}_{t-L}^{t-1})) \left(\sum_{\underline{z}^{t-1}} P_{\underline{Z}^{t-L-1}|\underline{Z}_{t-L}^{t-1}}(\underline{z}^{t-L-1}|\underline{z}_{t-L}^{t-1})x(\underline{z}^{t-1}) \right) \right) + 2(1 - \sigma)^L \quad (159) \end{aligned}$$

where (a) follows from Corollary 6 and (b) follows from $x(\underline{z}^{t-1}) \leq 1$ for all t and \underline{z}^{t-1} . If the sequence \underline{Z}^n is stationary, i.e. if $P_{\underline{Z}_{t-L}^{t-1}}(\underline{z}^L)$ does not depend on t but only on \underline{z}^L , then one can write the right hand side of (159) as

$$\sum_{\underline{z}^L} P_{\underline{Z}_{t-L}^{t-1}}(\underline{z}^L) (1 - \epsilon_1(\underline{z}^L)) \left(\frac{1}{n} \sum_{t=1}^n \sum_{\underline{z}^{t-L-1}} P_{\underline{Z}^{t-L-1}|\underline{Z}_{t-L}^{t-1}}(\underline{z}^{t-L-1}|\underline{z}^L)x(\underline{z}^{t-1}) \right) + 2(1 - \sigma)^L. \quad (160)$$

Abbreviating $\left(\frac{1}{n} \sum_{t=1}^n \sum_{\underline{z}^{t-L-1}} P_{\underline{Z}^{t-L-1}|\underline{Z}_{t-L}^{t-1}}(\underline{z}^{t-L-1}|\underline{z}^L)x(\underline{z}^{t-1}) \right)$ by $x(\underline{z}^L)$, we obtain

$$R_1 \leq 2(1 - \sigma)^L + \sum_{\underline{z}^L} P_{\underline{Z}^L}(\underline{z}^L)(1 - \epsilon_1(\underline{z}^L))x(\underline{z}^L). \quad (161)$$

With similar steps and adaption of Lemma 3 one obtains the inequalities in (50) - (53). Similar steps apply for the inner approximation.

APPENDIX E PACKET MOVEMENT AND NETWORK FLOW IN THE DEGENERATE CASE

One problem arises if we want to use proactive coding, i.e. $A_t = 4$, but $Q_1^{(1)}$ or $Q_1^{(2)}$ or both are empty. The flow-based models and backpressure schemes in Section VI-E require (72) and (75) - (80) to hold. This section shows that these conditions can be satisfied in the degenerate case.

Section VI-C describes the packet movement in the non-degenerate case, i.e. both $Q_1^{(1)}$ and $Q_1^{(2)}$ are nonempty when $A_t = 4$. The original packets involved in the poisoned packet are moved to $Q_3^{(1)}$, $Q_3^{(2)}$, respectively, if the poisoned packet is not erased at both Rx_1 and Rx_2 . That is, either both original packets move to $Q_3^{(1)}$, $Q_3^{(2)}$, or none of them. The flow dynamics in (75) - (80) show that a packet leaves $Q_3^{(1)}$ if and only if a packet leaves $Q_3^{(2)}$, provided that both $Q_3^{(1)}$ and $Q_3^{(2)}$ are nonempty. This implies that $Q_3^{(1)}$ and $Q_3^{(2)}$ always contain the same number of packets, provided that both queues are empty in the beginning and only non-degenerate cases occur.

Suppose $Q_{1,t}^{(1)} > 0$, $Q_{1,t}^{(2)} = 0$ and $A_t = 4$: In this case, the poisoned packet only consists of a single original packet $p_l^{(1)}$, because there is no packet in $Q_1^{(2)}$. Hence, this packet is uncoded in principle and could follow the same packet movement rules as if $A_t = 1$ was chosen. However, that would violate the flow dynamics in (76), which require that a packet moves from $Q_1^{(1)}$ to $Q_3^{(1)}$ for $A_t = 4$ unless erased at both Rx_1 and Rx_2 .

To deal with this case, we split the queues $Q_3^{(j)}$ into two subqueues $Q_3^{(j)\text{nondeg}}$ and $Q_3^{(j)\text{deg}}$, with

$$Q_{3,t}^{(j)} = Q_{3,t}^{(j)\text{nondeg}} + Q_{3,t}^{(j)\text{deg}}. \quad (162)$$

$Q_3^{(j)\text{nondeg}}$ contains only original packets that were involved in a non-degenerate poisoned packet. Each packet in $Q_3^{(1)\text{nondeg}}$ is linked to a packet in $Q_3^{(2)\text{nondeg}}$ with which it was combined in a poisoned packet. $Q_3^{(j)\text{deg}}$ contains original packets for degenerate poisoned packets. $Q_3^{(1)\text{nondeg}}$ and $Q_3^{(2)\text{nondeg}}$ always contain the same number of packets, but the number of packets in $Q_3^{(1)\text{deg}}$ and $Q_3^{(2)\text{deg}}$ may be different.

In the degenerate case we move the poisoned packet $p_l^{(1)}$ from $Q_1^{(1)}$ to $Q_3^{(1)\text{deg}}$ if it is not erased at both Rx₁ and Rx₂, as suggested by (76). We perform this movement even if $p_l^{(1)}$ was received by Rx₁ and hence already reached its destination⁹. Hence, this packet movement is suboptimal in principle, but ensures that (76) is satisfied. This applies similarly for $Q_{1,t}^{(1)} = 0$, $Q_{1,t}^{(2)} > 0$ and $A_t = 4$.

Remark 12. Note that the packet movement from $Q_1^{(1)}$ to $Q_3^{(1)}$ is independent of the number of packets in $Q_1^{(2)}$, as required by (76), and vice versa.

For $A_t = 5$, i.e. when moving packets out of $Q_3^{(j)}$, we want ensure that also (79) and (80) hold, regardless if we move the packet out of $Q_3^{(j)\text{nondeg}}$ or $Q_3^{(j)\text{deg}}$. Consider the following policy:

- Whenever $Q_3^{(1)\text{nondeg}}$ and $Q_3^{(2)\text{nondeg}}$ are nonempty and $A_t = 5$, we pick the pair of original packets in $Q_3^{(1)\text{nondeg}}$ and $Q_3^{(2)\text{nondeg}}$ that arrived first and apply the remedy packet transmission as described in Table I.
- When both $Q_3^{(1)\text{nondeg}}$ and $Q_3^{(2)\text{nondeg}}$ are empty, $Q_3^{(1)\text{deg}}$ is empty and $Q_3^{(2)\text{deg}}$ is nonempty, one can retransmit the packet $p_m^{(2)}$ as a remedy packet. This remedy transmission then follows the same rules as an uncoded transmission under $A_t = 2$ and hence satisfies (79) and (80). Similarly for $Q_3^{(1)\text{deg}}$ being nonempty and $Q_3^{(2)\text{deg}}$ empty.
- Suppose $Q_3^{(1)\text{nondeg}}$ and $Q_3^{(2)\text{nondeg}}$ are empty and both $Q_3^{(1)\text{deg}}$ and $Q_3^{(2)\text{deg}}$ are nonempty: Hence $Q_3^{(1)\text{deg}}$ contains $p_l^{(1)}$ and $Q_3^{(2)\text{deg}}$ contains $p_m^{(2)}$, but these packets arrived in different time slots at $Q_3^{(1)\text{deg}}$, $Q_3^{(2)\text{deg}}$, respectively. They were not combined to a poisoned packet, but they were both degenerate poisoned packets. In this case, it matters at which receivers $p_l^{(1)}$ and $p_m^{(2)}$ were received, respectively, and how the corresponding remedy packet looks like. All different possibilities are described in Table VI.

Example 3. For further illustration, we pick an example: Suppose poison $p_l^{(1)}$ is received at Rx₁ only and $p_m^{(2)}$ is also received at Rx₁ only. This corresponds to the first line in Table VI. Note that $p_l^{(1)}$ is - in principle - already known at its destination Rx₁. However, we do not account for this, i.e. we do not move it to $Q_4^{(1)}$.

We choose $p_m^{(2)}$ as the remedy packet and consider the following cases:

- If the remedy packet is received at Rx₁ only, we *release* $p_l^{(1)}$ at Rx₁. That is, $p_l^{(1)}$ has been received at Rx₁ before and was not counted, but we count it now and move it to $Q_4^{(1)}$. Because the remedy $p_m^{(2)}$ was received at Rx₁ we move it from $Q_3^{(2)}$ to $Q_2^{(2)}$. Note that we could have done that already before, as $p_m^{(2)}$ was received as a poisoned packet at Rx₁ before.
- If the remedy packet is received at Rx₂ only, we move $p_m^{(2)}$ to $Q_4^{(2)}$ as it was received at Rx₂. The flow dynamics in (79) require that $p_l^{(1)}$ should move from $Q_3^{(1)}$ to $Q_2^{(1)}$: We can achieve this by replacing $p_l^{(1)}$ with a dummy packet $p_\star^{(1)}$ that is known to Rx₂ and identified via a flag. Once this dummy packet $p_\star^{(1)}$ is combined in a reactive coding operation ($A_t = 3$), and received at Rx₁ we release (the previously already received) $p_l^{(1)}$ at Rx₁, satisfying the flow dynamics.
- If the remedy packet $p_m^{(2)}$ is received at Rx₁ and Rx₂, we release the (previously received) packet $p_l^{(1)}$ at Rx₁ and move it to $Q_4^{(1)}$. Packet $p_m^{(2)}$ is received at Rx₂, so we can also move it to $Q_4^{(2)}$.

The other cases require slightly different operations for the remedy packet, but the procedure is similar to this case. \square

Remark 13. In all cases, the packet movement from $Q_3^{(1)}$ to $Q_2^{(1)}$ or $Q_4^{(1)}$ is independent of the number of packets contained in $Q_3^{(2)}$, as required by (79) and (80).

⁹The header information can be used to distinguish whether an uncoded packet was transmitted due to $A_t = 1$ or $A_t = 4$.

poison $p_l^{(1)}$ received at	poison $p_m^{(2)}$ received at	remedy	remedy received at Rx ₁	remedy received at Rx ₂	remedy rec. at Rx ₁ and Rx ₂
Rx ₁ only	Rx ₁ only	$p_m^{(2)}$	Release $p_l^{(1)}$ at Rx ₁ ⇒ $p_l^{(1)}$ to $Q_4^{(1)}$ (exit) ⇒ $p_m^{(2)}$ to $Q_2^{(2)}$	⇒ $p_m^{(2)}$ to $Q_4^{(2)}$ (exit) ⇒ Replace $p_l^{(1)}$ with $p_\star^{(1)}$ and move to $Q_2^{(1)}$	Release $p_l^{(1)}$ at Rx ₁ ⇒ $p_l^{(1)}$ to $Q_4^{(1)}$ (exit) ⇒ $p_m^{(2)}$ to $Q_4^{(2)}$ (exit)
Rx ₁ only	Rx ₂ only	$p_m^{(2)}$	Release $p_l^{(1)}$ at Rx ₁ ⇒ $p_l^{(1)}$ to $Q_4^{(1)}$ (exit) ⇒ Put $p_m^{(2)}$ to $Q_2^{(2)}$	⇒ $p_m^{(2)}$ to $Q_4^{(2)}$ (exit) ⇒ Replace $p_l^{(1)}$ with $p_\star^{(1)}$ and move to $Q_2^{(1)}$	Release both $p_l^{(1)}$ and $p_m^{(2)}$ ⇒ $p_l^{(1)}$ to $Q_4^{(1)}$ (exit) ⇒ $p_m^{(2)}$ to $Q_4^{(2)}$ (exit)
Rx ₁ only	Rx ₁ and Rx ₂	$p_l^{(1)}$	Release $p_l^{(1)}$ at Rx ₁ ⇒ $p_l^{(1)}$ to $Q_4^{(1)}$ (exit) ⇒ Put $p_m^{(2)}$ to $Q_2^{(2)}$	Release $p_m^{(2)}$ at Rx ₂ ⇒ $p_m^{(2)}$ to $Q_4^{(2)}$ (exit) ⇒ Put $p_l^{(1)}$ to $Q_2^{(1)}$	Release both $p_l^{(1)}$ and $p_m^{(2)}$ ⇒ $p_l^{(1)}$ to $Q_4^{(1)}$ (exit) ⇒ $p_m^{(2)}$ to $Q_4^{(2)}$ (exit)
Rx ₂ only	Rx ₁ only	$p_l^{(1)} \oplus p_m^{(2)}$	Rx ₁ decodes $p_l^{(1)}$ ⇒ $p_l^{(1)}$ to $Q_4^{(1)}$ (exit) ⇒ Put $p_m^{(2)}$ to $Q_2^{(2)}$	Rx ₂ decodes $p_m^{(2)}$ ⇒ $p_m^{(2)}$ to $Q_4^{(2)}$ (exit) ⇒ Put $p_l^{(1)}$ to $Q_2^{(1)}$	Rx ₁ decodes $p_l^{(1)}$, Rx ₂ de- codes $p_m^{(2)}$ ⇒ $p_l^{(1)}$ to $Q_4^{(1)}$ (exit) ⇒ $p_m^{(2)}$ to $Q_4^{(2)}$ (exit)
Rx ₂ only	Rx ₂ only	$p_l^{(1)}$	Rx ₁ gets $p_l^{(1)}$ ⇒ $p_l^{(1)}$ to $Q_4^{(1)}$ (exit) ⇒ Replace $p_m^{(2)}$ with $p_\star^{(2)}$ and move to $Q_2^{(2)}$	Release $p_m^{(2)}$ at Rx ₂ ⇒ $p_m^{(2)}$ to $Q_4^{(2)}$ (exit) ⇒ Put $p_l^{(1)}$ to $Q_2^{(1)}$	Rx ₁ receives $p_l^{(1)}$, release $p_m^{(2)}$ at Rx ₂ ⇒ $p_l^{(1)}$ to $Q_4^{(1)}$ (exit) ⇒ $p_m^{(2)}$ to $Q_4^{(2)}$ (exit)
Rx ₂ only	Rx ₁ and Rx ₂	$p_l^{(1)}$	Rx ₁ gets $p_l^{(1)}$ ⇒ $p_l^{(1)}$ to $Q_4^{(1)}$ (exit) ⇒ Put $p_m^{(2)}$ to $Q_2^{(2)}$	Release $p_m^{(2)}$ at Rx ₂ ⇒ $p_m^{(2)}$ to $Q_4^{(2)}$ (exit) ⇒ Put $p_l^{(1)}$ to $Q_2^{(1)}$	Rx ₁ receives $p_l^{(1)}$, release $p_m^{(2)}$ at Rx ₂ ⇒ $p_l^{(1)}$ to $Q_4^{(1)}$ (exit) ⇒ $p_m^{(2)}$ to $Q_4^{(2)}$ (exit)
Rx ₁ and Rx ₂	Rx ₁	$p_m^{(2)}$	Release $p_l^{(1)}$ at Rx ₁ ⇒ $p_l^{(1)}$ to $Q_4^{(1)}$ (exit) ⇒ Put $p_m^{(2)}$ to $Q_2^{(2)}$	Rx ₂ receives $p_m^{(2)}$ ⇒ $p_m^{(2)}$ to $Q_4^{(2)}$ (exit) ⇒ Put $p_l^{(1)}$ to $Q_2^{(1)}$	Release $p_l^{(1)}$ at Rx ₁ ⇒ $p_l^{(1)}$ to $Q_4^{(1)}$ (exit) ⇒ $p_m^{(2)}$ to $Q_4^{(2)}$ (exit)
Rx ₁ and Rx ₂	Rx ₂	$p_m^{(2)}$	Release $p_l^{(1)}$ at Rx ₁ ⇒ $p_l^{(1)}$ to $Q_4^{(1)}$ (exit) ⇒ Put $p_m^{(2)}$ to $Q_2^{(2)}$	Release $p_m^{(2)}$ at Rx ₂ ⇒ $p_m^{(2)}$ to $Q_4^{(2)}$ (exit) ⇒ Put $p_l^{(1)}$ to $Q_2^{(1)}$	Release $p_l^{(1)}$ at Rx ₁ and $p_m^{(2)}$ at Rx ₂ ⇒ $p_l^{(1)}$ to $Q_4^{(1)}$ (exit) ⇒ $p_m^{(2)}$ to $Q_4^{(2)}$ (exit)
Rx ₁ and Rx ₂	Rx ₁ and Rx ₂	$p_l^{(1)}$	Release $p_l^{(1)}$ at Rx ₁ ⇒ $p_l^{(1)}$ to $Q_4^{(1)}$ (exit) ⇒ Put $p_m^{(2)}$ to $Q_2^{(2)}$	Release $p_m^{(2)}$ at Rx ₂ ⇒ $p_m^{(2)}$ to $Q_4^{(2)}$ (exit) ⇒ Put $p_l^{(1)}$ to $Q_2^{(1)}$	Release $p_l^{(1)}$ at Rx ₁ and $p_m^{(2)}$ at Rx ₂ ⇒ $p_l^{(1)}$ to $Q_4^{(1)}$ (exit) ⇒ $p_m^{(2)}$ to $Q_4^{(2)}$ (exit)

Resulting capacity:

$C_{34}^{(1)} = 1, C_{32}^{(2)} = 1$

$C_{32}^{(1)} = 1, C_{34}^{(2)} = 1$

$C_{34}^{(1)} = 1, C_{34}^{(2)} = 1$

TABLE VI: Packet movement for poisoned packets in $Q_3^{(1)}$ and $Q_3^{(2)}$ - degenerate cases.

APPENDIX F
PROOF OF PROPOSITION 7

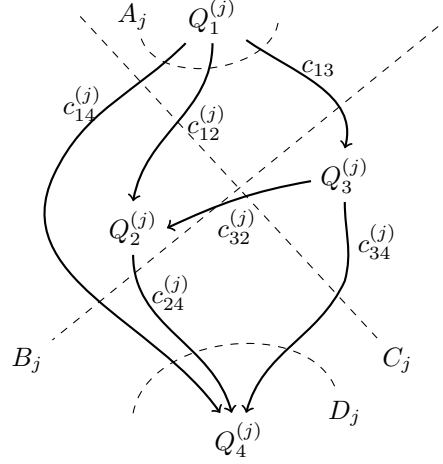


Fig. 19: Queue network and cuts.

We define the variables $A_j, B_j, C_j, D_j, j \in \{1, 2\}$ as the cut values in (90) - (93) (see Fig. 19):

$$\begin{aligned} A_j &= c_{12}^{(j)} + c_{13} + c_{14}^{(j)} \\ &= \sum_{s \in \mathcal{S}} \pi_s (1 - \epsilon_{12}(s)) [P_{A_t|S_{t-1}}(j|s) + P_{A_t|S_{t-1}}(4|s)] \end{aligned} \quad (163)$$

$$\begin{aligned} B_j &= c_{13} + c_{14}^{(j)} + c_{24}^{(j)} \\ &= \sum_{s \in \mathcal{S}} \pi_s \left[(1 - \epsilon_{12}(s)) P_{A_t|S_{t-1}}(4|s) + (1 - \epsilon_j(s)) [P_{A_t|S_{t-1}}(j|s) + P_{A_t|S_{t-1}}(3|s)] \right] \end{aligned} \quad (164)$$

$$\begin{aligned} C_j &= c_{12}^{(j)} + c_{14}^{(j)} + c_{32}^{(j)} + c_{34}^{(j)} \\ &= \sum_{s \in \mathcal{S}} \pi_s (1 - \epsilon_{12}(s)) [P_{A_t|S_{t-1}}(j|s) + P_{A_t|S_{t-1}}(5|s)] \end{aligned} \quad (165)$$

$$\begin{aligned} D_j &= c_{14}^{(j)} + c_{24}^{(j)} + c_{34}^{(j)} \\ &= \sum_{s \in \mathcal{S}} \pi_s (1 - \epsilon_j(s)) [P_{A_t|S_{t-1}}(j|s) + P_{A_t|S_{t-1}}(3|s) + P_{A_t|S_{t-1}}(5|s)] \end{aligned} \quad (166)$$

We omit the superscript (j) for c_{13} to emphasize that $c_{13}^{(1)} = c_{13}^{(2)} = c_{13}$.

Our goal is to show that for any link capacities $c_{rl}^{(j)}$ and associated cut values A_j, B_j, C_j, D_j induced by a distribution $P_{A_t|S_{t-1}}$, there is another distribution $P_{A_t|S_{t-1}}^*$ with associated link capacities $c_{rl}^{(j)*}$ and cut values $A_j^*, B_j^*, C_j^*, D_j^*$ such that

$$\min \{A_j^*, B_j^*, C_j^*, D_j^*\} = \min \{A_j, B_j, C_j, D_j\} \quad (167)$$

$$\min \{A_j^*, B_j^*, C_j^*, D_j^*\} = \min \{A_j^*, D_j^*\}. \quad (168)$$

That is, the minimal cut value does not change under $P_{A_t|S_{t-1}}^*$, but the cuts B_j^* and C_j^* are redundant. The next lemma states one sufficient condition:

Lemma 10. The cut values B_j and C_j are redundant for both $j = 1, 2$ if $P_{A_t|S_{t-1}}$ leads to

$$c_{13} = c_{32}^{(j)} + c_{34}^{(j)} \quad \forall j \in \{1, 2\}. \quad (169)$$

Proof: The condition in (169) is equivalent to

$$\sum_{s \in \mathcal{S}} \pi_s (1 - \epsilon_{12}(s)) P_{A_t|S_{t-1}}(4|s) = \sum_{s \in \mathcal{S}} \pi_s (1 - \epsilon_{12}(s)) P_{A_t|S_{t-1}}(5|s). \quad (170)$$

One can verify that $C_j = A_j$ in this case, so C_j can be omitted. Additionally, $D_j \leq B_j$ because

$$B_j - D_j = c_{13} + c_{14}^{(j)} + c_{24}^{(j)} - (c_{14}^{(j)} + c_{24}^{(j)} + c_{34}^{(j)})$$

$$\begin{aligned}
&= \left(\sum_{s \in \mathcal{S}} \pi_s (1 - \epsilon_{12}(s)) P_{A_t|S_{t-1}}(4|s) \right) - \left(\sum_{s \in \mathcal{S}} \pi_s (1 - \epsilon_j(s)) P_{A_t|S_{t-1}}(5|s) \right) \\
&= \left(\sum_{s \in \mathcal{S}} \pi_s (1 - \epsilon_{12}(s)) P_{A_t|S_{t-1}}(5|s) \right) - \left(\sum_{s \in \mathcal{S}} \pi_s (1 - \epsilon_j(s)) P_{A_t|S_{t-1}}(5|s) \right) \\
&\geq 0,
\end{aligned} \tag{171}$$

where the last inequality is due to $1 - \epsilon_{12}(s) \geq 1 - \epsilon_j(s)$ for all $s \in \mathcal{S}$ and $j \in \{1, 2\}$. \blacksquare

Remark 14. Note that one *cannot* simply set $P_{A_t|S_{t-1}}(4|s) = P_{A_t|S_{t-1}}(5|s)$, $\forall s \in \mathcal{S}$, to ensure (169). By the mapping in (98) - (99), this would require $x_s + y_s \geq 1$, $\forall s \in \mathcal{S}$ and hence permit only a limited set of values for x_s and y_s .

For any given distribution $P_{A_t|S_{t-1}}$, we choose $P_{A_t|S_{t-1}}^*$ such that $\forall s \in \mathcal{S}$:

$$P_{A_t|S_{t-1}}^*(0|s) = P_{A_t|S_{t-1}}(0|s) \tag{172}$$

$$P_{A_t|S_{t-1}}^*(1|s) = P_{A_t|S_{t-1}}(1|s) \tag{173}$$

$$P_{A_t|S_{t-1}}^*(2|s) = P_{A_t|S_{t-1}}(2|s) \tag{174}$$

$$P_{A_t|S_{t-1}}^*(4|s) = P_{A_t|S_{t-1}}(4|s) \tag{175}$$

$$P_{A_t|S_{t-1}}^*(3|s) + P_{A_t|S_{t-1}}^*(5|s) = P_{A_t|S_{t-1}}(3|s) + P_{A_t|S_{t-1}}(5|s) \tag{176}$$

By choosing $P_{A_t|S_{t-1}}^*(3|s) \neq P_{A_t|S_{t-1}}(3|s)$, $P_{A_t|S_{t-1}}^*(5|s) \neq P_{A_t|S_{t-1}}(5|s)$, the link capacities $c_{24}^{(j)*}$, $c_{34}^{(j)*}$ and $c_{32}^{(j)*}$, $j \in \{1, 2\}$ are varied. The other link capacities are not affected, hence

$$c_{12}^{(j)*} = c_{12}^{(j)}, \quad c_{13}^{(j)*} = c_{13}^{(j)}, \quad c_{14}^{(j)*} = c_{14}^{(j)}, \quad j \in \{1, 2\}. \tag{177}$$

In the following we therefore omit the superscript \star for those capacities that stay constant with $P_{A_t|S_{t-1}}$ and $P_{A_t|S_{t-1}}^*$.

Note that $A_j^* = A_j$, $D_j^* = D_j$, $j \in \{1, 2\}$ because

- A_j^* is not affected by changing $P_{A_t|S_{t-1}}^*(3|s)$ and $P_{A_t|S_{t-1}}^*(5|s)$ and
- D_j^* depends only on the sum $P_{A_t|S_{t-1}}^*(3|s) + P_{A_t|S_{t-1}}^*(5|s)$ that is kept constant (176), hence

$$c_{24}^{(j)} + c_{34}^{(j)} = c_{24}^{(j)*} + c_{34}^{(j)*}. \tag{178}$$

By changing $P_{A_t|S_{t-1}}^*(3|s)$ and $P_{A_t|S_{t-1}}^*(5|s)$ under the sum-constraint (176) one can obtain the maximal and minimal link capacities for $c_{24}^{(j)*}$ and $c_{34}^{(j)*}$, as follows:

- 1) $c_{24}^{(j)*} = D_j - c_{14}^{(j)}$, $c_{34}^{(j)*} = 0$, $j \in \{1, 2\}$,
by setting $P_{A_t|S_{t-1}}^*(3|s) = P_{A_t|S_{t-1}}(3|s) + P_{A_t|S_{t-1}}(5|s)$ and $P_{A_t|S_{t-1}}^*(5|s) = 0$, $\forall s \in \mathcal{S}$.
- 2) $c_{24}^{(j)*} = 0$, $c_{34}^{(j)*} = D_j - c_{14}^{(j)}$, $j \in \{1, 2\}$,
by setting $P_{A_t|S_{t-1}}^*(3|s) = 0$ and $P_{A_t|S_{t-1}}^*(5|s) = P_{A_t|S_{t-1}}(3|s) + P_{A_t|S_{t-1}}(5|s)$, $\forall s \in \mathcal{S}$.

Due to the continuity of the link capacities with respect to $P_{A_t|S_{t-1}}^*$, any convex combination of $(D_j - c_{14}^{(j)}, 0)$ and $(0, D_j - c_{14}^{(j)})$ can be obtained for $(c_{24}^{(j)*}, c_{34}^{(j)*})$.

We now show that choosing $P_{A_t|S_{t-1}}^*$ as in (172) - (176) suffices to ensure the desired criteria (167) - (168). We distinguish two cases. For one case, we use Lemma 10.

- Case I: $A_j \leq D_j$ for at least one $j \in \{1, 2\}$. This happens if we have

$$c_{12}^{(j)} + c_{13} \leq c_{24}^{(j)} + c_{34}^{(j)} \quad \text{for some } j \in \{1, 2\}. \tag{179}$$

In this case we choose $P_{A_t|S_{t-1}}^*(5|s)$ such that $c_{34}^{(j)*} = c_{13} - c_{32}^{(j)*}$. By Lemma 10, this suffices to ensure the criteria (167) - (168).

We can always find such values for $P_{A_t|S_{t-1}}^*(5|s)$ because, by definition of Case I in (179), there is a $j \in \{1, 2\}$ for which

$$D_j - c_{14}^{(j)} \geq c_{12}^{(j)} + c_{13}. \tag{180}$$

The LHS of (180) is the maximal possible link capacity for $c_{34}^{(j)*}$. The RHS of (180) is larger than (or equal to) $c_{13} - c_{32}^{(j)*}$, which is the desired value for $c_{34}^{(j)*}$. We can adjust $c_{34}^{(j)*}$ between 0 and $D_j - c_{14}^{(j)}$. As $c_{13} - c_{32}^{(j)*}$ lies in this interval, we can choose values for $P_{A_t|S_{t-1}}^*(5|s)$ such that $c_{34}^{(j)*} = c_{13} - c_{32}^{(j)*}$.

- Case II: $D_j < A_j$ for both $j \in \{1, 2\}$.

In this case the sufficient criterion in Lemma 10 cannot be guaranteed, since it is possible that there is no distribution $P_{A_t|S_{t-1}}^*(5|s)$ such that $c_{13} = c_{32}^{(j)*} + c_{34}^{(j)*}$. To satisfy the criteria (167) - (168), we need for both $j \in \{1, 2\}$:

$$D_j \leq B_j^* \Leftrightarrow c_{34}^{(j)*} \leq c_{13} \quad (181)$$

$$D_j \leq C_j^* \Leftrightarrow c_{24}^{(j)*} \leq c_{32}^{(j)*} + c_{12}^{(j)} \quad (182)$$

In this case we choose $P_{A_t|S_{t-1}}^*(5|s)$ such that $\max\{c_{34}^{(1)*}, c_{34}^{(2)*}\}$ is as large as possible, but at most equal to c_{13} , in order not to violate (181). Two sub-cases must be distinguished: leftmargin=+17mm

- Case IIa: One can choose $P_{A_t|S_{t-1}}^*(5|s)$ such that $\max\{c_{34}^{(1)*}, c_{34}^{(2)*}\} = c_{13}$.

The condition in (181) is satisfied by construction, so we have to check only (182). Note that the following inequalities always hold for Case IIa:

$$\begin{aligned} c_{24}^{(j)} + c_{34}^{(j)} &< c_{12}^{(j)} + c_{13}, && \text{because } D_j < A_j, \text{ and} \\ c_{24}^{(j)*} + c_{34}^{(j)*} &< c_{12}^{(j)} + c_{13}, && \text{because of (178). Hence,} \\ c_{24}^{(j)*} &< c_{12}^{(j)} + (c_{13} - c_{34}^{(j)*}). \end{aligned} \quad (183)$$

For condition (182) to hold, the term $(c_{13} - c_{34}^{(j)*})$ should be smaller than (or equal to) $c_{32}^{(j)*}$ for both $j \in \{1, 2\}$. For $j_{\max} = \operatorname{argmax}_{j \in \{1, 2\}} c_{34}^{(j)*}$, we have $c_{13} - c_{34}^{(j_{\max})*} = 0$, satisfying the condition. For $j_{\min} = \operatorname{argmin}_{j \in \{1, 2\}} c_{34}^{(j)*}$, we have $c_{13} - c_{34}^{(j_{\min})*} \geq 0$. We next show that $c_{13} - c_{34}^{(j_{\min})*} \leq c_{32}^{(j_{\min})*}$ holds for this case as well. As $c_{13} = c_{34}^{(j_{\max})*}$, we have

$$\begin{aligned} c_{13} - c_{34}^{(j_{\min})*} &= c_{34}^{(j_{\max})*} - c_{34}^{(j_{\min})*} \\ &= \sum_{s \in \mathcal{S}} \pi_s (\epsilon_{j_{\min}}(s) - \epsilon_{j_{\max}}(s)) P_{A_t|S_{t-1}}^*(5|s) \geq 0. \end{aligned}$$

The following statement shows that $c_{13} - c_{34}^{(j_{\min})*} \leq c_{32}^{(j_{\min})*}$:

$$\begin{aligned} c_{13} - c_{34}^{(j_{\min})*} - c_{32}^{(j_{\min})*} &= \sum_{s \in \mathcal{S}} \pi_s [(\epsilon_{j_{\min}}(s) - \epsilon_{j_{\max}}(s)) - (\epsilon_{j_{\min}}(s) - \epsilon_{12}(s))] P_{A_t|S_{t-1}}^*(5|s) \\ &= \sum_{s \in \mathcal{S}} \pi_s [\epsilon_{12}(s) - \epsilon_{j_{\max}}(s)] P_{A_t|S_{t-1}}^*(5|s) \leq 0, \end{aligned} \quad (184)$$

as $\epsilon_{12}(s) - \epsilon_{j_{\max}}(s) \leq 0$ for all $s \in \mathcal{S}$, $j \in \{1, 2\}$. This shows that the choice of $P_{A_t|S_{t-1}}^*(5|s)$ such that $\max\{c_{34}^{(1)*}, c_{34}^{(2)*}\} = c_{13}$ suffices to achieve the criteria (167) - (168).

- Case IIb: Choosing the maximal $P_{A_t|S_{t-1}}^*(5|s) \forall s \in \mathcal{S}$ leads to $\max\{c_{34}^{(1)*}, c_{34}^{(2)*}\} < c_{13}$.

This immediately satisfies the condition in (181). As $P_{A_t|S_{t-1}}^*(5|s)$ is maximal, we have $P_{A_t|S_{t-1}}^*(3|s) = 0 \forall s \in \mathcal{S}$.

Hence, we have $c_{24}^{(j)*} = 0, \forall j \in \{1, 2\}$, satisfying the condition (182).

This completes the proof.

APPENDIX G PROOF OF MAX-WEIGHT SCHEMES

A. Visible Case

The objective is to show that the max-weight criterion in (100) strongly stabilizes all queues in the network, as defined in (7). We use Lyapunov-drift theory to prove the result.

Recall the dynamics of queues $Q_{1,t}^{(j)}$, $Q_{2,t}^{(j)}$ and $Q_{3,t}^{(j)}$ defined in (72):

$$Q_{1,t+1}^{(j)} \leq [Q_{1,t}^{(j)} - F_{12,t}^{(j)} - F_{13,t}^{(j)} - F_{14,t}^{(j)}]^+ + F_{01,t}^{(j)} \quad (185)$$

$$Q_{2,t+1}^{(j)} \leq [Q_{2,t}^{(j)} - F_{24,t}^{(j)}]^+ + F_{12,t}^{(j)} + F_{32,t}^{(j)} \quad (186)$$

$$Q_{3,t+1}^{(j)} \leq [Q_{3,t}^{(j)} - F_{32,t}^{(j)} - F_{34,t}^{(j)}]^+ + F_{13,t}^{(j)} \quad (187)$$

The flow variables $F_{lm,t}^{(j)}$ depend on the action A_t , the activation variables \underline{E}_t and the erasures \underline{Z}_t , so the queue state Q_{t+1} is a function of Q_t , A_t , \underline{E}_t and \underline{Z}_t . Actions are restricted to depend only on the current queue state and on the previous channel

state, hence are according to a distribution $P_{A_t|Q_t, S_{t-1}}$. Packet movement decisions may depend on the current queue state, hence are according to $P_{E_t|Q_t}$. This may be a suboptimal choice, but we will see that it suffices to achieve all rate points inside $\underline{C}_{fb+s}^{\text{mem}}$. All dependencies are depicted in the Bayesian network in Fig. 20.

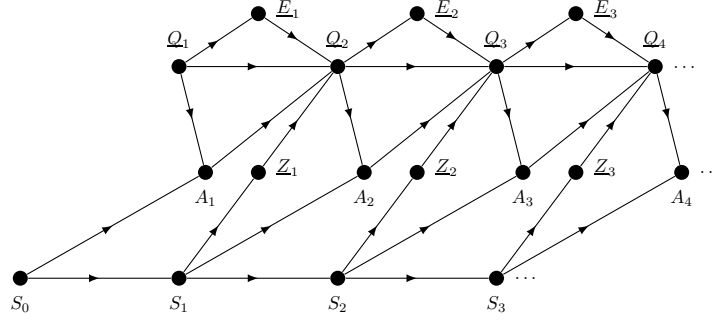


Fig. 20: Bayesian network of the queuing system. Actions at time t may depend on the previous channel state S_{t-1} and the current buffer state Q_t . Note that Q_t denotes the buffer state *before* executing action A_t .

Define the Lyapunov function $\mathbb{L}(Q_t)$ as

$$\mathbb{L}(Q_t) = \sum_{j=1}^2 \sum_{l=1}^3 \left(Q_{l,t}^{(j)} \right)^2 \quad (188)$$

and the T -slot conditional Lyapunov drift $\Delta(Q_t)$ as

$$\Delta(Q_t) = \mathbb{E} \left[\mathbb{L}(Q_{t+T}) - \mathbb{L}(Q_t) \mid Q_t \right], \quad (189)$$

where the expectation is with respect to the possibly random actions $A_t, A_{t+1}, \dots, A_{t+T-1}$, erasures $\underline{Z}_t, \dots, \underline{Z}_{t+T-1}$, packet movement decisions $\underline{E}_t, \dots, \underline{E}_{t+T-1}$ and queues Q_{t+1}, \dots, Q_{t+T} . $\Delta(Q_t)$ measures the expected reduction or increase of the aggregate queue lengths from slot t to slot $t+T$, conditioned on Q_t , and will be useful to prove strong stability.

Split $\Delta(Q_t)$ into the telescoping sum

$$\begin{aligned} \Delta(Q_t) &= \mathbb{E} \left[\sum_{\tau=t}^{t+T-1} \mathbb{L}(Q_{\tau+1}) - \mathbb{L}(Q_{\tau}) \mid Q_t \right] \\ &= \sum_{\tau=t}^{t+T-1} \mathbb{E} \left[\mathbb{L}(Q_{\tau+1}) - \mathbb{L}(Q_{\tau}) \mid Q_t \right]. \end{aligned} \quad (190)$$

Note that the individual expectation terms of the sum in (190) depend on the conditioning Q_t only through Q_{τ} and $S_{\tau-1}$, as $Q_{\tau+1} A_{\tau} \underline{Z}_{\tau} - Q_{\tau} S_{\tau-1} - Q_t$ forms a Markov chain for $\tau \geq t$. Hence, one can use the law of total expectation and write

$$\Delta(Q_t) = \sum_{\tau=t}^{t+T-1} \mathbb{E} \left[\mathbb{E} \left[\mathbb{L}(Q_{\tau+1}) - \mathbb{L}(Q_{\tau}) \mid Q_{\tau} S_{\tau-1} \right] \mid Q_t \right]. \quad (191)$$

We will bound the individual terms inside the inner expectation of (191).

We can use [32, Lemma 4.3], which states that for any nonnegative numbers v, u, μ, α satisfying $v \leq [u - \mu]^+ + \alpha$, we have

$$v^2 \leq u^2 + \mu^2 + \alpha^2 - 2u(\mu - \alpha). \quad (192)$$

We apply this lemma and combine it with $(C_{lm,\tau}^{(j)})^2 = C_{lm,\tau}^{(j)} \leq 1$ because $C_{lm,\tau}^{(j)}$ is either 1 or 0 and obtain the following bound:

$$\mathbb{L}(Q_{\tau+1}) - \mathbb{L}(Q_{\tau}) \leq 12 - 2 \sum_{j=1}^2 Q_{1,\tau}^{(j)} D_{1,\tau}^{(j)} + Q_{2,\tau}^{(j)} D_{2,\tau}^{(j)} + Q_{3,\tau}^{(j)} D_{3,\tau}^{(j)}, \quad (193)$$

where $D_{l,\tau}^{(j)}$ is the flow divergence defined in (70).

The bound in (193) is used to develop a bound on $\Delta(Q_t)$. First, we insert (193) into (191) to obtain

$$\Delta(Q_t) \leq \sum_{\tau=t}^{t+T-1} 12 - 2 \cdot \mathbb{E} \left[\sum_{j=1}^2 \sum_{l=1}^3 \mathbb{E} \left[Q_{l,\tau}^{(j)} D_{l,\tau}^{(j)} \mid Q_{\tau} S_{\tau-1} \right] \mid Q_t \right] \quad (194)$$

$$= \sum_{\tau=t}^{t+T-1} 12 - 2 \cdot \mathbb{E} \left[\sum_{j=1}^2 \sum_{l=1}^3 \sum_{m \in \mathcal{O}_l} \mathbb{E} \left[F_{lm,\tau}^{(j)} \left(Q_{l,\tau}^{(j)} - Q_{m,\tau}^{(j)} \right) \middle| \underline{Q}_\tau S_{\tau-1} \right] - Q_{1,\tau}^{(j)} R_j \middle| \underline{Q}_t \right] \quad (195)$$

$$= \sum_{\tau=t}^{t+T-1} 12 - 2 \cdot \mathbb{E} \left[\sum_{j=1}^2 \sum_{l=1}^3 \sum_{m \in \mathcal{O}_l} \mathbb{E} \left[E_{lm,\tau}^{(j)} C_{lm,\tau}^{(j)} \left(Q_{l,\tau}^{(j)} - Q_{m,\tau}^{(j)} \right) \middle| \underline{Q}_\tau S_{\tau-1} \right] - Q_{1,\tau}^{(j)} R_j \middle| \underline{Q}_t \right], \quad (196)$$

where \mathcal{O}_l contains all queue indices m for which a link from queue $Q_l^{(j)}$ to $Q_m^{(j)}$ exists, with the understanding that $Q_{4,\tau}^{(j)} = 0$.

In (196), we have to maximize the inner expectation with respect to $P_{\underline{E}_\tau | \underline{Q}_\tau}$ and $P_{A_\tau | \underline{Q}_\tau S_{\tau-1}}$ to find the tightest upper bound on $\Delta(\underline{Q}_t)$. Because $C_{lm,\tau}^{(j)}$ is nonnegative, we can first choose $E_{lm,\tau}^{(j)} = 1$ if $(Q_{l,\tau}^{(j)} - Q_{m,\tau}^{(j)}) > 0$ and 0 otherwise, hence we obtain

$$\Delta(\underline{Q}_t) \leq \sum_{\tau=t}^{t+T-1} 12 - 2 \cdot \mathbb{E} \left[\sum_{j=1}^2 \sum_{l=1}^3 \sum_{m \in \mathcal{O}(l)} \left[Q_{l,\tau}^{(j)} - Q_{m,\tau}^{(j)} \right]^+ \mathbb{E} \left[C_{lm,\tau}^{(j)} \middle| \underline{Q}_\tau S_{\tau-1} \right] - Q_{1,\tau}^{(j)} R_j \middle| \underline{Q}_t \right]. \quad (197)$$

The individual terms inside the inner expectation are derived in the following, using the definitions in (75) - (80):

$$\mathbb{E} \left[C_{12,\tau}^{(j)} \middle| \underline{Q}_\tau S_{\tau-1} \right] = \Pr[A_\tau = j | \underline{Q}_\tau S_{\tau-1}] (\epsilon_j(S_{\tau-1}) - \epsilon_{12}(S_{\tau-1})) \quad (198)$$

$$\mathbb{E} \left[C_{13,\tau}^{(j)} \middle| \underline{Q}_\tau S_{\tau-1} \right] = \Pr[A_\tau = 4 | \underline{Q}_\tau S_{\tau-1}] (1 - \epsilon_{12}(S_{\tau-1})) \quad (199)$$

$$\mathbb{E} \left[C_{14,\tau}^{(j)} \middle| \underline{Q}_\tau S_{\tau-1} \right] = \Pr[A_\tau = j | \underline{Q}_\tau S_{\tau-1}] (1 - \epsilon_j(S_{\tau-1})) \quad (200)$$

$$\mathbb{E} \left[C_{24,\tau}^{(j)} \middle| \underline{Q}_\tau S_{\tau-1} \right] = \Pr[A_\tau = 3 | \underline{Q}_\tau S_{\tau-1}] (1 - \epsilon_j(S_{\tau-1})) \quad (201)$$

$$\mathbb{E} \left[C_{32,\tau}^{(j)} \middle| \underline{Q}_\tau S_{\tau-1} \right] = \Pr[A_\tau = 5 | \underline{Q}_\tau S_{\tau-1}] (\epsilon_j(S_{\tau-1}) - \epsilon_{12}(S_{\tau-1})) \quad (202)$$

$$\mathbb{E} \left[C_{34,\tau}^{(j)} \middle| \underline{Q}_\tau S_{\tau-1} \right] = \Pr[A_\tau = 5 | \underline{Q}_\tau S_{\tau-1}] (1 - \epsilon_j(S_{\tau-1})), \quad (203)$$

where the expectation on the LHS is with respect to a distribution $P_{A_\tau | \underline{Q}_\tau S_{\tau-1}}$. All three relations follow because $\underline{Z}_\tau - S_{\tau-1} - A_\tau \underline{Q}_\tau$ forms a Markov chain.

The action in (100) results in the tightest upper bound on $\Delta(\underline{Q}_t)$ in (196): The distribution $P_{A_\tau | \underline{Q}_\tau S_{\tau-1}}$ that maximizes the expression inside the conditional expectation for every outcome of \underline{Q}_τ and $S_{\tau-1}$ also minimizes the upper bound in (196). The associated optimization problem is a linear program, constrained only by conditions that $P_{A_\tau | \underline{Q}_\tau S_{\tau-1}}$ must be a probability distribution. The optimizer of a linear program lies at the boundary of the constraint set, and thus the optimal conditional distribution is deterministic. Hence, choosing one action with probability 1 optimizes the max-weight criterion in (100).

Remark 15. Note that

- the criterion in (100) does not depend on τ ,
- actions are chosen only if the corresponding queues are nonempty, so no transmissions are wasted and $\tilde{F}_{lm,\tau}^{(j)} = C_{lm,\tau}^{(j)}$, unless there is a nonpositive differential backlog $Q_{l,\tau}^{(j)} - Q_{m,\tau}^{(j)}$.

The action in (100) results in the tightest upper bound in (196) under the assumption that actions can depend on \underline{Q}_τ and $S_{\tau-1}$. Hence, the deterministic scheme in Section VI-E always leads to a tighter upper bound on $\Delta(\underline{Q}_t)$ than any stationary probabilistic scheme that bases its decisions for A_τ only on $S_{\tau-1}$, according to a distribution $P_{A_\tau | S_{\tau-1}}$, and its decisions for \underline{E}_τ randomly on a distribution $P_{\underline{E}_\tau}$.

Given that the probabilistic scheme is used, we write the inner expectation in (194)

$$\mathbb{E} \left[Q_{l,\tau}^{(j)} D_{l,\tau}^{(j)} \middle| \underline{Q}_\tau S_{\tau-1} \right] = Q_{l,\tau}^{(j)} \mathbb{E} \left[D_{l,\tau}^{(j)} \middle| S_{\tau-1} \right] = Q_{l,\tau}^{(j)} d_l^{(j)}(S_{\tau-1}), \quad (204)$$

where the expectation on the LHS is with respect to some distributions $P_{A_\tau | S_{\tau-1}}$ and $P_{\underline{E}_\tau}$.

We use these arguments to further bound $\Delta(\underline{Q}_t)$ as follows. The individual steps are explained below.

$$\Delta(\underline{Q}_t) \stackrel{(a)}{\leq} \sum_{\tau=t}^{t+T-1} 12 - 2 \cdot \mathbb{E} \left[\sum_{j=1}^2 \sum_{l=1}^3 Q_{l,\tau}^{(j)} d_l^{(j)}(S_{\tau-1}) \middle| \underline{Q}_t \right] \quad (205)$$

$$\leq \sum_{\tau=t}^{t+T-1} 12 + 12(\tau - t) - 2 \cdot \mathbb{E} \left[\sum_{j=1}^2 \sum_{l=1}^3 Q_{l,t}^{(j)} d_l^{(j)}(S_{\tau-1}) \middle| \underline{Q}_t \right] \quad (206)$$

$$\stackrel{(c)}{=} 12T + 6T(T-1) - 2 \sum_{j=1}^2 \sum_{l=1}^3 \sum_{\tau=t}^{t+T-1} \sum_{s \in S} \Pr[S_{\tau-1} = s | \underline{Q}_t] Q_{l,t}^{(j)} d_l^{(j)}(s) \quad (207)$$

$$\stackrel{(d)}{=} 12T + 6T(T-1) - 2 \sum_{j=1}^2 \sum_{l=1}^3 Q_{l,t}^{(j)} \sum_{s \in \mathcal{S}} d_l^{(j)}(s) \sum_{\tau=t}^{t+T-1} \Pr[S_{\tau-1} = s | \underline{Q}_t] \quad (208)$$

$$\stackrel{(e)}{\leq} 12T + 6T^2 - 2T \sum_{j=1}^2 \sum_{l=1}^3 Q_{l,t}^{(j)} \left(\left[\sum_{s \in \mathcal{S}} \pi_s d_l^{(j)}(s) \right] - \varepsilon_T \right) \quad (209)$$

$$\stackrel{(f)}{\leq} 12T + 6T^2 - 2T(\delta - \varepsilon_T) \sum_{j=1}^2 \sum_{l=1}^3 Q_{l,t}^{(j)}. \quad (210)$$

Step (a) follows from the argumentation above.

For step (b) we follow similar steps as in [26, Sect. 4.9]: The buffer level $Q_{l,\tau}^{(j)}$ can decrease by at most one per slot, because at most one packet can depart in each time slot:

$$Q_{l,\tau}^{(j)} \geq Q_{l,t}^{(j)} - (\tau - t), \quad \text{for } \tau \geq t. \quad (211)$$

One obtains (206), where the expression inside the expectation does not depend on \underline{Q}_τ anymore. Steps (c) and (d) write out the expectation and rearrange terms.

Define the mixture distribution

$$\bar{P}^T(s|\underline{q}) = \frac{1}{T} \sum_{\tau=t}^{t+T-1} P_{S_{\tau-1}|\underline{Q}_t}(s|\underline{q}). \quad (212)$$

The constant T can be chosen large enough such that $\left| \sum_{s \in \mathcal{S}} d_l^{(j)}(s)(\pi_s - \bar{P}^T(s|\underline{q})) \right|$ is small, for all l, j and \underline{q} . This follows from

$$\begin{aligned} \left| \sum_{s \in \mathcal{S}} d_l^{(j)}(s)(\pi_s - \bar{P}^T(s|\underline{q})) \right| &\leq \sum_{s \in \mathcal{S}} |d_l^{(j)}(s)| |\pi_s - \bar{P}^T(s|\underline{q})| \\ &\leq \sum_{s \in \mathcal{S}} |\pi_s - \bar{P}^T(s|\underline{q})| \leq \varepsilon_T, \quad \forall \underline{q} \end{aligned} \quad (213)$$

for some arbitrarily small $\varepsilon_T > 0$. The first inequality follows from the triangle inequality, the second one follows from $|d_l^{(j)}(s)| \leq 1$. The final step is a bound on the variational distance between the steady state distribution and the mixture distribution. A value of T for an arbitrarily small $\varepsilon_T > 0$ exists if the Markov chain of the channel state process is irreducible and aperiodic¹⁰: In this case the steady-state distribution π is unique (see, e.g., [51, Theorem 4.3.1]) and the distribution $P_{S_{\tau-1}|\underline{Q}_t}$ converges to π for any initial distribution $P_{S_{t-1}|\underline{Q}_t}$, $\tau > t$. If $P_{S_{\tau-1}|\underline{Q}_t}$ converges to π , so does the mixture distribution defined in (212). The constant T is thus related to the mixing time of the channel state Markov chain. The decay of ε_T with respect to T is $\sim \frac{1}{T}$. A more detailed derivation on the dependency of ε_T on T is given in Section G-C.

For step (e), we replace the expression $\sum_{s \in \mathcal{S}} d_l^{(j)}(s) \sum_{\tau=t}^{t+T-1} \Pr[S_{\tau-1} = s | \underline{Q}_t]$ by its lower bound $T \left(\sum_{s \in \mathcal{S}} d_l^{(j)}(s) \pi_s \right) - T\varepsilon_T$.

For step (f), note that if the rate pair is in the interior of the rate region $\bar{C}_{\text{fb}+s}^{\text{mem}}$, i.e. if $(R_1 + \bar{\delta}, R_2 + \bar{\delta}) \in \bar{C}_{\text{fb}+s}^{\text{mem}}$, then there exists a constant $\delta > 0$ that goes to zero when $\bar{\delta} \rightarrow 0$ such that

$$\sum_{s \in \mathcal{S}} \pi_s d_l^{(j)}(s) = d_l^{(j)} \geq \delta, \quad \forall l, j \in \{1, 2\}, \quad (214)$$

where δ has to be chosen such that $\delta > \varepsilon_T$.

Using the result in (210) and the law of total expectation, we can bound

$$\begin{aligned} \mathbb{E} [\mathbb{L}(\underline{Q}_{t+T}) - \mathbb{L}(\underline{Q}_t)] &= \mathbb{E} [\Delta(\underline{Q}_t) | \underline{Q}_t] \\ &\leq 18T^2 - 2T(\delta - \varepsilon_T) \sum_{j=1}^2 \sum_{l=1}^3 \mathbb{E} [Q_{l,t}^{(j)}]. \end{aligned} \quad (215)$$

Summing over all time slots $t = 1, \dots, n$ yields

$$\sum_{t=1}^n \mathbb{E} [\mathbb{L}(\underline{Q}_{t+T}) - \mathbb{L}(\underline{Q}_t)] = \sum_{t=1}^T \mathbb{E} [\mathbb{L}(\underline{Q}_{t+n}) - \mathbb{L}(\underline{Q}_t)]$$

¹⁰Aperiodicity is not necessarily required due to the Cesàro mean in (213), but this is beyond the scope of this work. See [50, Theorem 8.6.1] for details.

$$\leq 18nT^2 - 2T(\delta - \varepsilon_T) \sum_{t=1}^n \sum_{j=1}^2 \sum_{l=1}^3 \mathbb{E} [Q_{l,t}^{(j)}]. \quad (216)$$

Rearranging terms gives

$$\frac{1}{n} \sum_{t=1}^n \sum_{j=1}^2 \sum_{l=1}^3 \mathbb{E} [Q_{l,t}^{(j)}] \leq \frac{9T}{\delta - \varepsilon_T} + \frac{\sum_{t=1}^T \mathbb{E}[\mathbb{L}(\underline{Q}_t)]}{2(\delta - \varepsilon_T)Tn}, \quad (217)$$

and taking a limsup with respect to n on both sides proves strong stability of the queuing network, given that we have $1/T \sum_{t=1}^T \mathbb{E}[\mathbb{L}(\underline{Q}_t)] < \infty$. This is true if the constant T is finite and $\mathbb{E}[\mathbb{L}(\underline{Q}_1)] < \infty$. Hence, for a chosen δ , one needs to choose a large but finite value of T such that the corresponding ε_T satisfies $\delta > \varepsilon_T$: the closer the distance to the boundary of $\bar{C}_{fb+s}^{\text{mem}}$, the higher the bound on the expected buffer size. This proves Theorem 8.

B. Hidden Case

The proof is similar to the visible case, with \underline{Z}^{t-1} taking the role of S_{t-1} , with some necessary adaptations.

An action at time t can depend only on the current queue state \underline{Q}_t and on the previous channel feedback messages \underline{Z}^{t-1} . Hence it can be represented by a distribution $P_{A_t|\underline{Q}_t\underline{Z}^{t-1}}$. \underline{E}_t is chosen according to $P_{\underline{E}_t|\underline{Q}_t}$. All dependencies are depicted in the Bayesian network in Fig. 21.

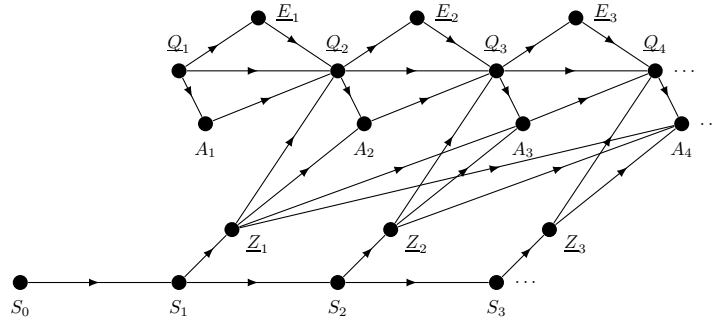


Fig. 21: Bayesian network of the queuing system. Actions at time t may depend on the previous feedback messages \underline{Z}^{t-1} and the current buffer state \underline{Q}_t , where \underline{Q}_t denotes the buffer state *before* executing action A_t .

We can split the T -slot conditional Lyapunov drift $\Delta(\underline{Q}_t)$ as defined in (189) into the telescoping sum

$$\Delta(\underline{Q}_t) = \sum_{\tau=t}^{t+T-1} \mathbb{E} [\mathbb{L}(\underline{Q}_{\tau+1}) - \mathbb{L}(\underline{Q}_\tau) | \underline{Q}_t] \quad (218)$$

$$= \sum_{\tau=t}^{t+T-1} \mathbb{E} \left[\mathbb{E} [\mathbb{L}(\underline{Q}_{\tau+1}) - \mathbb{L}(\underline{Q}_\tau) | \underline{Q}_\tau \underline{Z}^{\tau-1}] | \underline{Q}_t \right], \quad (219)$$

where the last equality is because $\underline{Q}_{\tau+1}$ is a deterministic function of \underline{Q}_τ , A_τ , \underline{Z}_τ and $\underline{Q}_\tau A_\tau \underline{Z}_\tau - \underline{Q}_\tau \underline{Z}_\tau^{\tau-1} - \underline{Q}_t$ forms a Markov chain for $\tau \geq t$.

We use (219) together with (193) to obtain

$$\Delta(\underline{Q}_t) \leq \sum_{\tau=t}^{t+T-1} 12 - 2 \cdot \mathbb{E} \left[\sum_{j=1}^2 \sum_{l=1}^3 \mathbb{E} \left[Q_{l,\tau}^{(j)} D_{l,\tau}^{(j)} | \underline{Q}_\tau \underline{Z}^{\tau-1} \right] | \underline{Q}_t \right]. \quad (220)$$

With the same arguments as in the visible case, we obtain the bound

$$\Delta(\underline{Q}_t) \leq \sum_{\tau=t}^{t+T-1} 12 - 2 \cdot \mathbb{E} \left[\sum_{j=1}^2 \sum_{l=1}^3 \sum_{m \in \mathcal{O}(l)} [Q_{l,\tau}^{(j)} - Q_{m,\tau}^{(j)}]^+ \mathbb{E} \left[C_{lm,\tau}^{(j)} | \underline{Q}_\tau \underline{Z}^{\tau-1} \right] - Q_{1,\tau}^{(j)} R_j | \underline{Q}_t \right]. \quad (221)$$

As before, the terms inside the inner expectation are as follows:

$$\mathbb{E} \left[C_{12,\tau}^{(j)} | \underline{Q}_\tau \underline{Z}^{\tau-1} \right] = \Pr[A_\tau = j | \underline{Q}_\tau \underline{Z}^{\tau-1}] (\epsilon_j(\underline{Z}^{\tau-1}) - \epsilon_{12}(\underline{Z}^{\tau-1})) \quad (222)$$

$$\mathbb{E} \left[C_{13,\tau}^{(j)} | \underline{Q}_\tau \underline{Z}^{\tau-1} \right] = \Pr[A_\tau = 4 | \underline{Q}_\tau \underline{Z}^{\tau-1}] (1 - \epsilon_{12}(\underline{Z}^{\tau-1})) \quad (223)$$

$$\mathbb{E} \left[C_{14,\tau}^{(j)} | \underline{Q}_\tau \underline{Z}^{\tau-1} \right] = \Pr[A_\tau = j | \underline{Q}_\tau \underline{Z}^{\tau-1}] (1 - \epsilon_j(\underline{Z}^{\tau-1})) \quad (224)$$

$$\mathbb{E} \left[C_{24,\tau}^{(j)} | \underline{Q}_\tau \underline{Z}^{\tau-1} \right] = \Pr[A_\tau = 3 | \underline{Q}_\tau \underline{Z}^{\tau-1}] (1 - \epsilon_j(\underline{Z}^{\tau-1})) \quad (225)$$

$$\mathbb{E} \left[C_{32,\tau}^{(j)} | \underline{Q}_\tau \underline{Z}^{\tau-1} \right] = \Pr[A_\tau = 5 | \underline{Q}_\tau \underline{Z}^{\tau-1}] (\epsilon_j(\underline{Z}^{\tau-1}) - \epsilon_{12}(\underline{Z}^{\tau-1})) \quad (226)$$

$$\mathbb{E} \left[C_{34,\tau}^{(j)} | \underline{Q}_\tau \underline{Z}^{\tau-1} \right] = \Pr[A_\tau = 5 | \underline{Q}_\tau \underline{Z}^{\tau-1}] (1 - \epsilon_j(\underline{Z}^{\tau-1})), \quad (227)$$

The criterion in (101) finds the tightest upper bound in (220) under the assumption that actions can depend on Q_τ and $\underline{Z}^{\tau-1}$. Hence, any stationary probabilistic scheme that bases its decisions only on $\underline{Z}_{\tau-L}^{\tau-1}$, according to a distribution $P_{A_\tau | \underline{Z}_{\tau-L}^{\tau-1}}$, leads to a looser upper bound on $\Delta(\underline{Q}_t)$.

To that end, we write the inner expectation in (220) similar to the visible case:

$$\mathbb{E} \left[Q_{l,\tau}^{(j)} D_{l,\tau}^{(j)} | \underline{Q}_\tau \underline{Z}^{\tau-1} \right] = Q_{l,\tau}^{(j)} \mathbb{E} \left[D_{l,\tau}^{(j)} | \underline{Q}_\tau \underline{Z}^{\tau-1} \right] = Q_{l,\tau}^{(j)} d_l^{(j)}(\underline{Z}_{\tau-L}^{\tau-1}), \quad (228)$$

where the expectation on the LHS is with respect to a distribution $P_{A_\tau | \underline{Z}_{\tau-L}^{\tau-1}}$. The average flow divergence does not depend on the queue state \underline{Q}_τ and $\underline{Z}^{\tau-L-1}$ in this case. Hence we can write

$$\Delta(\underline{Q}_t) \leq \sum_{\tau=t}^{t+T-1} 12 - 2 \cdot \mathbb{E} \left[\sum_{j=1}^2 \sum_{l=1}^3 Q_{l,\tau}^{(j)} d_l^{(j)}(\underline{Z}_{\tau-L}^{\tau-1}) | \underline{Q}_t \right] \quad (229)$$

$$\stackrel{(a)}{\leq} \sum_{\tau=t}^{t+T-1} 12 + 12(\tau - t) - 2 \cdot \mathbb{E} \left[\sum_{j=1}^2 \sum_{l=1}^3 Q_{l,t}^{(j)} d_l^{(j)}(\underline{Z}_{\tau-L}^{\tau-1}) | \underline{Q}_t \right] \quad (230)$$

$$\stackrel{(b)}{\leq} 12T + 6T^2 - 2 \sum_{j=1}^2 \sum_{\tau=t}^{t+T-1} \sum_{\underline{z}_{\tau-L}^{\tau-1}} \Pr[\underline{Z}_{\tau-L}^{\tau-1} = \underline{z}_{\tau-L}^{\tau-1} | \underline{Q}_t] \sum_{l=1}^3 Q_{l,t}^{(j)} d_l^{(j)}(\underline{z}_{\tau-L}^{\tau-1})$$

$$\stackrel{(c)}{=} 12T + 6T^2 - 2 \sum_{j=1}^2 \sum_{l=1}^3 Q_{l,t}^{(j)} \sum_{\underline{z}^L} d_l^{(j)}(\underline{z}^L) \sum_{\tau=t}^{t+T-1} \Pr[\underline{Z}_{\tau-L}^{\tau-1} = \underline{z}^L | \underline{Q}_t] \quad (231)$$

$$\stackrel{(d)}{\leq} 12T + 6T^2 - 2T \sum_{j=1}^2 \sum_{l=1}^3 Q_{l,t}^{(j)} \left(\left[\sum_{\underline{z}^L} P_{\underline{Z}^L}(\underline{z}^L) d_l^{(j)}(\underline{z}^L) \right] - \epsilon_{L,T} \right) \quad (232)$$

$$\stackrel{(e)}{\leq} 12T + 6T^2 - 2T(\delta - \epsilon_{L,T}) \sum_{j=1}^2 \sum_{l=1}^3 Q_{l,t}^{(j)}. \quad (233)$$

Step (a) follows because the buffer level $Q_{l,\tau}^{(j)}$ can decrease by at most one per slot, as stated in (211). The expression inside the expectation in (230) does not depend on \underline{Q}_τ anymore. Step (b) writes out the expectation and rearranges terms. Because the sequence \underline{Z}^n is stationary and also the probabilistic strategy is stationary, $d_l^{(j)}(\underline{z}_{\tau-L}^{\tau-1})$ does not depend on τ but only on the realization $\underline{Z}_{\tau-L}^{\tau-1} = \underline{z}^L$. This is used in step (c).

Define the mixture distribution

$$\bar{P}^T(\underline{z}^L | \underline{q}) = \frac{1}{T} \sum_{\tau=t}^{t+T-1} P_{\underline{Z}_{\tau-L}^{\tau-1} | \underline{Q}_t}(\underline{z}^L | \underline{q}). \quad (234)$$

The constant T can be chosen large enough such that $\left| \sum_{\underline{z}^L} d_l^{(j)}(\underline{z}^L) (P_{\underline{Z}^L}(\underline{z}^L) - \bar{P}^T(\underline{z}^L | \underline{q})) \right|$ is small, for all l, j and \underline{q} . This follows because

$$\left| \sum_{\underline{z}^L} d_l^{(j)}(\underline{z}^L) (P_{\underline{Z}^L}(\underline{z}^L) - \bar{P}^T(\underline{z}^L | \underline{q})) \right| \leq \sum_{\underline{z}^L} |d_l^{(j)}(\underline{z}^L)| |P_{\underline{Z}^L}(\underline{z}^L) - \bar{P}^T(\underline{z}^L | \underline{q})|$$

$$\leq \sum_{\underline{z}^L} |P_{\underline{Z}^L}(\underline{z}^L) - \bar{P}^T(\underline{z}^L | \underline{q})| \leq \epsilon_{L,T}, \quad \forall \underline{q} \quad (235)$$

for some $\epsilon_{L,T} > 0$. Hence, the variational distance between $P_{\underline{Z}^L}$ and \bar{P}^T needs to become small.

Recall that the channel state Markov chain is irreducible and aperiodic. Define the random variable $M_t = (S_{t-L}^{t-1} \underline{Z}_{t-L}^{t-1})$. Note that the sequence M^n is Markov and the corresponding Markov chain is irreducible and aperiodic. One may verify that $M_{\tau+1}$ is independent of \underline{Q}_t given M_τ for $\tau \geq t$ and hence the distribution of M_τ converges to the steady state distribution of the corresponding Markov chain, for any given initial distribution of $P_{M_t | \underline{Q}_t}$. If M_τ is distributed according to the steady state distribution, so is its component $\underline{Z}_{\tau-L}^{\tau-1}$, i.e. according to $P_{\underline{Z}_{\tau-L}^{\tau-1}}(\underline{z}^L)$. This distribution does not depend on τ because \underline{Z}^n is stationary, so we can replace it with $P_{\underline{Z}^L}(\underline{z}^L)$. If $P_{\underline{Z}_{\tau-L}^{\tau-1} | \underline{Q}_t}$ converges to $P_{\underline{Z}^L}$, so does the Cesàro mean in (235). In

general the constant T will have to be larger than L . A detailed derivation on the dependency of $\varepsilon_{L,T}$ on L and T is given in Appendix G-C.

For step (d), we lower bound the expression $\sum_{\underline{z}^L} d_l^{(j)}(\underline{z}^L) \sum_{\tau=t}^{t+T-1} \Pr [\underline{Z}_{\tau-L}^{\tau-1} = \underline{z}^L | \underline{Q}_t]$ by $T \left(\sum_{\underline{z}^L} d_l^{(j)}(\underline{z}^L) P_{\underline{z}^L}(\underline{z}^L) \right) - T\varepsilon_{L,T}$.

For step (e), note that if the rate pair is in the interior of the L -order approximation of the outer bound in (59) - (63), i.e. if $(R_1 + \bar{\delta}, R_2 + \bar{\delta}) \in \bar{\mathcal{C}}_{\text{pb}}^{\text{mem}}(L)$, then there exists a constant $\delta > 0$ that goes to zero when $\bar{\delta} \rightarrow 0$ such that

$$\sum_{\underline{z}^L} P_{\underline{z}^L}(\underline{z}^L) d_l^{(j)}(\underline{z}^L) \geq \delta, \quad \forall l \in \{1, 2, 3\}, j \in \{1, 2\}, \quad (236)$$

where δ should be chosen such that $\delta > \varepsilon_{L,T}$.

Using the result in (233) and the law of total expectation, we can bound

$$\begin{aligned} \mathbb{E} [\mathbb{L}(\underline{Q}_{t+T}) - \mathbb{L}(\underline{Q}_t)] &= \mathbb{E} [\Delta(\underline{Q}_t) | \underline{Q}_t] \\ &\leq 18T^2 - 2T(\delta - \varepsilon_{L,T}) \sum_{j=1}^2 \sum_{l=1}^3 \mathbb{E} [Q_{l,t}^{(j)}]. \end{aligned} \quad (237)$$

Summing over all time slots $t = 1, \dots, n$ yields

$$\begin{aligned} \sum_{t=1}^n \mathbb{E} [\mathbb{L}(\underline{Q}_{t+T}) - \mathbb{L}(\underline{Q}_t)] &= \sum_{t=1}^T \mathbb{E} [\mathbb{L}(\underline{Q}_{t+n}) - \mathbb{L}(\underline{Q}_t)] \\ &\leq 18nT^2 - 2T(\delta - \varepsilon_{L,T}) \sum_{t=1}^n \sum_{j=1}^2 \sum_{l=1}^3 \mathbb{E} [Q_{l,t}^{(j)}]. \end{aligned} \quad (238)$$

Rearranging terms gives

$$\frac{1}{n} \sum_{t=1}^n \sum_{j=1}^2 \sum_{l=1}^3 \mathbb{E} [Q_{l,t}^{(j)}] \leq \frac{9T}{\delta - \varepsilon_{L,T}} + \frac{\sum_{t=1}^T \mathbb{E}[\mathbb{L}(\underline{Q}_t)]}{2(\delta - \varepsilon_{L,T})Tn}, \quad (239)$$

and taking a lim sup with respect to n on both sides proves strong stability of the queuing network, given that $1/T \sum_{t=1}^T \mathbb{E}[\mathbb{L}(\underline{Q}_t)] < \infty$. This is true if the constant T is finite and $\mathbb{E}[\mathbb{L}(\underline{Q}_1)] < \infty$. The dependency of L and T is studied in more detail in Appendix G-C.

C. Speed of Convergence

Consider an irreducible aperiodic finite state Markov chain $M_t \in \mathcal{M}$ with transition matrix \mathbf{P} and corresponding stationary distribution π . \mathbf{P}_{ji} corresponds to $P_{M_t | M_{t-1}}(i|j)$, and by the Chapman-Kolmogorov equations, $P_{M_t | M_{t-k}}(i|j)$ is represented by $\mathbf{P}_{ji}^{(k)}$, with $\mathbf{P}^{(k)} = \mathbf{P}^k$.

For finite state irreducible aperiodic Markov chains, [52, Theorem 8.9] states the following exponential convergence result:

$$\left| \mathbf{P}_{ji}^{(k)} - \pi_i \right| \leq K \rho^k, \quad \forall j, \quad (240)$$

where $K \geq 0$ and $0 \leq \rho < 1$.

An immediate consequence is the following corollary:

Corollary 11. The variational distance between P_{M_k} and π is bounded for any initial distribution on M_0 by

$$\sum_{i=1}^{|\mathcal{M}|} |P_{M_k}(i) - \pi_i| \leq K |\mathcal{M}| \rho^k. \quad (241)$$

Proof: Let the row vector \underline{x} represent the initial distribution of M_0 on \mathcal{M} , and let x_j denote $P_{M_0}(j)$. P_{M_k} can be represented by the row vector $\underline{x} \mathbf{P}^k$. With $\underline{\pi}$ representing the steady state distribution π , we can write

$$\begin{aligned} \sum_{i=1}^{|\mathcal{M}|} |P_{M_k}(i) - \pi_i| &= \|\underline{x} \mathbf{P}^k - \underline{\pi}\|_1 = \sum_{i=1}^{|\mathcal{M}|} \left| \sum_{j=1}^{|\mathcal{M}|} x_j \mathbf{P}_{ji}^{(k)} - \pi_i \right| \\ &= \sum_{i=1}^{|\mathcal{M}|} \left| \sum_{j=1}^{|\mathcal{M}|} x_j (\mathbf{P}_{ji}^{(k)} - \pi_i) \right| \end{aligned}$$

$$\begin{aligned}
&\leq \sum_{i=1}^{|\mathcal{M}|} \sum_{j=1}^{|\mathcal{M}|} x_j \left| \mathbf{P}_{ji}^{(k)} - \pi_i \right| \\
&\leq \sum_{i=1}^{|\mathcal{M}|} \sum_{j=1}^{|\mathcal{M}|} x_j K \rho^k = K |\mathcal{M}| \rho^k,
\end{aligned} \tag{242}$$

where the first inequality is due to the triangle inequality and the second one due to (240). \blacksquare

We are interested in the variational distance between some mixture distribution $\frac{1}{T} \sum_{t=0}^{T-1} P_{M_t}$ and the stationary distribution π as a function of T , for some arbitrary initial distribution P_{M_0} .

Corollary 12. For any given distribution on M_0 , the variational distance between the mixture distribution $\frac{1}{T} \sum_{t=0}^{T-1} P_{M_t}$ and π is bounded by

$$\sum_{i=1}^{|\mathcal{M}|} \left| \frac{1}{T} \sum_{t=0}^{T-1} P_{M_t}(i) - \pi_i \right| \leq \frac{K |\mathcal{M}|}{T} \cdot \frac{1}{1-\rho}. \tag{243}$$

Proof: We have

$$\begin{aligned}
\sum_{i=1}^{|\mathcal{M}|} \left| \frac{1}{T} \sum_{t=0}^{T-1} P_{M_t}(i) - \pi_i \right| &= \sum_{i=1}^{|\mathcal{M}|} \left| \frac{1}{T} \sum_{t=0}^{T-1} \sum_{j=1}^{|\mathcal{M}|} x_j \mathbf{P}_{ji}^{(t)} - \pi_i \right| \\
&= \sum_{i=1}^{|\mathcal{M}|} \left| \frac{1}{T} \sum_{t=0}^{T-1} \sum_{j=1}^{|\mathcal{M}|} x_j (\mathbf{P}_{ji}^{(t)} - \pi_i) \right| \\
&\leq \frac{1}{T} \sum_{t=0}^{T-1} \sum_{i=1}^{|\mathcal{M}|} \sum_{j=1}^{|\mathcal{M}|} x_j \left| \mathbf{P}_{ji}^{(t)} - \pi_i \right| \\
&\leq \frac{1}{T} \sum_{i=1}^{|\mathcal{M}|} \sum_{j=1}^{|\mathcal{M}|} x_j \sum_{t=0}^{T-1} K \rho^t = \frac{K}{T} |\mathcal{M}| \frac{1-\rho^T}{1-\rho} \leq \frac{K |\mathcal{M}|}{T} \cdot \frac{1}{1-\rho},
\end{aligned} \tag{244}$$

where the first inequality is due to the triangle inequality and the second one due to (240). \blacksquare

The result in (244) can be used for the visible case in (213), where the Markov chain M_t corresponds to the state sequence S_t and the state space has cardinality $|\mathcal{S}|$. Hence, $\varepsilon_T \sim \frac{|\mathcal{S}|}{T}$.

For the hidden case in (235), M_t corresponds to the random variable $(S_{t-L}^{t-1} \underline{Z}_{t-L}^{t-1})$ with cardinality $|\mathcal{M}| = |\mathcal{S}|^L |\mathcal{Z}|^L$. The result in (244) proves the convergence of M_t towards its stationary distribution π . In (235) we are interested in the convergence of $\underline{Z}_{t-L}^{t-1}$ towards its steady state distribution. For this, denote the mixture distribution $\frac{1}{T} \sum_{t=0}^{T-1} P_{M_t}(m)$ by $\bar{P}^T(m)$, where the initial distribution P_{M_0} corresponds to $P_{S_{t-L}^{t-1} \underline{Z}_{t-L}^{t-1} | \mathcal{Q}_t}$. We can split m into its components $m = (s^L, \underline{z}^L)$ and write

$$\begin{aligned}
\frac{K |\mathcal{S}|^L |\mathcal{Z}|^L}{T} \cdot \frac{1}{1-\rho} &\geq \sum_{m \in \mathcal{M}} |\bar{P}^T(m) - \pi(m)| = \sum_{\underline{z}^L} \sum_{s^L} |\bar{P}^T(s^L, \underline{z}^L) - \pi(s^L, \underline{z}^L)| \\
&\geq \sum_{\underline{z}^L} \left| \sum_{s^L} \bar{P}^T(s^L, \underline{z}^L) - \pi(s^L, \underline{z}^L) \right| \\
&= \sum_{\underline{z}^L} |\bar{P}^T(\underline{z}^L) - \pi(\underline{z}^L)|,
\end{aligned} \tag{245}$$

where the first inequality is due to (244) and the second one due to the triangle inequality. Hence, we have

$$\varepsilon_{T,L} \sim \frac{|\mathcal{S}|^L |\mathcal{Z}|^L}{T}. \tag{246}$$

For a given value of L , the constant T must be chosen on the order of $\exp(L)$ to make $\varepsilon_{T,L}$ small.

ACKNOWLEDGMENT

The authors would like to thank Navid Reyhanian, Gerhard Kramer and Chih-Chun Wang for comments and remarks that led to significant improvements of the paper.

REFERENCES

- [1] A. El Gamal, "The feedback capacity of degraded broadcast channels," *IEEE Trans. Inf. Theory*, vol. 24, no. 3, pp. 379–381, May 1978.
- [2] L. Ozarow and S. Leung-Yan-Cheong, "An achievable region and outer bound for the Gaussian broadcast channel with feedback," *IEEE Trans. Inf. Theory*, vol. 30, no. 4, pp. 667–671, July 1984.
- [3] G. Kramer, "Capacity results for the discrete memoryless network," *IEEE Trans. Inf. Theory*, vol. 49, no. 1, pp. 4–21, January 2003.
- [4] G. Dueck, "Partial feedback for two-way and broadcast channels," *Information and Control*, vol. 46, no. 1, pp. 1–15, June 1980.
- [5] S. Bhaskaran, "Gaussian broadcast channel with feedback," *IEEE Trans. Inf. Theory*, vol. 54, no. 11, pp. 5252–5257, November 2008.
- [6] O. Shayevitz and M. Wigger, "On the capacity of the discrete memoryless broadcast channel with feedback," *IEEE Transactions on Information Theory*, vol. 59, no. 3, pp. 1329–1345, March 2013.
- [7] R. Venkataramanan and S. S. Pradhan, "An achievable rate region for the broadcast channel with feedback," *IEEE Transactions on Information Theory*, vol. 59, no. 10, pp. 6175–6191, October 2013.
- [8] Y. Wu and M. Wigger, "Coding schemes with rate-limited feedback that improve over the no feedback capacity for a large class of broadcast channels," *IEEE Transactions on Information Theory*, vol. 62, no. 4, pp. 2009–2033, April 2016.
- [9] L. Georgiadis and L. Tassiulas, "Broadcast erasure channel with feedback-capacity and algorithms," in *IEEE Int. Symp. Network Coding*, June 2009, pp. 54–61.
- [10] M. Gatzianas, L. Georgiadis, and L. Tassiulas, "Multiuser broadcast erasure channel with feedback – capacity and algorithms," *IEEE Trans. Inf. Theory*, vol. 59, no. 9, pp. 5779–5804, September 2013.
- [11] M. Gatzianas, S. Saeedi Bidokhti, and C. Fragouli, "Feedback-based coding algorithms for broadcast erasure channels with degraded message sets," in *IEEE Int. Symp. Network Coding*, 2012.
- [12] C.-C. Wang, "On the capacity of 1-to-K broadcast packet erasure channels with channel output feedback," *IEEE Trans. Inf. Theory*, vol. 58, no. 2, pp. 931–956, February 2012.
- [13] P. Bergmans, "Random coding theorem for broadcast channels with degraded components," *IEEE Trans. Inf. Theory*, vol. 19, no. 2, pp. 197–207, March 1973.
- [14] R. G. Gallager, "Capacity and coding for degraded broadcast channels," *Problemy Peredachi Informatsii*, vol. 10, no. 3, pp. 3–14, 1974.
- [15] C.-C. Wang and J. Han, "The capacity region of two-receiver multiple-input broadcast packet erasure channels with channel output feedback," *IEEE Trans. Inf. Theory*, vol. 60, no. 9, pp. 5597–5626, September 2014.
- [16] E. Lutz, D. Cygan, M. Dippold, F. Dolainsky, and W. Papke, "The land mobile satellite communication channel-recording, statistics, and channel model," *IEEE Trans. Veh. Technol.*, vol. 40, no. 2, pp. 375–386, May 1991.
- [17] E. Lutz, "A Markov model for correlated land mobile satellite channels," *Int. Journal Satellite Comm.*, vol. 14, no. 4, pp. 333–339, July 1996.
- [18] F. P. Fontán, M. Vázquez-Castro, C. E. Cabado, J. P. Garcia, and E. Kubista, "Statistical modeling of the LMS channel," *IEEE Trans. Veh. Technol.*, vol. 50, no. 6, pp. 1549–1567, November 2001.
- [19] M. Ibnkahla, Q. M. Rahman, A. I. Sulyman, H. A. Al-Asady, J. Yuan, and A. Safwat, "High-speed satellite mobile communications: technologies and challenges," *Proc. IEEE*, vol. 92, no. 2, pp. 312–339, February 2004.
- [20] R. G. Gallager, *Information theory and reliable communication*. John Wiley and Sons, Inc., 1968.
- [21] P. Sadeghi, R. A. Kennedy, P. B. Rapajic, and R. Shams, "Finite-state Markov modeling of fading channels—a survey of principles and applications," *IEEE Signal Process. Mag.*, vol. 25, no. 5, pp. 57–80, September 2008.
- [22] H. Viswanathan, "Capacity of Markov channels with receiver CSI and delayed feedback," *IEEE Transactions on Information Theory*, vol. 45, no. 2, pp. 761–771, March 1999.
- [23] S. Tatikonda and S. Mitter, "The capacity of channels with feedback," *IEEE Transactions on Information Theory*, vol. 55, no. 1, pp. 323–349, January 2009.
- [24] H. H. Permuter, T. Weissman, and A. J. Goldsmith, "Finite state channels with time-invariant deterministic feedback," *IEEE Transactions on Information Theory*, vol. 55, no. 2, pp. 644–662, February 2009.
- [25] Y. H. Kim, "A coding theorem for a class of stationary channels with feedback," *IEEE Transactions on Information Theory*, vol. 54, no. 4, pp. 1488–1499, April 2008.
- [26] M. J. Neely, *Stochastic network optimization with application to communication and queueing systems*. Morgan & Claypool Publishers, 2010, vol. 3, no. 1.
- [27] W.-C. Kuo and C.-C. Wang, "Robust and optimal opportunistic scheduling for downlink 2-flow inter-session network coding with varying channel quality," in *IEEE INFOCOM*, April 2014, pp. 655–663.
- [28] R. Dabora and A. J. Goldsmith, "Capacity theorems for discrete, finite-state broadcast channels with feedback and unidirectional receiver cooperation," *IEEE Trans. Inf. Theory*, vol. 56, no. 12, pp. 5958–5983, December 2010.
- [29] E. N. Gilbert, "Capacity of a burst-noise channel," *Bell System Technical Journal*, vol. 39, no. 5, pp. 1253–1265, September 1960.
- [30] E. Elliott, "Estimates of error rates for codes on burst-noise channels," *Bell System Technical Journal*, vol. 42, no. 5, pp. 1977–1997, September 1963.
- [31] M. J. Neely, "Stability and capacity regions of discrete time queueing networks," *arXiv*, 2010. [Online]. Available: <http://arxiv.org/abs/1003.3396>
- [32] L. Georgiadis, M. J. Neely, and L. Tassiulas, *Resource allocation and cross-layer control in wireless networks*. NOW Publishers, 2006.
- [33] L. Jiang and J. Walrand, "Stable and utility-maximizing scheduling for stochastic processing networks," in *Allerton Conf. on Commun., Control, and Computing*, 2009, pp. 1111–1119.
- [34] T. Cover and J. Thomas, *Elements of Information Theory*. John Wiley and Sons, Inc., 2006.
- [35] A. Dana and B. Hassibi, "The capacity region of multiple input erasure broadcast channels," in *IEEE Int. Symp. Inf. Theory*, 2005.
- [36] F. Le Gland and L. Mevel, "Exponential forgetting and geometric ergodicity in Hidden Markov Models," *Mathematics of Control, Signals and Systems*, vol. 13, no. 1, pp. 63–93, February 2000.
- [37] M. J. Neely and R. Uргаonkar, "Optimal backpressure routing for wireless networks with multi-receiver diversity," *Ad Hoc Networks*, vol. 7, no. 5, pp. 862 – 881, 2009. [Online]. Available: <http://www.sciencedirect.com/science/article/pii/S1570870508001157>
- [38] D. Traskov, N. Ratnakar, D. Lun, R. Koetter, and M. Medard, "Network coding for multiple unicasts: An approach based on linear optimization," in *IEEE Int. Symp. Inf. Theory*, 2006, pp. 1758–1762.
- [39] D. P. Bertsekas, *Network Optimization: Continuous and Discrete Methods*. Athena Scientific, 1998.
- [40] G. S. Paschos, L. Georgiadis, and L. Tassiulas, "Scheduling with pairwise XORing of packets under statistical overhearing information and feedback," *Queueing Systems*, vol. 72, no. 3–4, pp. 361–395, April 2012.
- [41] L. Tassiulas and A. Ephremides, "Stability properties of constrained queueing systems and scheduling policies for maximum throughput in multihop radio networks," *IEEE Trans. Autom. Control*, vol. 37, no. 12, pp. 1936–1948, December 1992.
- [42] —, "Dynamic server allocation to parallel queues with randomly varying connectivity," *IEEE Trans. Inf. Theory*, vol. 39, no. 2, pp. 466–478, March 1993.
- [43] M. J. Neely, E. Modiano, and C. E. Rohrs, "Dynamic power allocation and routing for time-varying wireless networks," *IEEE J. Sel. Areas Commun.*, vol. 23, no. 1, pp. 89–103, January 2005.
- [44] A. Pantelidou, A. Ephremides, and A. L. Tits, "A cross-layer approach for stable throughput maximization under channel state uncertainty," *Wireless Networks*, vol. 15, no. 5, pp. 555–569, July 2009.

- [45] L. Tassiulas, "Scheduling and performance limits of networks with constantly changing topology," *IEEE Trans. Inf. Theory*, vol. 43, no. 3, pp. 1067–1073, May 1997.
- [46] C.-p. Li and M. J. Neely, "Exploiting channel memory for multi-user wireless scheduling without channel measurement: Capacity regions and algorithms," *Performance Evaluation*, August 2011.
- [47] —, "Network utility maximization over partially observable Markovian channels," *Performance Evaluation*, vol. 70, no. 7, pp. 528–548, July 2013.
- [48] L. Ying and S. Shakkottai, "On throughput optimality with delayed network-state information," *IEEE Trans. Inf. Theory*, vol. 57, no. 8, pp. 5116–5132, August 2011.
- [49] D. Traskov, M. Heindlmaier, M. Médard, and R. Koetter, "Scheduling for network-coded multicast," *IEEE/ACM Trans. Netw.*, vol. 20, no. 5, pp. 1479–1488, October 2012.
- [50] R. A. Horn and C. R. Johnson, *Matrix analysis*. Cambridge University Press, 2012.
- [51] R. G. Gallager, *Stochastic Processes: Theory for Applications*. Cambridge University Press, 2013.
- [52] P. Billingsley, *Probability and measure*. John Wiley and Sons, Inc., 1995.